TEMPORAL STUDIES OF ATMOSPHERIC ELECTRICAL PARAMETERS CLOSE TO THE EARTH'S SURFACE

THESIS SUBMITTED TO

MANONMANIAM SUNDARANAR UNIVERSITY

IN PARTIAL FULFILMENT OF THE REQUIREMENTS

FOR THE AWARD OF DEGREE OF

DOCTOR OF PHILOSOPHY

BY

C. PANNEERSELVAM

(Reg. No. 1548)

EQUATORIAL GEOPHYSICAL RESEARCH LABORATORY

INDIAN INSTITUTE OF GEOMAGNETISM

TIRUNELVELI – 627011, INDIA

FEBRUARY 2012

Dr. S. Gurubaran,
Professor 'F',
Equatorial Geophysical Research Laboratory,
Indian Institute of Geomagnetism,
Krishnapuram,
Tirunelveli-627011, Tamilnadu,
India

CERTIFICATE

This thesis entitled "**TEMPORAL STUDIES OF ATMOSPHERIC ELECTRICAL PARAMETERS CLOSE TO THE EARTH'S SURFACE** " submitted by C**. Panneerselvam** for the award of **Degree of Doctor of Philosophy in Physics** of Manonmaniam Sundaranar University is a record of bonafide research work done by him and it has not been submitted for the award of any degree, diploma, associateship, fellowship of any University/Institution.

Place: Tirunelveli
Date: 06-02-2012 **S. GURUBARAN**

C. Panneerselvam

Technical Officer-III,

Equatorial Geophysical Research Laboratory,

Indian Institute of Geomagnetism,

Krishnapuram,

Tirunelveli-627011, Tamilnadu,

India

DECLARATION

I hereby declare that the thesis entitled "**TEMPORAL STUDIES OF ATMOSPHERIC ELECTRICAL PARAMETERS CLOSE TO THE EARTH'S SURFACE**" submitted by me for the **Degree of Doctor of Philosophy in Physics** is the result of my original and independent research work carried out under the guidance of **Dr. S. Gurubaran**, Professor, Equatorial Geophysical Research Laboratory, Indian Institute of Geomagnetism, Tirunelveli, and it has not been submitted for the award of any degree, diploma, associateship, fellowship of any University or Institution.

Station: Tirunelveli

Date: 06-02-2012 **(C. Panneerselvam)**

Acknowledgement

Pursuing a Ph.D. is a difficult and scrupulous yet enjoyable task, in which one learns much more over the period and evolves in all aspects. During this period, my belief on the fact that, "Any difficult task can be accomplished, with hard work, perseverance and patience", grew all the stronger. However, a person's efforts, when alone are not sufficient to bear fruitful outcomes, the cooperation and coordination of many people involved, impart motivation, encouragement and moral support is almost essential. It gives me pleasure to thank all the people who made this thesis possible.

First of all, my deep gratitude goes to my thesis guide Prof. S. Gurubaran, Head, EGRL, Tirunelveli for his invaluable guidance, suggestions and constant encouragement during the entire period of work and for writing thesis. I believe no word could fully encompass the amount of gratitude I have for his supervision and loving support.

My sincere thanks are due to Prof. R. Rajaram who taught me this new subject in physics. During the course work I gathered subject knowledge and experience from Prof. R.Rajaram through many useful discussions. I owe my gratitude to him for having taught me some basic aspects of life which I found to be very useful in day to day life.

I express my sincere thanks to the Director of IIG, Prof. Mita Rajaram for her cooperation, encouragement. I owe immense thanks to my ex-Director Prof. Archana Bhattacharyya for her motivation, invaluable help for registering my Ph.D at M.S. University, Tirunelveli.

I thank Prof. A. K. Kamra, Indian Institute of Tropical meteorology, Pashan, Pune for his support and encouragement which helped me in completing this work. The knowledge I have gathered from him is enormous. I am grateful to him for the good arrangement made for my stay at Pune and having spent so much time amidst his busy schedule to go through my research work.

I also thank my colleagues (lab engineer's) Mr. K.U. Nair, Mr. C.Selvaraj and Mr. Gopal Singh Rathod who cheerfully welded, soldered, fixed, assembled, cleaned, and installed all the instruments in this project involved, including digging of enormous pits and installation of mast at Maitri, Antarctica too on my request.

I am grateful to my colleagues Mr. K. Jeeva, Mr. K. Emperumal, Dr. K. Jawahar, Mr. Laxman, Mr. Sheik Bareeth for their patience, during field work.

I should not miss the opportunity to thank my colleague and also classmate from school days, Mr. P. Elango, who is well known to me from the childhood for his constant enragement, motivation, in time moral support and affection throughout this course of work

I thank Mr. Thiyagarajan, Associate Professor, Dept. of physics, KGS Arts & Science College, Srivaikuntam, and Mr. N.Johonson Jeyakumar, Associate Professor, Dept. of physics, Pope's College, Sawyerpuram for friendly discussions during this course of work.

I thank our institute members who went to Maitri, Antarctica, installed the GEC equipments and collected valuable data in the extreme climatic conditions. I thank the Leaders &

members of 19th and 28th Indian Scientific Expeditions to Antarctica, who helped me on various aspects to install and smooth operation of our instruments during my stay at Maitri, Antarctica.

I thank Ms. A. Selvarajeswari, Librarian for her efforts in getting the scientific reprints from IIG, Mumbai in time. I would like to acknowledge all the staffs of Balaji Security Services and Joshoph Man Power for their assistance rendered.

I am dedicating this thesis work to my parents (late) both of them uneducated but they were having too much affection and love for me and they were interested in my Doctoral Degree. Finally, I thank my beloved wife and my only son who have been extremely supportive and encouraging, particularly during difficult and challenging times.

PREFACE

The study of atmospheric electrical parameters (Global Electric Circuit, GEC) will provide a platform for understanding the solar-terrestrial relationship and offers possibilities of exploring one of the traditional scientific problems of mankind in the last few centuries, namely, that of associating changes in lower atmospheric weather with the solar output. In spite of several mechanisms having been proposed there still lie uncertainties in identifying the actual physical processes that govern the envisioned relationship between the sun and the changes in weather. Continuous measurements of atmospheric electrical parameters, namely, the vertical electric field, the conductivity and the air-earth current density, that characterize the GEC, are considered useful in any study aiming towards understanding fully the electrical environment of the Earth. Further, since the global circuit links the lower troposphere, the ionosphere and the magnetosphere, the measurements of atmospheric electrical parameters will be handy in any integrated approach that involve all these regions. Day to day variability of thunderstorm activity there are diurnal, seasonal, interannual variations in the potential differences and currents, as well as solar influences on the properties of the circuit. Maxwell currents, electric field and conductivity measurements made from a low latitude station, Tirunelveli (8.7°N, 77.8°E), near the southern tip of the Indian peninsula and at Maitri, Antarctica, as a part of ongoing GEC study, are made use of for examining the possibility of detecting global signatures in the tropical Indian zone and polar regions to evaluating the contributions of local processes in the variabilities of atmospheric electrical parameters as measured during the course of the work. The installation of Passive antenna, Wilson's plate antenna for the measurements of atmospheric potential, conduction current and convection current will be carried out in this course of work for the both the stations. Atmospheric

electrical measurements made at Antarctica are expected to be relatively unperturbed by local meteorological conditions.

In this investigation we have analyzed more than a decade data from a tropical equatorial station. The measured atmospheric electrical parameters in both the stations during fair-weather days follow the famous Carnegie's curve with a minimum about 3:00 UT and a maximum at about 18:00 UT except morning sunrise effect which is local effect. As far the polar station we have used the data for the years 2001 – 2006. The diurnal variation follows clearly with well defined Carnegie's curve. With 3:00 UT minimum and a maximum with 18:00 UT during fair-weather conditions. The upper atmospheric contribution to the GEC separated using principle component analysis. During geomagnetic quiet days the measured GEC parameters follows the regular diurnal pattern and during geomagnetic disturbed days the regular diurnal pattern modified by the ionospheric / magnetospheric contribution. The data from the both the stations will provide good information about the relationship between the sun and the changes in weather. Long-term measurements would be considered useful for addressing some of the problems associated with global change.

(C.PANNEERSELVAM)

Equatorial Geophysical Research Laboratory,

Indian Institute of Geomagnetism,

Krishnapuram,

Tirunelveli – 627011

List of Publications

1. **C. Panneerselvam**, K. U. Nair, K. Jeeva, C. Selvaraj, S. Gurubaran and R. Rajaram, A comparative study of atmospheric Maxwell current and electric field from a low latitude station, Tirunelveli, Earth, Planets and Space, 55, 697-703, 2003.

2. **C. Panneerselvam,** C. Selvaraj, K. Jeeva, K. U. Nair, C. P. Anil Kumar and S. Gurubaran, Fairweather atmospheric electricity at an Indian station, Maitri, Antarctica during Antarctic summer, Journal of Earth System Science, 116, 179-186, 2007

3. **C. Panneerselvam,** K. U. Nair, C. Selvaraj, K. Jeeva, C. P. Anil Kumar and S. Gurubaran, Diurnal variation of atmospheric Maxwell current over the low latitude continental station, Tirunelveli, India, Earth, Planets and Space, 59, 429-435, 2007.

4. C. P. Anil Kumar, **C. Panneerselvam**, K. U. Nair, K. Jeeva, C. Selvaraj, S. Gurubaran and R. Rajaram, Influence of coronal mass ejections on global electric circuit, Indian Journal of Radio and Space Physics, 37, 39-45, 2008

5. C. P. Anil Kumar, **C. Panneerselvam**, K. U. Nair, K. Jeeva, C. Selvaraj, H. Johnson Jeyakumar and S. Gurubaran, Measurement of atmospheric air- earth current density from a tropical station using improvised Wilson's plate antenna, Earth Planets Space, 61, 919-926, 2009.

6. C. P. Anil Kumar, **C. Panneerselvam**, K. U. Nair, C. Selvaraj, S. Gurubaran and C. Venugopal, Apposite of atmospheric electric parameters with the energy coupling function (å) during geomagnetic storms at high latitude, Atmospheric Research, 91, 201-205, 2009. doi:10.1016/j.atmosres.2008.06.005

7. **C. Panneerselvam**, C. P. Anil Kumar, Ajay Dhar, K. U. Nair, C. Selvaraj, S. Gurubaran, and B. M. Pathan, Instrumentation for the surface measurements of atmospheric electrical parameters at Maitri, Antarctica: First results, *Earth Planets Space*, **62**, 545–549, 2010 *DOI: 10.5047/eps.2010.06.001*

8. K. Jeeva, **C. Panneerselvam**, K. U. Nair, C. Selvaraj, Ajay Dhar, B.M.Pathan and S. Gurubaran, Global electric circuit parameters and their variability observed over Maitri, Antarctica, Journal of geological society of India, Vol.78, September 2011, pp.199-210 DOI**:** http://dx.doi.org/10.1007/s12594-011-0088-2

CONTENTS

CHAPTER 5: Observation of the global atmospheric electric circuit

CHAPTER 6: Influence of upper atmospheric electric generators on GEC

And separation of different atmospheric currents

CHAPTER 7: Conclusions and suggestions for future work

Nomenclature

Symbol	Description
J_C	Conduction current density
J_D	Displacement current density
J_P	Precipitation current density
J_S	Total air-Earth current density
J_T	Turbulent current density
J_M	Maxwell current density
PG	Potential Gradient
R_C	Columnar resistance
E	Electric field
V_I	Ionosphere-earth potential difference
J_L	Lightning current density
C	Electrical capacitance
σ	air conductivity
ε_0	permittivity of free space
ω	Angular frequency
Q	Total charge on the Earth's surface
S_d	Static effective area of the antenna
S	Effective area of the antenna
H	Height of the antenna
L	Length of the antenna wire
r_o	Radius of the antenna wire

ε	Solar wind – magnetosphere energy coupling function
B	Geomagnetic field
B_Z	North-south magnetic field
V_s	Velocity of solar wind
IMF	Interplanetary Magnetic Field
GEC	Global Electric Circuit
FM	Field Mill
EFM	Electric Field Meter
RC	Time constant used in the electrometer circuit
UT	Universal Time
IST	Indian Standard Time
LT	Local Time
ELF	Extreme Low Frequency
VLF	Very Low Frequency
GCR	Galactic Cosmic Rays
CME	Coronal Mass Ejection
WMO	World Meteorological Organization
EGRL	Equatorial Geophysical Research Laboratory
NPL	National Physical Laboratory
OTD	Optical Transient Detector
PCA	Principle Component Analysis
ADC	Analog to Digital Converter
AWS	Automatic Weather Station

CHAPTER 1

Introduction

1.1 Historical overview

Before more specific details on this study are provided, a brief historical introduction to key revelations in atmospheric electricity is given in this section to introduce the general background of this area of research. The quantitative study of atmospheric electricity in the United Kingdom began over 250 years ago, with detection of electric charge in a clear atmosphere reported by John Canton in 1753. From his experiments, Canton (1753) discovered that the air was generally positively charged with respect to the ground during fair-weather, with changes in this charge associated with different meteorological phenomena, such as precipitation and fog. The mid-nineteenth century marked an advancement of atmospheric electrical sensors, noticeably Lord Kelvin's "water dropper" electric field sensor. When combined with the newly-discovered method of photographic recording, the water-dropper allowed continuous measurement of the electric field at Kew Observatory, London in 1861 (Everett, 1868; Harrison and Aplin, 2002). The close connection between the electrical state of the atmosphere and changes in the weather provided motivation for continued study of atmospheric electricity. Lord Kelvin confidently predicted that electric field measurements were to eventually form a basis for weather forecasting (Thomson, 1872).

Kelvin and previous researchers such as Canton observed a continuous and varying electric field in the atmosphere. The air was also known to be weakly

electrically conductive from experiments by Gerdien (1905a), implying the presence of an atmospheric electrical current. A vertical current flowing through the electrically resistive atmosphere was considered to be the source of the fair weather electric field by the Nobel Prize winner C.T.R. Wilson in 1906, which is shown in Fig.1.1.

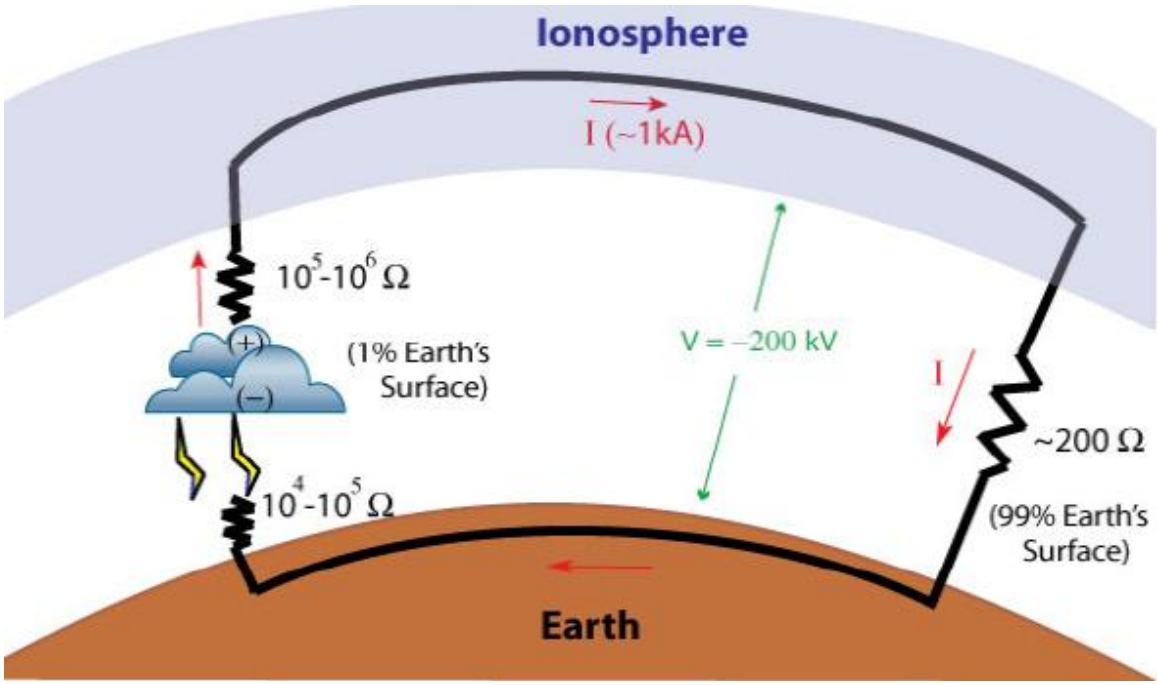

Fig. 1.1 The global electric circuit by C.T.R. Wilson.

The concept of a global atmospheric electrical circuit and the description of a new type of sensor capable of directly measuring this vertical current density, as well as the associated electric field, were given by Wilson (1906). The personal significance of this direct measurement of the air-Earth current density was recalled by Wilson in a later publication about his work (Wilson, 1960).

An additional motivation to investigate temporal patterns in atmospheric electricity measurements came later in the early twentieth century, with the discovery of a universal global diurnal variation in electric field. Careful measurements made in clear oceanic air during the 1915-1928 cruises of the geophysical research ship Carnegie, showed a distinct diurnal cycle that was independent of geographical location. This significant finding suggested a global source of diurnal variation of surface electric field. The global source was thought to directly relate to the intensity of global thunderstorm activity, as demonstrated by Whipple (1929), who found the shape and phase of the observed cycle to be closely related to the estimated diurnal variation of global thunderstorm area with universal time. A global signal in surface atmospheric electric field measurements (Carnegie curve) was further evidence for the suggestion originally proposed before the cruises by Wilson (1906), that the diurnal variation of the electric current and field had global origins, visible when local meteorological influences were low. Wilson's air-Earth current density has since been recognised as the most fundamental electrical parameter of the global electric circuit that can be measured at the surface (e.g. Chalmers (1967), Dolezalek (1978)).

Worldwide thunderstorm activity is believed to maintain the global electric potential between the ionosphere and the earth's surface (Wilson 1925). Tropical thunderstorms are considered as the main source for the electric field in the lower atmosphere, drawing current upward to the ionosphere. In this way, the global thunderstorm activity is able to maintain a time varying electric potential difference of nearly 300 kV, directed downward between the equipotential surfaces of the ionosphere and the ground (Alderman and Williams 1996). The atmospheric vertical electric field, conductivity and total current density are the three closely related

parameters of atmospheric electricity that are required to obtain an adequate description of the fairweather atmospheric electric circuit (Israel 1973).

The study of Global Electric Circuit (GEC) can help in understanding the electrical environment of the earth's atmosphere. This approach can provide a good framework for exploring interconnections and coupling of various regions of the atmosphere. It can also provide information on the solar-terrestrial weather relationship and offers possibilities for exploring one of the traditional scientific problems, namely, that of associating changes in surface weather with the solar output (Herman and Goldberg 1978). Thunderstorms are electrical generators whose global activity provides a current output that maintains a vertical potential difference between the ground and ionosphere. The GEC links the electric field and currents flowing in the lower atmosphere, the ionosphere and the magnetosphere. Measurements of atmospheric electrical parameters will prove handy for any integrated approach involving all these regions. Long-term measurements would be considered useful for addressing some of the problems associated with global change.

1.2 Climate-global circuit interaction

A modern motivation for the study of atmospheric electricity is to determine what extent the global electric circuit is a forcing effect on climate. The global circuit provides a physical link between solar and geophysical change with the Earth's climate, through the effect of the air-Earth current density on cloud microphysics, although further research is required to understand the exact mechanisms involved. Evaluating the importance of this link requires detailed observations, analysis and modeling of electrical properties. Global thunderstorm and shower cloud activity are

considered the primary source of the global circuit. A feedback of the global circuit-climate interaction exists as increased global surface temperature is expected to cause an increase in convection and therefore global thunderstorm activity (Williams, 1992), with associated enhancements of the global circuit. Measurement of the intensity of this circuit may therefore provide insight into global climate change (Markson, 2007), providing the only method of global climate monitoring to use a single point on the Earths surface.

Atmospheric electrical quantities are sensitive to aerosol. If the electrical parameters are known for a site, information on the aerosol concentration can be retrieved (although further research is required to quantify the electrical-aerosol relationships sufficiently for general acceptance by the scientific community). As highlighted by the International Panel on Climate Change (IPCC) a large contribution (~±50%) of the uncertainty in the radiative forcing of climate models is due to inadequate knowledge in the areas of chemical and microphysical properties of anthropogenic aerosol and their interaction with cloud, as well as their geographical and vertical distribution (IPCC Working Group I Report, 1995). Measurement of atmospheric electricity may provide a further method of studying global aerosol profiles as well as improving the understanding of aerosol-cloud interactions, as the charge associated with atmospheric electrical processes is expected to modify aerosol-cloud microphysics and affect the formation of clouds. Although satellite and surface-based optical methods of aerosol profile retrievals provide estimates of aerosol radiative properties, they do not provide information on the ultra fine particle spectrum, unlike atmospheric electrical methods.

A general motivation for study of the global circuit is therefore a better understanding of the extent of climate forcing through interaction of the air-Earth current density with cloud microphysics (Harrison, 2004c). In order that this can be achieved, detailed measurements of surface electrical parameters and how they can be used to monitor the global circuit are required. The variability of these parameters results from local and global sources, so it is crucial that a method of separation of these sources is found. The objectives of this project are to provide detailed measurements of surface atmospheric electrical parameters for analysis, and separate their observed variability into that due to local and global sources.

1.3 Ions

The existence of ions in the atmosphere is the fundamental reason for atmospheric electricity. An absence of ions would mean zero electric field in the atmosphere and most probably no thunderstorms or lightning. The concept of positive and negative ions as charge carriers in the atmosphere was first put forward by J. Elster and H. Geitel (1899) in order to explain the electric conductivity of air. Much work has since been done on ions and their role in atmospheric electric phenomena. Today we know there are mainly three classes of ions, namely small ions, intermediate ions and large ions. Most important are the small ions since their higher mobility allows them to take a more active part in the transfer of charge throughout the atmosphere. The mobility of ions can be measured in meters per second per volt per meter which signifies the velocity that an ion will reach when subjected to an electric field of one volt per meter. For small ions the mobility is of the order of 0.0001 with a slight edge of the negative ion over its positive counterpart. In fact, the negative to positive mobility ratio of small ions is about 1.25 (Wåhlin 1985) which is

a paradox since negative ions are believed to be more massive than positive ions. One explanation (Papoular, 1965) is that for part of its lifetime a negative ion is really an electron jumping from molecule to molecule. Molecules such as NO and NO2 are believed to dominate the negative small ion population while oxonium and water might make up the positive small ions in the atmosphere. Their true molecular structure and mass are not well known because it is difficult to get spectroscopic mass analysis of small ions in the lower atmosphere. The problem is their relative short life time, about 100 seconds, which is much shorter than the transit time required for molecules or ions to reach the source end of a mass analyser.

The ionization in the lower atmosphere is mostly caused by cosmic rays and natural radioactivity. Ions are also produced in and near thunderclouds by lightning and corona processes. Cosmic rays originate from solar flares and other galactic objects such as supernovas and exploding stars. One interesting thought is; do stellar events affect our lives here on earth? We know that cosmic rays are by far the major ion producers in the lower atmosphere and if thunderstorms need ions to feed on in order to charge, we certainly would not have thunderstorms if there were no cosmic rays. Ancient man would not have had access to fires and the many thousands deaths each year from lightning strokes would have been avoided. Cosmic rays originate from deep space and usually consist of very high-velocity atoms that have been stripped of their orbiting electrons. There are also electrons present in space that travel with near-light velocities, but such particles are usually absorbed at very high altitudes in the earth's atmosphere. However, heavy cosmic rays penetrate the atmosphere quite far and often reach the earth's surface. During such an encounter numerous secondary electrons are produced (electron showers) along its track from

ionizing collisions with atmospheric molecules. The secondary electrons in turn might ionize a fair amount of molecules themselves before they slow down and attach themselves to atmospheric molecules to form negative ions. The average production rate at sea level is about ten million ion pairs per cubic meter per second. However, the average ion population at any given time is nearly one hundred times more, and ion mobility with altitude as air gets thinner has a drastic effect on the electric structure of the atmosphere. Typical conductivity data as a function of altitude are shown in Fig. 1.2 The conductivity is the inverse of specific resistance and is usually measured with a Gerdien cylinder (Gerdien 1905).

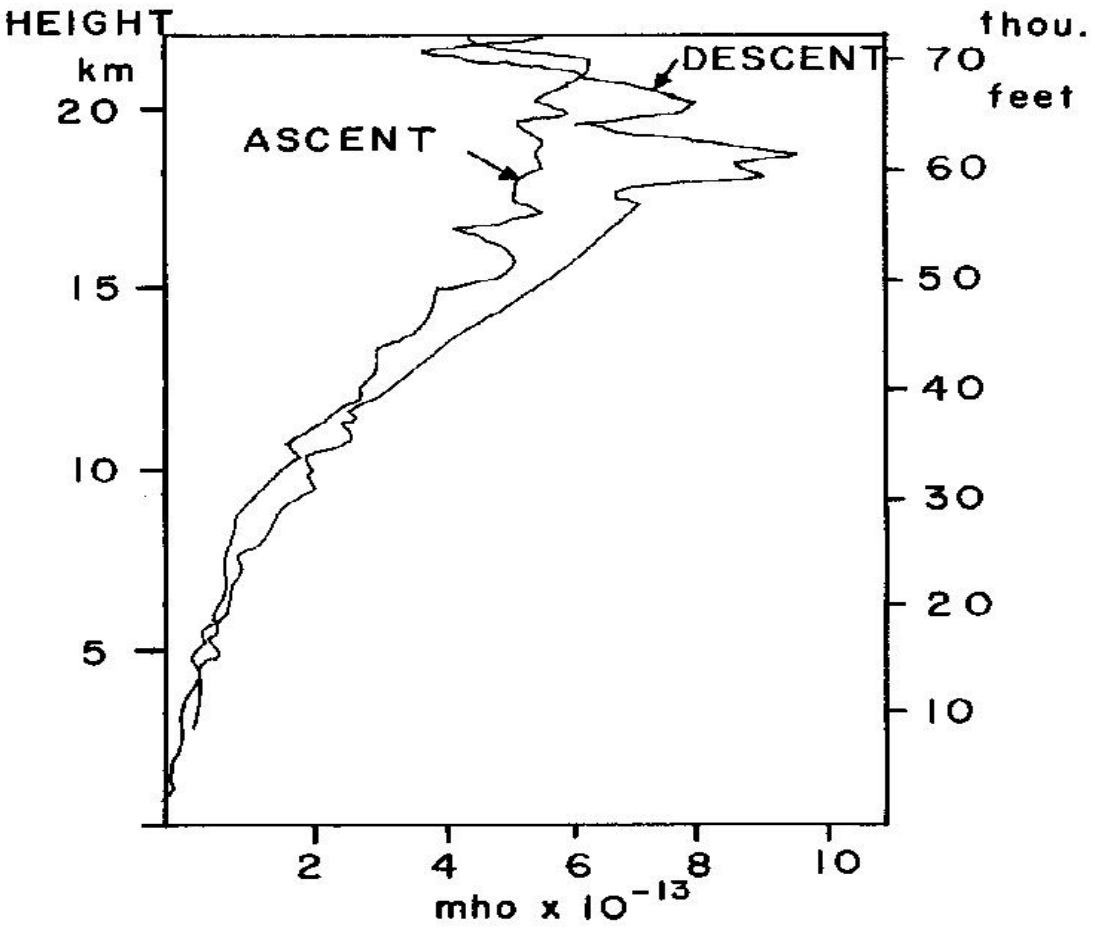

Fig. 1.2 Conductivity as a function of altitude (Rocket data).

1.4 The global atmospheric electric circuit

Harrison (2004c) provides details on all aspects of the global electrical circuit, including historical instrumentation, observations and the proposed connection with climate. Thunderstorms and shower clouds cause separation of electric charge between the ground and ionosphere, an electrically conductive layer about 60km above the surface (the term electrically conductive layer refers to a layer with sufficiently high conductivity compared to the lower (tropospheric) atmosphere to be considered a perfect conductor). This charge separation causes the ionosphere to have a potential (V_I) of approximately +300kV with respect to the surface. Ionisation from cosmic rays and terrestrial sources produce cluster ions (small ions) which make the atmosphere weakly electrically conductive. These ions flow vertically because of the vertical potential difference, causing the air-Earth conduction current density, J_C, of order 10^{-12} Am^{-2}. The total electrical resistance for a unit area of the atmospheric column from the surface to the ionosphere is called the columnar resistance, R_C. A schematic of the global circuit is given in Figure 1.3. The ionosphere-earth potential difference (V_I), columnar resistance and conduction current are related by Ohms law,

$$V_I = J_C \times R_C$$

The physical units of R_C are Ωm^2. V_I represents the electric potential of a layer at a height above the surface (the zero potential reference) so the units are in volts (usually quoted in kV). At the surface, the PG arises because of J_C flowing through the electrically conductive air. It is therefore J_C that is the parameter that permits the effect of the global circuit to be measured at the surface, either directly through

measurement of J_C itself, or by PG. However, PG is also a function of the local air conductivity (σ). Away from sources of charge separation, the air conductivity (σ), electric field (E) and conduction current density are related by Ohm's Law:

$$J = \sigma E$$

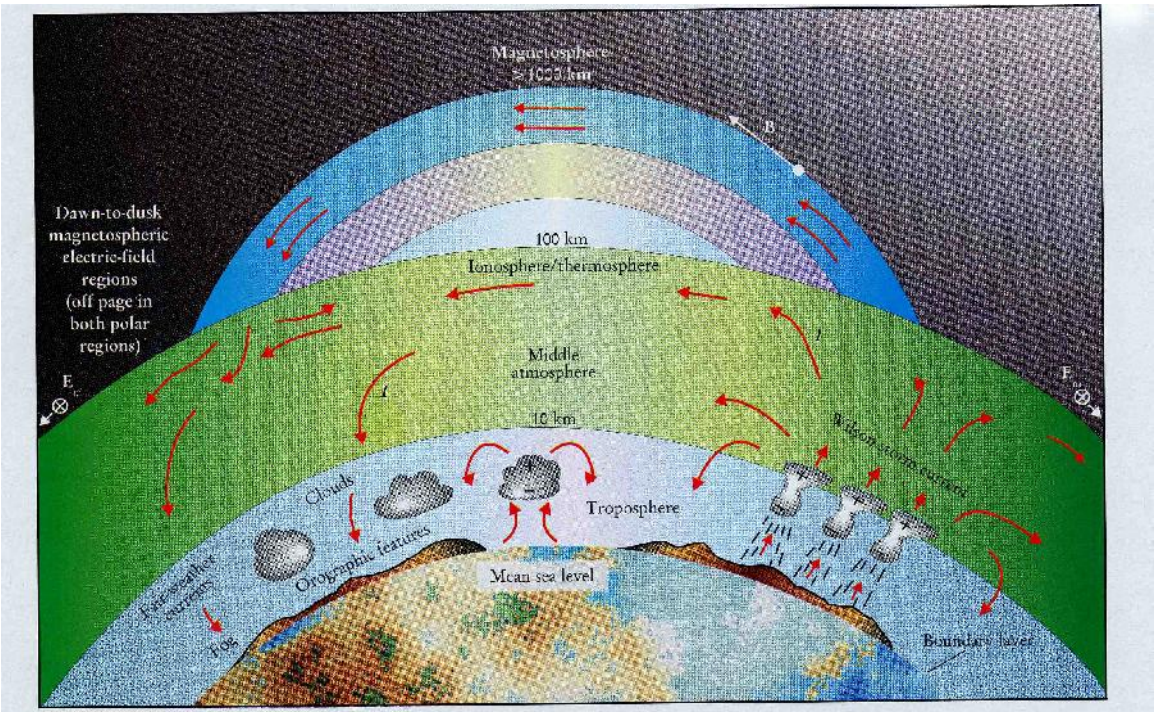

Fig. 1.3 Schematic diagram of GEC

The atmosphere is positively charged with respect to the ground during fair weather. This produces a downward pointing (negative) electric field (E) so PG is positive for fair weather conditions. In the fair-weather part of the circuit, small ions dominate the charge transport since they have a large electrical mobility. Therefore an increase in small ion concentration will increase the air conductivity by providing more charge carriers. Aerosol in the atmosphere removes small ions by attachment. An increase in aerosol number concentration therefore reduces the ion number concentration and decreases the air conductivity. A change in aerosol number

concentration subsequently modifies the total columnar resistance (R_C) between the ionosphere and the surface.

1.5 Measurement of current density

Of the quantities which can be measured at the surface, the air-Earth conduction current density (J_C) presents one of the most fundamental parameters of the global circuit (Chalmers, 1967). It is therefore of great importance in this study, with its continuous measurement being one of the aims of this thesis. A positive current density occurs when positive charge is moved downward. The conduction current density is one of several components contributing to the total current density, J_S, received by a horizontal conducting electrode at the earth's surface, electrically isolated from the ground. J_S comprises contributions from turbulence J_T, conduction J_C, displacement J_D and precipitation J_P,

$$J_S = J_C + J_{Dis} + J_T + J_P + Jpt + J_L$$

where J_C is the component flowing as a result of the global electric circuit (Rycroft et al. 2000). Here displacement current density (J_{Dis}) is induced by changes in the PG. Jpt is the point discharge current, the turbulent current density (J_T) arises due to the transport of space charge by air turbulence. Charged precipitation falling on the electrode will also transfer a precipitation charge, J_P. Current due to lightning is J_L, The current density is considered positive if positive charge is brought from the atmosphere to the surface (or electrode to surface in the case of J_D). J_C is the contribution to J_S arising from the global atmospheric electric circuit.. J_P is of course confined only to times of falling precipitation. A description of instrumentation to

measure J_C (when the J_T and J_P components are negligible), and the methods used to separate J_D and J_C from the directly measured J_S are discussed in Chapters 6.

1.5.1 The conduction current

As already mentioned, the atmosphere is weakly conducting and the earth's electric potential or field must cause a current to flow in the atmosphere. Since there is an excess of positive ions residing in the atmosphere and an opposite negative charge bound on the earth's surface, charge must flow to earth in the form of a positive ion current. Direct measurements of electric currents in the atmosphere are difficult if not impossible. Therefore, ion current values at different altitudes are almost always computed indirectly from conductivity and electric field data by the use of Ohm's law. Direct current measurements can be made, however, at ground level by isolating a portion of the earth's surface and measure the charge collected over a given time. Several methods can be used (Wilson 1906, 1916, Thompson 1910, and Kasemir 1951) but in almost all cases the indirect current gives a value often twice as large as the direct method (Lutz 1939, Israel 1954). Whipple (1932) pointed out that the discrepancy in currents can be explained by the fact that there is always convection and eddy diffusion in the atmosphere which will mechanically move charges upwards in the atmosphere thus generating a mechanical or convection current in the opposite direction of the leakage current (the Austauch generator). As later explained, the question whether or not the convection and leakage current on the average are equal is crucial to the electrochemical charging theory and is a problem which has not yet been settled. From direct current measurements it is possible to estimate the total fairweather current over the whole earth to be nearly 2000 amperes which corresponds to a current density of about 3 $X10^{-12}$ amperes per square meter.

Other charge transfer mechanisms in the atmosphere of importance are point discharges, precipitation currents and lightning discharges.

1.5.2 Point discharge current

It is difficult to determine the total charge brought to the earth's surface by means of point discharge currents under electrified clouds. Wormell (1930) has made some estimates from the amount of charge brought down by a single point over a period of 4 years. He made a guess that the total point discharge current around the world brings negative charge to the surface at a rate of about 1500 amperes which would supply about 75% of the total fairweather leakage current. Other investigators give slightly lower values for the average point discharge current but not less than 25% of the fairweather current. The source of point discharge currents are the electrified clouds which of course also bring charge to ground by lightning. The point discharge current is, to a certain extent, canceled by the large amount of positive lightning flashes to ground and through positive charge reaching the earth's surface by precipitation.

1.5.3 Precipitation current

The electricity associated with precipitation has played an important role in atmospheric research due to the belief that charging of precipitation particles in some way must relate to whatever charging mechanism is active in clouds. Paradoxically, this is not always true because the final charge on a cloud drop is determined in the space between the cloud base and ground and is usually of opposite sign to the charge

of the cloud base where it came from. This peculiar phenomenon is called the mirror-image effect and is demonstrated in Fig. 1.4 by the two curves which show the change in electric field strength and amount of precipitation charge reaching the earth's surface as a function of time.

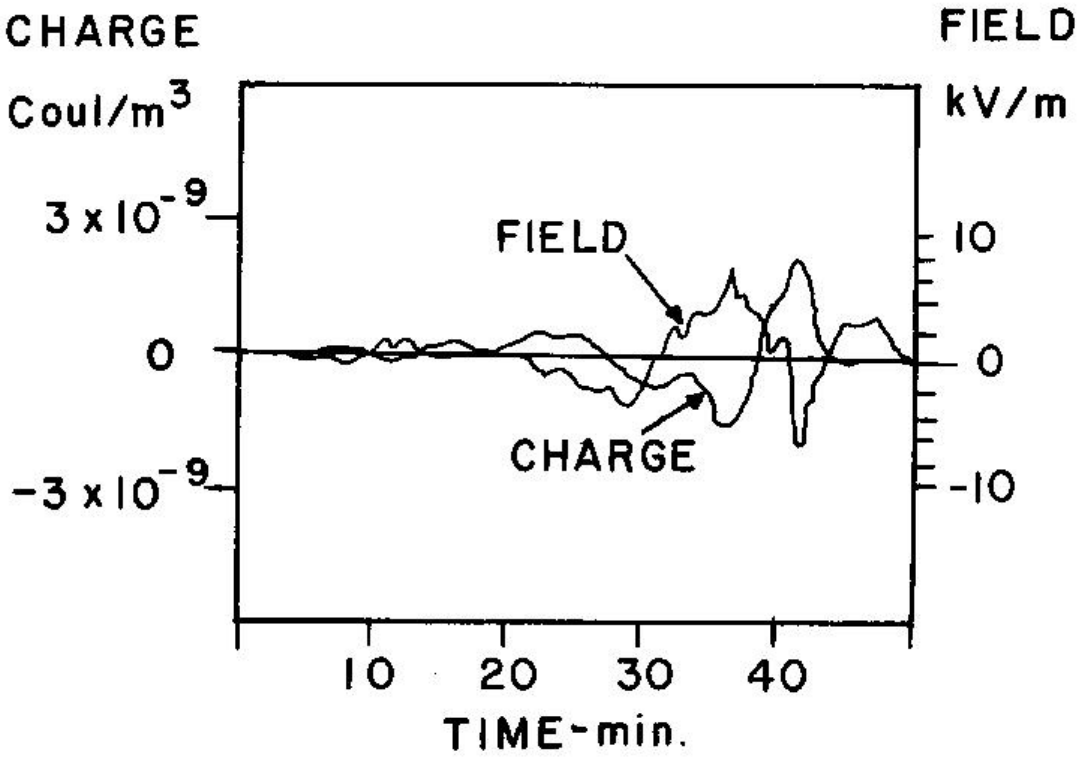

Fig. 1.4 The mirror-image effect.

One can easily see that when the electric field goes negative (negative charge in the cloud base) the precipitation current becomes positive and vice versa. As pointed out by Chalmers, a drop must take several minutes to fall from the cloud base to ground. Since the precipitation charge changes with the potential gradient below

the cloud, it must mean that the drops also obtain their final charge below the cloud or very near ground. The electrochemical charging process can possibly explain the mirror-image effect if one assumes that the positive to negative ion concentration ratio near ground is affected by the strong electric field under the cloud. For example, a positive charge on the earth's surface, caused by a strong negative cloud charge above, would attract and remove part of the negative ion population near the surface. The result would be a higher than normal positive to negative ion concentration ratio at lower levels. When the positive to negative ion ratio exceeds 1.2 a positive cloud charge above would reverse the effect because drops now fall through an environment containing a higher negative to positive ion concentration ratio which will generate negative electrochemical charges on their surfaces. Other explanations of the mirror-image effect take the Wilson charging mechanism into consideration. This charging mechanism is based on the idea that rain drops become electrically polarized when immersed in an electric field such as under an electrified cloud. A negative cloud charge above will induce a positive charge on the top surface of a drop and the bottom surface will acquire a negative charge induced by the positive charge on the earth's surface. The total net charge on the drop, however, would remain zero. As the drop falls through the ionized region below a cloud it would preferentially sweep up positive ions by its negatively-charged bottom. Calculations, however, show that the Wilson mechanism is too feeble to account for the amounts of charge normally collected by drops. In contrast to rain, precipitation currents carried to ground by snow are usually always negative under potential gradients between ±800 V/m (Chalmers 1956). The total precipitation current around the earth is estimated to be about +340 amperes.

1.5.4 Lightning current

The charge brought to earth by lightning is estimated to average -340 amperes which would cancel the precipitation current. It must be remembered that a mean current of -340 amperes represents the excess of negative charge over positive charge reaching ground by lightning and that the ratio of negative to positive ground strokes equals about 10:1. The average current in a negative lightning stroke to ground is about 25,000 amperes but the total charge averages is only 25 coulomb. Positive ground strokes usually carry as much as 10 times more charge and current than do negative strokes although they are outnumbered by 10:1. The ratio of negative to positive ground strokes seems to vary with global location. It is believed that about 2,000 thunderstorms are active at one time around the earth which amounts to a total number of 50,000 thunderstorms per day.

1.6 The fairweather electric field

The fairweather electric field discovered by Lemonnier and Beccaria is almost entirely due to the excess of positive ions over negative ions in the atmosphere. The fairweather field is best understood if we assume that the earth's surface has absorbed a certain number of negative ions from the atmospheric ion pair population. It will create a slight excess of negative charge on the earth's surface with an equal excess of opposite charge in the form of positive ions left behind in the atmosphere. If we imagine that each captured charge on the earth's surface will produce an electric field line which must terminate on a positive excess ion left behind in the atmosphere one obtains a fairly accurate picture of the electric fairweather field in the atmosphere. The excess positive ions are more or less uniformly mixed in the lower 3 km of the

atmosphere which, to the meteorologist, is known as the "Austauch" or mixing region. The mixing is produced by convection and eddy-diffusion and the ionic distribution follows the mixing patterns of other constituents in the atmosphere such as radon for example. Radon is a radioactive gas emitted by the earth's surface and is constantly released into the atmosphere**.** The radon profiles are obtained from airborne radioactive counters that detect the daughter products of the decaying radon gas. The number of field lines per unit surface area produced by the positive charge or space charge above the earth's surface is also a measure of the electric field strength. Obviously the electric field strength reaches a maximum at the earth's surface since it contains the largest number of field lines per unit area. The average field strength at the earth's surface is on the average 100 volts per meter and decreases to less than 10 volts per meter at an altitude of 3 km. If one integrates the electric field as a function of altitude one obtains the total potential difference V_I at different heights. A typical value of V_I at 3 km is 200 kV with respect to the earth's surface. The total charge Q on the earth's surface is

$$Q = AE\,\varepsilon_0$$

where A is the surface area of the Earth, E the electric field strength at the surface and ε_0 the permittivity of free space ($\varepsilon_0 = 8.85 \times 10^{-12}$ Farad m^{-1}). The total energy of the fairweather field is

$$W = 1/2\,VQ$$

Fig. 1.5 shows the total electric energy, charge and potential in the atmosphere as a function of altitude. More than 90% of the energy is confined to an altitude below 3

km which together with the charge distribution curve seems to indicate that convection and eddy diffusion play a predominant part in the distribution of the fair-weather electric field and that the bulk of its energy is distributed throughout the mixing region by the so called "Austauch Generator" (Kasemir 1950).

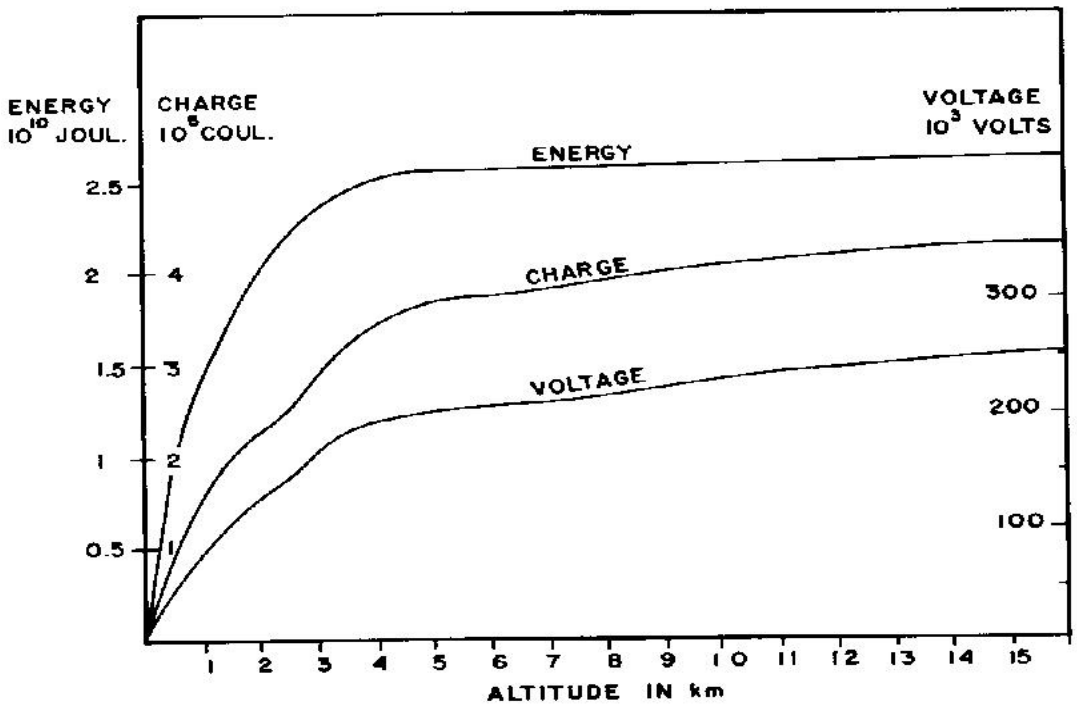

Fig. 1.5 Electric energy, charge and potential vs. altitude.

One crucial question still remains to be answered. What causes the positive space charge in the atmosphere and how is the opposite negative charge maintained on the earth's surface?

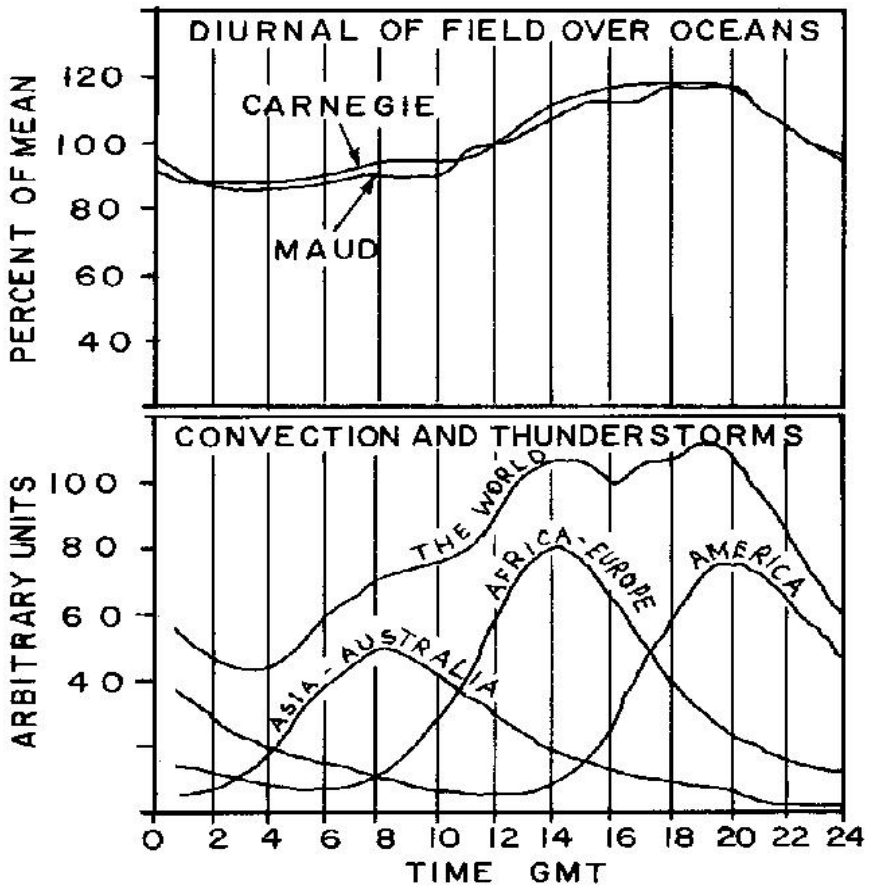

Fig. 1.6 Diurnal variations in the fairweather field compared to world-wide Convection

Thunderstorms around the world are believed to charge the earth-atmosphere system (Wilson 1929), which considers the electrochemical effect as a charging mechanism where negative atmospheric ions are preferentially captured by the earth's surface leaving a space charge of positive ions behind in the surrounding atmosphere. Both theories might be supported by the evidence of a small systematic diurnal variation in the fairweather field, which is believed to be related to the world-wide atmospheric convection activity. The effect was first discovered in Lappland 1905 by Simpson whose findings were later augmented by Hoffmann (1923) and Mauchly (1923). The effect is illustrated in Fig. 1.6 where the average variation in the world-

wide potential gradient is compared to the estimated world-wide convection activity at different times of day (by GMT). The top graph shows the global variations in the electric field measured at sea in the absence of local disturbances such as pollution, fog, etc. The top graph seems to coincide with the lower graph which gives an estimate of the world-wide convection activity produced by the heat of the sun during a diurnal period. The steady convection over oceans, however, is thought to smooth out the electric field variations as is evident from the top graph. Before discussing the electrochemical and global thunderstorm circuits as possible generators of the fairweather field, it is necessary to examine the global leakage current and its implications.

1.7 Thesis structure

In this thesis chapter 2 provides the conceptual origins and measurement of the global atmospheric electric circuit. Chapter 3 deals with Instrumentation used in this work. Chapter 4, 5 and 6 present surface observation of atmospheric electrical parameters at equatorial station Triunelveli (including local effect and global circuit). Influence of upper atmospheric electric generators on GEC and separation of different atmospheric currents discussed in chapter. 6. Conclusions and suggestions for further work resulting from this study are summarized in chapter 7.

CHAPTER 2

Conceptual origins and measurement of the global atmospheric electric circuit

2.1 Introduction

The scientific study of atmospheric electricity began in the 18th century, with investigation into the electrical nature of thunderstorms such as that famously undertaken by Benjamin Franklin, producing a spark from his aerial apparatus in 1750. Realisation that the atmosphere was electrified even in fair weather was made by the French botanist and physicist L.G. Le Monnier (Watson, 1746) who reproduced Franklin's experiment with an aerial in 1752 (although he removed the grounding pole from the aerial and placed some dust particles near the apparatus to investigate electrostatic attraction). This positive atmospheric charge was also found by John Canton in 1753. Le Monnier later went on to demonstrate the clear-sky electrification of the atmosphere and the diurnal variation of atmospheric electricity, by observing changes in the electrostatic attraction of a suspended wire insulated from the ground and exposed to the atmosphere. The English physicist Benjamin Wilson visited Le Monnier in Paris in 1753, who stated in a letter to the President of the Royal Society:

The regular diurnal variation of electric field found by Le Monnier was also found by the Italian physicist Giambatista Beccaria, (Beccaria, 1775). An advocate of the scientific ideas of Benjamin Franklin, Beccaria determined that the atmosphere was positively charged with respect to the Earth during fair weather in 1775. Ten years later the French physicist Charles Coulomb discovered that atmospheric air was

not a perfect electrical insulator as previously thought, but was in fact weakly conductive. Unfortunately however, this aspect of his work was ignored at the time.

In the 1860s William Thomson (later Lord Kelvin) invented the water-dropping discharger (Thompson, 1910). With this instrument it was possible to transport charge induced by an insulated tube in equilibrium with the atmosphere on water droplets from a reservoir, being collected by a metal funnel that was connected to an electrometer. That way charge could be measured from a collector whilst still being electrically isolated from the ground, allowing the atmospheric potential (and therefore electric field, given a further reference potential) to be determined. Kelvin recognized the necessity for regular recordings of atmospheric electricity, preferably simultaneously at different locations in the study of atmospheric electricity, following what was described by Kelvin as the "incessant" recordings by Beccaria a century before (Thomson, 1859). Almost fifty years later, C.T.R. Wilson developed a method to measure the air-earth conduction current density (J_C) at the surface in Kew Observatory, London (Wilson, 1906). By this time the presence of ions in the air was known and the Wilson instrument could also measure total air conductivity (σ) and potential gradient (PG) simultaneously, as described in detail by Harrison and Ingram (2005). This invention permitted the beginning of regular measurements of all three major variables in atmospheric electricity in the United Kingdom: air-earth current density, potential gradient and air conductivity. In addition to knowledge that natural radioactivity had sources in the ground that ionized the air, a balloon flight in 1912 by Austrian physicist Victor Hess carrying an ionization chamber demonstrated that ionization rate actually increased with height (after an initial decrease), demonstrating that the ground was not the only source of ionization (Hess, 1912). The extra-terrestrial source of this ionization was determined to be cosmic radiation, with

ionization rate increasing with height as the absorbing mass of atmosphere above decreased. The cosmic origins that produced an increased ion production rate (and therefore air conductivity) with height offered an explanation in addition to decreased aerosol concentration with height for the results from previous balloon flights measuring atmospheric electrical parameters (e.g. Gerdien, 1905a, 1905b), that noticed an increase in conductivity and decrease in potential gradient with height.

2.2 The Carnegie cruises 1915-1921 (cruises 4, 5 and 6)

The research vessel Carnegie was built in New York for the Carnegie Institution of Washington, USA with the purpose of scientific investigation and logging of geomagnetic and atmospheric electrical phenomena throughout the world's oceans. It was a sailing ship constructed out of wood or, if wood was not possible, non-magnetic metal (to prevent local magnetic distortion). Indeed, even the crew's cutlery was made from Mexican silver (Bunker, 1982). The ship was nearly 48m long, weighed 323 Tons and robust enough to withstand heavy seas. After 20 years of successful deployment, the Carnegie tragically caught fire during the seventh global cruise in 1929: it was not replaced. Of the many new discoveries during the cruises, the Carnegie showed the global presence of "penetrating radiation" (now known to be produced by cosmic rays), of approximately uniform intensity at the surface (Fleming, 1949), although a variation with geomagnetic latitude was present (Aplin et al. 2005). In confirmation of the earlier discovery by Hess (1912) it was shown from air and sea-water radioactivity measurements that penetrating (cosmic) radiation could not be attributed to any known source from within the oceans (Fleming, 1949). It was noted that no significant variation of PG with small-scale position was found at sea (unlike on land) with an average PG of about $130 Vm^{-1}$ (Fleming, 1949). However, PG was

found to be about 10 percent less in low latitudes than in high latitudes, or even up to 20 percent allowing for observed annual change in PG (Fleming, 1949). This annual variation is likely to be due to changes in local air conductivity since although PG had an annual variation, the average air-earth current (found as a product of PG and total air conductivity) was found to be nearly constant (Fleming, 1949).

2.2.1 Cruise geographical details

The Carnegie surveyed all oceans from 80°N to 60°S, covering a distance of nearly 480,000 kilometers over 7 cruises (Fleming, 1949). The three longest, most instrumented cruises were IV, V and VI, details of their tracks are as follows.

Cruise IV

The ship began cruise IV from Brooklyn on 6 March 1915. The first stop was Hawaii, followed by Alaska (60°N) then New Zealand. From New Zealand the Carnegie began a four-month circumnavigation of the globe, generally confined to between 50°S and 60°S. After reaching New Zealand again, the ship traveled clockwise near the Pacific Rim, past Japan, before arriving at San Francisco in September 1916. The final leg of the cruise was down the western coast of North and South America, round Cape Horn and concluding the cruise in Buenos Aires on 2 February 1917.

Cruise V

The Carnegie set sail from Buenos Aires on 4 December 1917. The route went round Cape Horn and up the western coast of South America, through the Panama Canal and ending at Washington, USA on 10 June 1918.

Cruise VI

From Washington on 9 October 1919, the Carnegie began a global circumnavigation cruise, confined mostly between 40°N and 40°S, arriving back in Washington on 10 November 1921.

2.2.2 Overview of measurements made during cruises IV-VI

The instruments on board the Carnegie were refined and improved for cruises IV, V and VI but remained essentially the same as the preceding cruises, with observational procedure and skill also improving with time (Mauchly,1926). The atmospheric electrical instruments measured PG, small ion number concentration and mobility (both polarities), air conductivity (both polarities), “penetrating” (gamma) radiation and terrestrial (beta/alpha) radiation. The conduction current density was determined indirectly using PG and total air conductivity.

Mauchly (1926) stated that each instrument for all the cruises showed considerable variation even under ideal conditions and even with the same observer. This was thought to be due to a lack of appreciation of the importance of contact potential effects and the adequate screening of all connections against inductive effects. Despite this, it was found that accuracy (compared to the calibration equipment) better than 5 percent was possible during the voyages for all the measurements, assuming normal precautions were observed. However, with an electrometer of suitable sensitivity and a more highly refined 10-observation technique, probable errors in the atmospheric electrical measurements could be reduced to about 1 percent (Mauchly, 1926).

2.2.3 Diurnal variation of the potential gradient measured by the Carnegie

Perhaps the most significant finding of the Carnegie cruises for the study of atmospheric electricity was that of the mean diurnal variation of PG away from the polluted continents. Despite limitations when the PG could be accurately measured (involving the orientation of the ship's boom and mainsail) and correction factors that needed to be made even for ideal boom and sail positions (Mauchly, 1926), a characteristic diurnal cycle emerged that would later from the standard for diurnal variation of the global atmospheric electric circuit. This average variation is shown in Figure 2.1, for cruises 4-6.

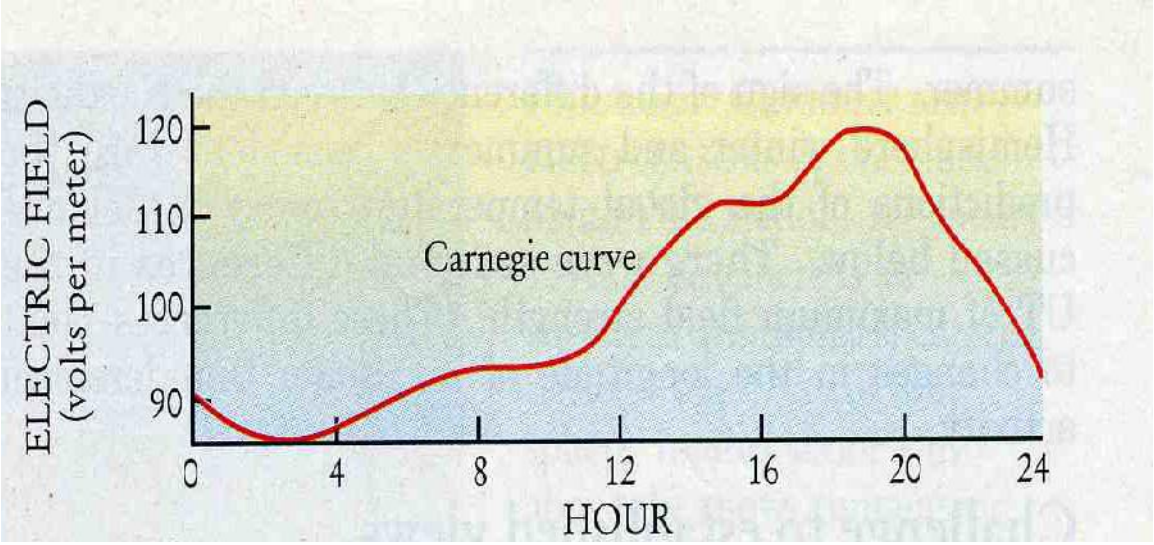

Fig. 2.1 Average diurnal variation of the electric field measured on cruises 4, 5 and 6 time in UT hrs

2.3 The origin of the global circuit concept

It was Wilson (1906) who proposed that the air-earth current (and consequent potential gradient) had its source in “wet weather” areas, and flowed large distances in the conductive upper atmosphere to areas of fair weather as a conduction current,

produced from the movement of free ions due to the potential difference (of order 100,000V) between the surface and upper atmosphere. Wilson even theorized an effect of aerosol on the circuit (Wilson, 1906). It was these "showers of the appropriate kind" that act as batteries to the global atmospheric electrical circuit. By the late 1920s there was gathering evidence that the diurnal variation of potential gradient with respect to Universal Time was similar for stations throughout the world, especially at unpolluted sites such as during the oceanographic cruises of the Carnegie. Evidence for the universal diurnal variation of potential gradient was first published by S.J. Mauchly from observations made on board the Carnegie, as shown in Figure 2.1 (Mauchly, 1921).

With the establishment of a global network of meteorological stations it became possible to compare the diurnal variation reported by Mauchly (1921) with the diurnal cycle of global thunderstorm activity. This was first investigated by Whipple (1929) who compared the diurnal variation of thunderstorm area and assumptions about the typical storm occurrence in local time and the frequency of oceanic storms, with the Carnegie, Maud, Arctic and Antarctic diurnal variation of potential gradient (Figure 2.2). There appeared to be good agreement, with the minima and maxima of both curves occurring at approximately the same time, thereby strongly supporting the Wilson theory of a global circuit (Whipple, 1929). However, this conclusion ignored shower clouds and other areas of disturbed weather, since thunderstorms were expected to be the main, but not only, mechanism for powering the global circuit. Harrison (2004c) extrapolated the linear fit between PG from the Carnegie curve and thunderstorm area and found that the intercept on the PG axis was

non-zero, demonstrating that thunderstorm activity accounted for most, but not all, of the Carnegie PG variation.

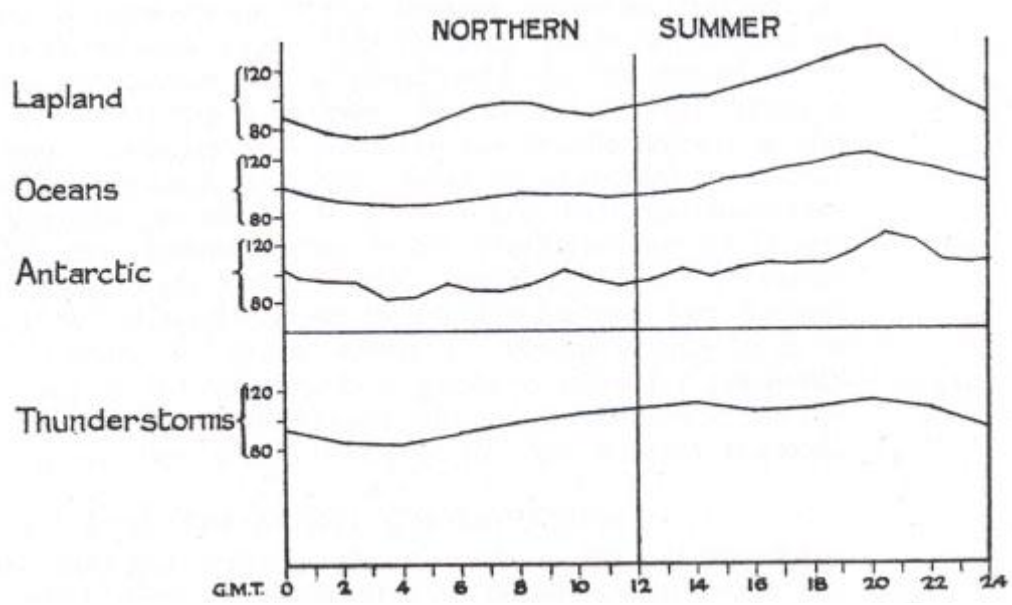

Figure 2.2 Comparison between average diurnal PG cycles from clean-air sites and estimated global thunderstorm area diurnal variation for the Northern Hemisphere summer, as a percentage of the mean from Whipple (1929).

Despite the close agreement between global thunderstorm area and diurnal variation of PG, the Wilson theory was not universally accepted, with leading authorities on atmospheric electricity of the time such as G.C. Simpson remaining to be convinced that there was any physical support to Wilson's hypothesis (Whipple, 1929). As the source of the fair weather PG is the air-Earth conduction current density (J_C), the Carnegie curve would also be expected to be observed in the diurnal variation of J_C during times of negligible variability in columnar resistance (R_C). Such a similarity of J_C diurnal variation to the Carnegie curve has indeed been reported (e.g. Cobb (1967), Anderson (1969), Retalis (1991), Isrealsson and Tammet (2001)).

2.4 Evidence for the global atmospheric electric circuit concept

The theory of Wilson's global atmospheric electrical circuit concept is still regarded as the best explanation for the global variation of PG and J_C, due to the increasing weight of observations in agreement with the main principles of the theory, the details of which will be discussed in this section.

2.4.1 Columnar Resistance

During fair weather (away from any local sources of charge separation), the conduction current density J_C is related only to the ionospheric potential V_I and columnar resistance R_C. Since J_C is the most fundamental parameter of the global circuit measurable from the surface due to it being largely unaffected by local surface conditions (e.g. Dolezalek, 1978), it offers the best method of global circuit monitoring. For this, the variation of R_C must either be known or assumed to be negligible for the diurnal variation of J_C to represent the strength of the global circuit via ionospheric charging by global thunderstorm activity. It is therefore of significant importance to investigate changes in R_C at all timescales and under different conditions.

One of the principal components to the Wilson theory of a global electric circuit is that of the large but finite electrical resistance between the ionosphere and surface. This resistance, termed the columnar resistance, R_C, by Gish (1944) can be determined experimentally by measuring the vertical profile of total air conductivity. This was first done using the stratospheric balloon flight of *Explorer II* in 1935 (Gish, 1944), obtaining a columnar resistance of the order $100 P\Omega m^{-2}$ (Sagalyn and Faucher, 1954). The relative contribution of the atmosphere to this columnar resistance was

strongly height dependent, with Sagalyn and Faucher (1954) reporting columnar resistances of between 90-250PΩm^{-2}, of which 40-73% originated from the surface boundary layer. These observations have been used to explain the large air-earth current densities found at the summit of mountains (e.g. Kasemir, 1951 reported a J_C of up to ten times higher than at sea level) where the mass of atmosphere above is less (and generally cleaner).

The first investigation of the diurnal variation of R_C was made by Sagalyn and Faucher (1956) using equipment carried by balloons to measure the total conductivity profile from the surface to 4.57 km (Figure 2.3). The shape of the profile was demonstrated to be a function of the height of the boundary layer, with the upward transport of aerosols by turbulent mixing around midday increasing the total aerosol number concentration in the column and hence R_C. The shape of the curve and the 40% daily variation are in approximate agreement with modern estimation of the diurnal variation of boundary layer turbulence (Hoppel et al., 1986).

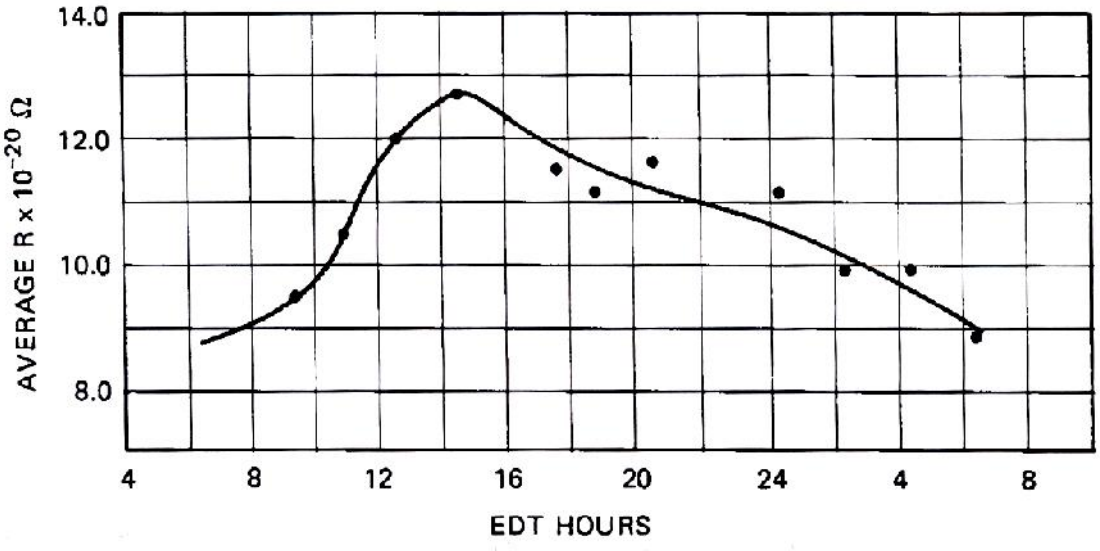

Figure 2.3 Average diurnal variation of R_C of a 1cm^2 column from the surface to 4.57km with local time (from Sagalyn and Faucher, 1956).

Tropospheric balloon flights measuring negative conductivity between 1957-1962 were used to calculate the seasonal variation in R_C near Tokyo, Japan (Uchikawa, 1972). It was found that a distinct seasonal variation existed, being proportionally greater in the winter (December) than the summer (June). However, no seasonal variation was found over the Hachijojima, an island in the Pacific Ocean, 200km south of Tokyo, making the clean-air site more suitable for assessing seasonal variation of V_I using measurements of J_C as any seasonal variation would be attributed to V_I alone. The difference between these two results may be attributed to the greater influence of air pollution near Tokyo than at Hachijojima, as aerosol removes small ions in the column by attachment, increasing R_C. The seasonal variation in R_C over Tokyo varied in the opposite sense to the air-earth current density calculated in the stratosphere by the balloon soundings, but only half the relative amplitude. This difference in variations of R_C and current density was approximately equal to the variation in V_I observed in Weissenau, Germany, thereby suggesting an Ohmic relationship (Uchikawa, 1972).

The Ohmic assumption between J_C and V_I was used more recently by Harrison (2005b) to calculate R_C using coincident J_C data from the Wilson apparatus at Kew, London and V_I soundings from Weissenau. The R_C over Kew varied between ~50 to 400PΩm^{-2}. The reason for this variability was not straightforward, with cosmic ray-induced aerosol formation being a suggested factor. A method of remotely detecting the total number of cluster ions in the atmospheric column using infrared absorption was investigated by Aplin and McPheat (2005). Remote sensing of total number of ions in the atmospheric column could provide a method of measuring R_C, providing

appropriate assumptions about the vertical distribution of the ions and the ion mobility vertical profile are made.

2.4.2 Source of the global circuit

More work was done on the source term of the global circuit by Krumm (1962) who reinvestigated the relationship between global thunderstorm area and the Carnegie curve using more modern and extensive data (from the 1956 World Meteorological Organisation thunder days dataset) than available during the first investigation by Whipple (1929). Although the variation found by Krumm (Figure 2.5) appears to have a similar minima time as the Carnegie curve (Figure 2.1), the maximum number of global thunderstorms appears to be at a sooner time than that found by Whipple (Figure 2.6) and the Carnegie curve, although an offset between thunderstorm area and the Carnegie was also acknowledged by Whipple.

Reasons for this discrepancy between the Whipple (1929) and Krumm (1962) analyses seem to be due to the inclusion of oceanic data with a maximum of around 13 UT (unlike Whipple who included no maximum time for oceanic storms) and the similar maximum amount of Asian/American storms used by Krumm (Figure 2.5), with Whipple using a lower occurrence of Asian storms relative to American, although conversely, the annual global thunder days used by Krumm (Figure 2.4) still appear to imply a greater occurrence of American storms. The differences between Whipple and Krumm's thunderstorm estimations are likely to be a result of improved spatial representative of global thunderstorm occurrence due to a longer recording history of more frequent and reliable meteorological stations in 1959 than those available to Whipple in 1929. It is therefore of interest that the departure of estimated

global thunderstorm area produced by Krumm (1962) from the Carnegie curve is greater than that of Whipple (1929). The discrepancy between the calculated thunderstorm areas of Krumm (1962) and Whipple (1929) was discussed by Dolezalek (1972) where concern was expressed over the lack of more recent evidence supporting the close correlation between global thunderstorm area and the Carnegie curve as suggested by Whipple (1929). Due to this lack of modern evidence, Dolezalek (1972) states that:

"…It is obvious that the assessment of the global thunderstorm activity is the weakest point in our attempts to understand the global circuit…"

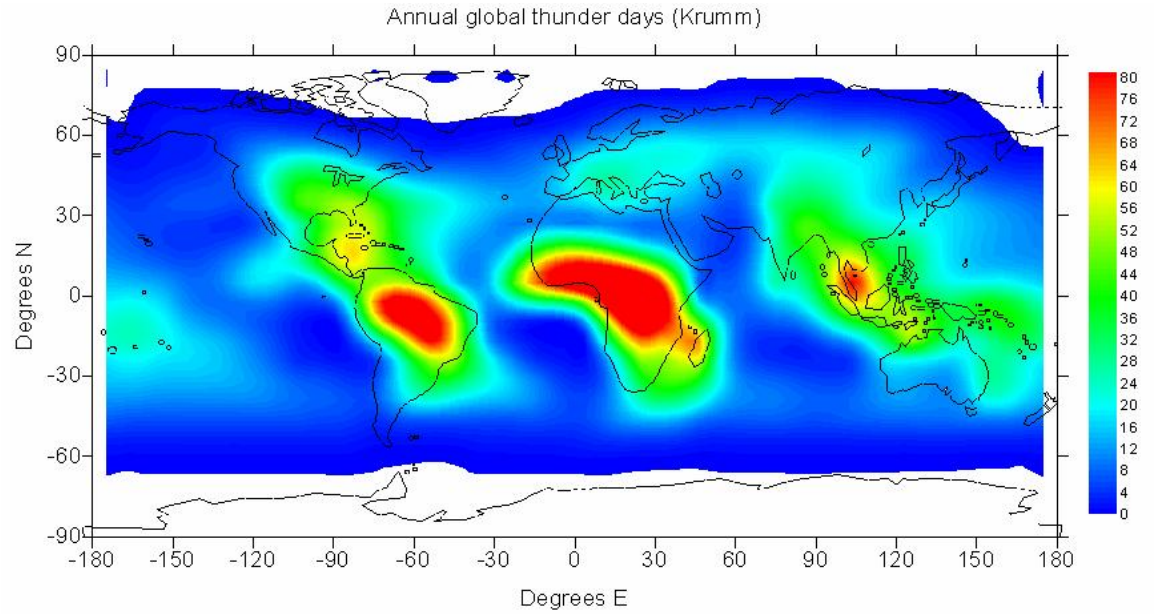

Figure 2.4 Global thunderstorm frequency as measured by the annual number of days when thunder was heard using the WMO 1956 dataset (adapted from Krumm, 1962).

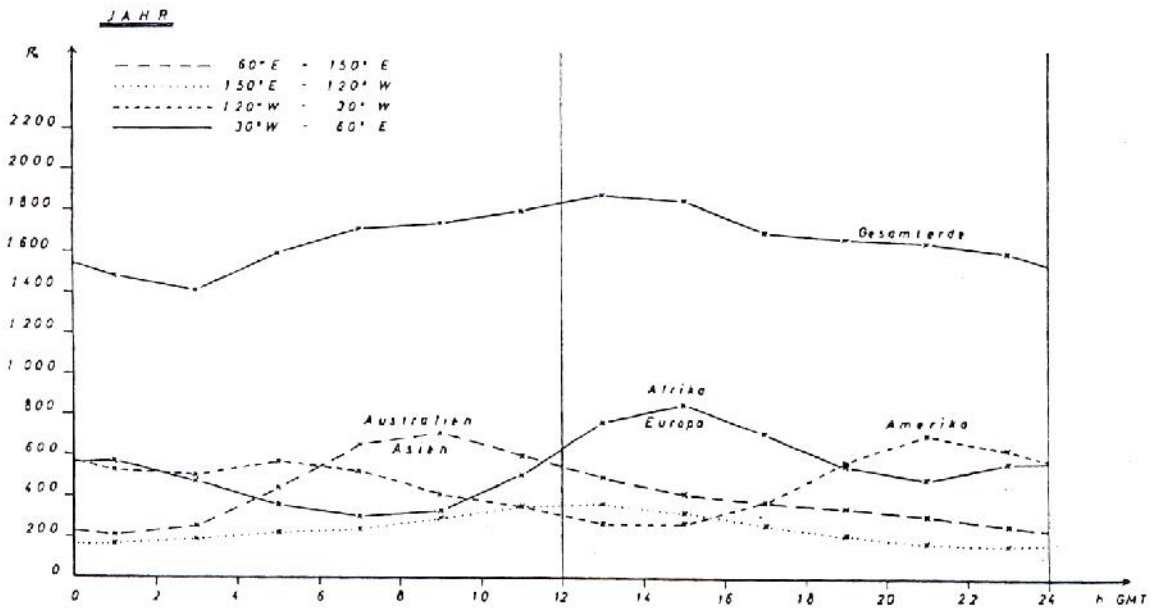

Figure 2.5 Estimated global (top line) and regional (Asia/Australia, Africa/Europe, America and Ocean (lowest line)) mean number of thunderstorms at 2-hour intervals in Universal Time from Krumm (1962).

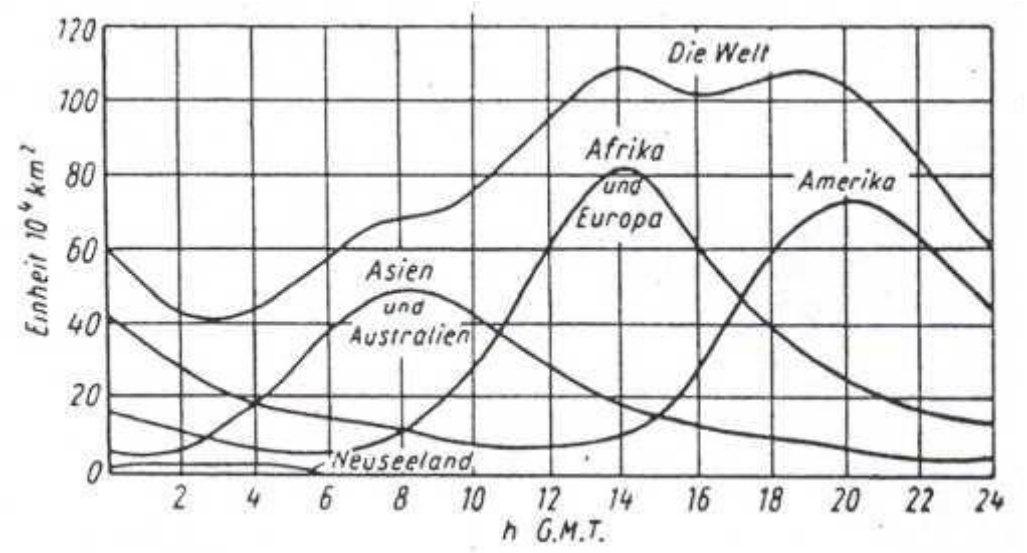

Figure 2.6 Diurnal variation of thunderstorm area over the entire world (top line) and major land regions calculated by Whipple (1929) from Krumm (1962).

Dolezalek (1972) does not, however, dispute the observed uniform global diurnal cycle of (clean-air) PG and J_C. Dolezalek (1972) suggests that the air-earth current density was the "safest" surface parameter for investigating the diurnal cycle of the global circuit, with thunderstorm numbers being the most tenuous. Reasons suggested are due partly to the questionable accuracy and limited density of global thunderstorm observations at the time and also the unproven assumption of a linear proportionality between thunderstorm area and ionospheric charging, or that this charging rate does not vary with the geographical source of the thunderstorm generators. As was then suggested by other researchers (e.g. Kasemir, 1972) that long term monitoring of ELF or VLF (extremely and very low radio frequency respectively) intensity generated by global lightning activity, especially in Polar regions, would provide a more reliable (and in near-real time) method of determining the global thunderstorm activity than meteorological statistics in order to further investigate this fundamental aspect of the global circuit theory. The technique of using ELF measurements in the Antarctic and Greenland as a means of global circuit monitoring was investigated by Füllekrug et al. (1999). A remarkably close correlation in both shape and phase between the mean diurnal variation of the ELF magnetic field intensity and the surface PG at the South Pole during December 1992 was found. However, correlations between hourly values of ELF and PG were low, suggesting the presence of local variations in PG at hourly timescales. From the ELF and PG comparison, Füllekrug et al. (1999) estimated that global cloud-to-ground lightning activity contributed to ~40±10% of the strength of the atmospheric electric field.

It has always been noted (e.g. Wilson, 1906 and Kasemir, 1972) that mechanisms other than just global thunderstorm activity may be responsible for modulation of the global circuit, such as shower clouds. A more recent investigation of the possible contribution of shower clouds on the global electric circuit (as originally hypothesised by Wilson, 1906) has been discussed by Williams and Sátori (2004), suggesting a significant contribution of electrified shower clouds in South America. Mechanisms for charge separation within thunderstorms have been investigated recently by Bürgesser et al. (2006), with the importance of rapid convective updrafts and the presence of mixed-phase cloud hydrometeors shown.

2.4.3 Modern measurements of the global circuit

The use of instrumented aircraft to study the worldwide variations in atmospheric electricity was seen as the most promising technique by Anderson (1967), who also criticized the lack of "care and effort" employed by aircraft campaigns in the past. In particular, Anderson (1967) states that surface-based instrumentation is subject to too much local variation caused by the turbulent motion of space charge, terrain and electrode layers, even for "exotically placed" instrumentation. Instrumented aircraft measuring both potential gradient and air conductivity in order that J_C could be derived and flying over a large body of water during fair-weather conditions was suggested to be the most reliable method of monitoring the global circuit, with a collection of such measurements suggested to be able to provide the "final" answer to the source(s) and variability of the global atmospheric electrical circuit (Anderson, 1967).

Continuing the initiative of using J_C measured indirectly by aircraft to study variation of the global circuit, Anderson compared measurements of the mean UT diurnal cycle of J_C made in this manner above the Mediterranean and Tasman Seas, although separated by four months (Anderson, 1969). Both diurnal cycles exhibited similar general patterns, although with different emphasis in parts. This was expected to be due to the proximity of the storm group that caused the global variation to the point of observation, such that accentuations of the global pattern due to storm activity in the same hemisphere would occur, with attenuation of that from further away (Anderson, 1969). A similar result was also reported by Takagi and Masahiro (1972) who found that better correlations between clean-air stations measuring PG were found when the stations were in the same hemisphere. Recently, Kamra et al., (1994) measured the mean PG diurnal variation during a cruise in the Bay of Bengal and obtained a curve with characteristics dominated more by the contribution of local (Asian) thunderstorms than seen in the typical Carnegie curve. This implies that although thunderstorm activity encompasses entire globe as expected by the Wilson theory, the signal does attenuate with distance from source to point of observation, particularly when crossing the equator. An attenuated global signal is likely to be overpowered by local sources of variability.

Aircraft measurements were later used by Markson (1976) to calculate the mean diurnal variation of V_I from profiles of PG, to further investigate the global circuit hypothesis. This percentage variation was shown to agree well with the Carnegie curve (correlation coefficient of 0.96) as expected from the Wilson theory if R_C remained constant, which was likely as measurements were conducted over the ocean. In addition, a comparison between PG using an aircraft at constant altitude

over the Bahamas and J_C measured near-simultaneously by an aircraft over the Gulf of Alaska. The same Carnegie curve-type variation was apparent at both sites, adding confidence to the global circuit hypothesis (Markson, 1976). Similar trends in coincident ionospheric potential measurements, as well as surface PG have also been reported (Harrison, 2005b). Additionally, it was suggested by Markson (1976) that aircraft measurements were capable of recording temporal variation of V_I with a resolution of minutes, which as not possible with ground instrumentation. This was presumably due to the improved signal-to-noise ratio for measurements above the boundary layer and the reduced electrical relaxation time in the mid-upper troposphere, allowing more rapid coupling between the airborne measurements and the Ionosphere. Interestingly, Markson commented that the overall average of 120 V_I soundings was lower than estimates made 10-20 years earlier, suggesting a possible decrease in the strength of the global circuit with time (Markson, 1976). However, the effect of nuclear weapons testing in the 1960s may have had an influence on this, an effect mentioned earlier by Uchikawa (1972). It is also noted during research in the 1970s that despite the term "ionospheric potential" V_I the majority of this potential is reached within the troposphere (in accordance with the majority of columnar resistance, R_C) as illustrated by Israelsson (1978) who found the diurnal variation of V_I (using radiosonde ascents) to be of a similar appearance to the Carnegie curve as expected, with the potential at the top of the tropopause being 88% (standard deviation of 9%) of the assumed V_I (by extrapolation) based on 24 soundings. This finding illustrates the importance of the troposphere, and therefore meteorological processes, in the global atmospheric electrical circuit, as well as the significant meteorological influence on local atmospheric electrical parameters, especially during high static stability in the boundary layer (Israelsson, 1978). However, it is quite

possible that meteorological phenomena either directly or indirectly affect ionosphere even at altitudes such as the F2-layer (Rishbeth, 2006).

More recent investigations of the global circuit diurnal and seasonal variation have been made by Burns et al. (2005). In this paper, the mean diurnal and seasonal variation of PG measured in Antarctica between 1998-2002 was analyzed. It is evident that the diurnal variation was very much like that of the Carnegie curve, although even in Antarctica, local influences such as wind speed and blowing snow were still evident under certain meteorological conditions. Seasonal trends in this diurnal cycle were also observed, such as a reduction in the diurnal range (as a % of the mean) in May-June (29% variation) compared to November-December (59%) as well as seasonal changes to the curve shape, expected to be due to changes in the location of main global thunderstorm activity. Although suggestive of seasonal variation in the global circuit, the authors advise that care should be taken when considering the global generators as the only source of this variation in PG due to the relative sparseness of fair-weather measurements around the time of the November-December minimum and the influence of local meteorological conditions on the measurements (Burns et al, 2005). Due to the cross-polar cap potential, a model must be used to account for this influence on surface atmospheric electrical effects, which would also have possibility of introducing errors. It was also emphasized that measurement of the air-earth conduction current density (J_C) would potentially provide more reliable measurements of the global circuit as they are less influenced by changes in local air conductivity than the PG (Burns et al., 2005), especially as significant seasonal variation of air conductivity at the South Pole occurs (Reddell et al., 2004). A list of preferred measurements and locations for global circuit

monitoring is given by Märcz and Harrison (2005), which states that V_I is the primary quantity of interest, followed by J_C then PG in oceanic, mountain, continental rural and finally urban air.

The advent of modern, satellite-based instrumentation suitable for monitoring lightning flashes (both day and night) has allowed a detailed investigation of the link between diurnal variation of global lightning activity and that of the global circuit as seen by the Carnegie curve. Using data from the OTD (Optical Transient Detector, based on sensors originally designed for the detection of atmospheric nuclear explosions) between April 1995 and March 2000 Nickolaenko et al. (2006) produced a map of the global distribution of lightning activity (Figure 2.7).

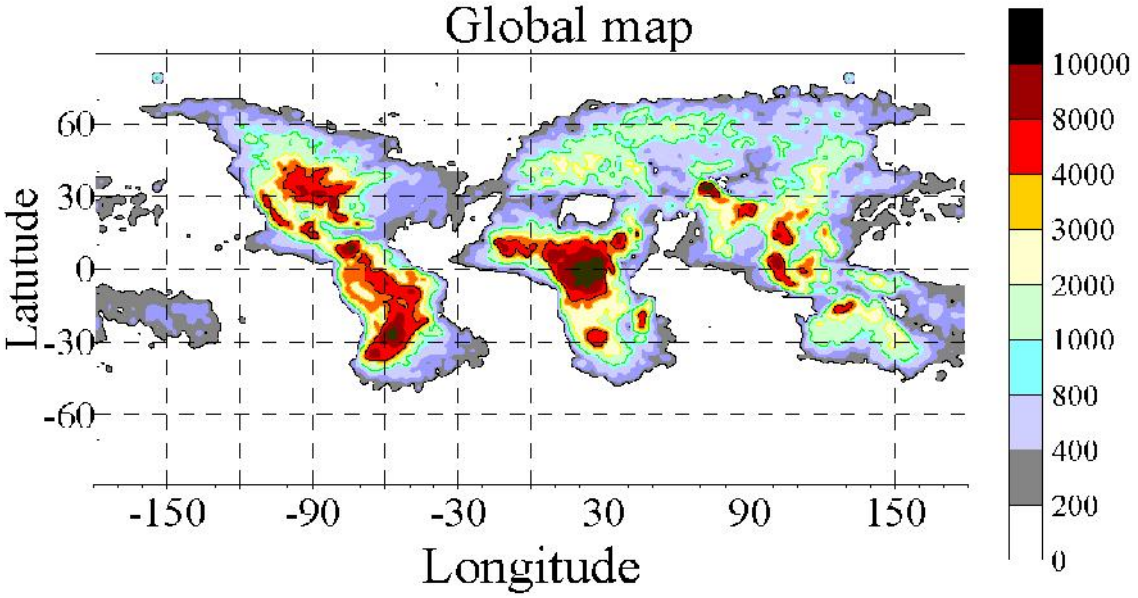

Figure 2.7 Cumulative global lightning flash frequency per 2.5° grid box

In summary, it is clear that observations made throughout the 100 years since the concept of a global atmospheric electrical circuit (Wilson, 1906) continue to support its hypothesis. Perhaps the greatest uncertainly lies in quantitative connection between global thunderstorm activity and ionospheric potential (Dolezalek, 1972) as

well as the physical mechanisms of charge separation and transport to the upper atmosphere, although the recent discovery of upward plasma discharges from the tops of thunderstorms (e.g. “Sprites”) are likely to provide clues to this missing link. The attenuation of this thunderstorm signal as it passes along the ionosphere has been noticed (Anderson (1969), Takagi and Masahiro (1972) and Kamra et al., 1994), offering further insights into the interactions present in this circuit. Despite the increasing evidence, further research and suitably dense networks of good quality and simultaneous monitoring of J_C, PG, air conductivity and preferably V_I and R_C via radiosondes or other vertical profiling as well as global thunderstorm activity are required for more conclusive proof of the Wilson (1906) global electric circuit theory.

2.5 Solar activity and the global circuit

The total electrical resistance of the global circuit is determined by the amount of small ions, which are mostly produced by cosmic radiation. Therefore any process that modulates the strength of cosmic radiation below the ionosphere will also effect the global circuit. As the activity of the Sun increases (such as during the peak of the 11-year cycle) so too does its magnetic field. This magnetic field diverts galactic cosmic rays from the Earth, causing a decrease in the ionisation of the atmosphere and subsequent increase in R_C. Shorter period solar activity can also produce variation of the solar field strength and therefore the intensity of galactic cosmic rays reaching the Earth’s atmosphere. Coronal Mass Ejection (CME) causes a rapid decrease in the observed galactic cosmic rays reaching Earth a few days after the event due to the enhanced magnetic field carried by the solar wind (called a Forbush decrease) thereby increasing R_C. However, a solar flare event will cause an increase in cosmic ray

intensity originating from the Sun itself (solar cosmic rays) that will enhance the ionisation of the Earth's atmosphere and decrease R_C.

The air-earth conduction current density, J_C, is a function of both V_I and R_C so any change in cosmic radiation that alters R_C will consequently be observed in J_C at the surface, for a given V_I. Of course, R_C varies naturally at timescales of hours to seasons with changes in the aerosol vertical profile, so if modulation by cosmic ray changes is to be observed, the observation site must be unpolluted so that variation of R_C due to aerosol is kept to a minimum. This criterion makes remote sites such as oceanic or polar stations best suited to monitor changes in the global circuit from solar activity (although the effects are believed to be latitude dependent as will be discussed later). However, for the case of polar sites, the cross-polar cap potential (a horizontal potential difference between the nocturnal and daylight sides of the ionosphere), makes changes in cross-polar ionospheric potential unrepresentative of global variation and a model is required to account for this additional (non-global circuit) source of V_I variability. Direct measurements of J_C using an automatic "Wilson-plate" at the relatively unpolluted site of the Pacific Island of Hawaii were made by Cobb (1967). The observations identified an increase of approximately 10% in daily mean J_C (and PG) above their normal values following solar flare events, demonstrating an effect of solar flares on the global circuit. The effect of an individual flare caused an increase of about 5 or 6% with the increase usually lasting lass than a day although the clustered nature of solar flare emissions meant that the cumulative effect of a rapid sequence of flares produces the typical 10% overall increase, visible over the duration of the flare cluster arrivals (Figure 2.8). Short periods of greatly enhanced J_C were also observed following a multiple flare burst, where J_C increased by 75% for a 6-

hour period (Cobb, 1967). A similar increase in J_C and PG after solar flares was also observed at two European mountain top sites (Ogawa, 1985).

Hays and Roble (1979) modeled the effect of a solar flare and Forbush decrease on the total air conductivity at different altitude and latitude (Figure 2.9). The results show an altitude variation parallel to the modeled conductivity profile, of noticeable but reasonably small magnitude compared to the variation of observed profiles. The decrease in conductivity due to the reduction in galactic cosmic rays during a Forbush decrease appears to be approximately equal to the increase in conductivity with increased solar cosmic rays after a solar flare.

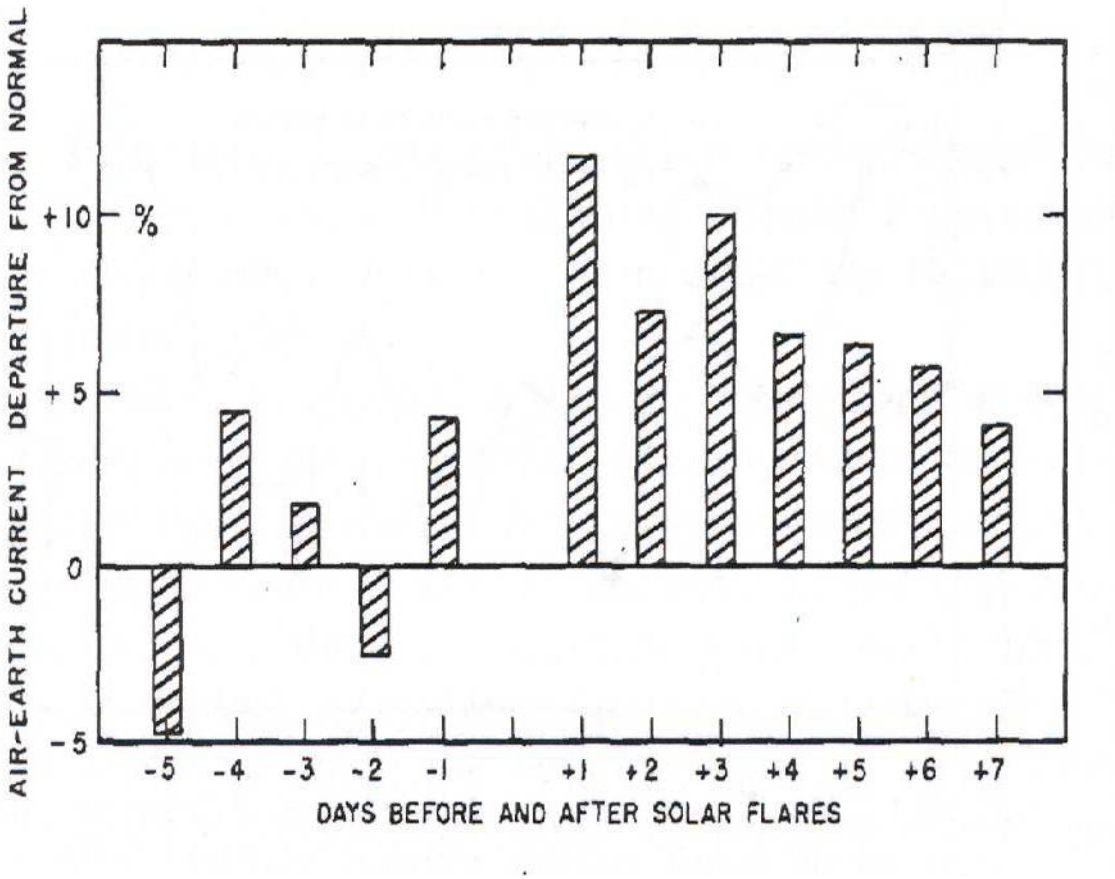

Figure 2.9 Percentage variation of daily mean J_C from the normal due to solar flares observed in Hawaii (Cobb, 1967).

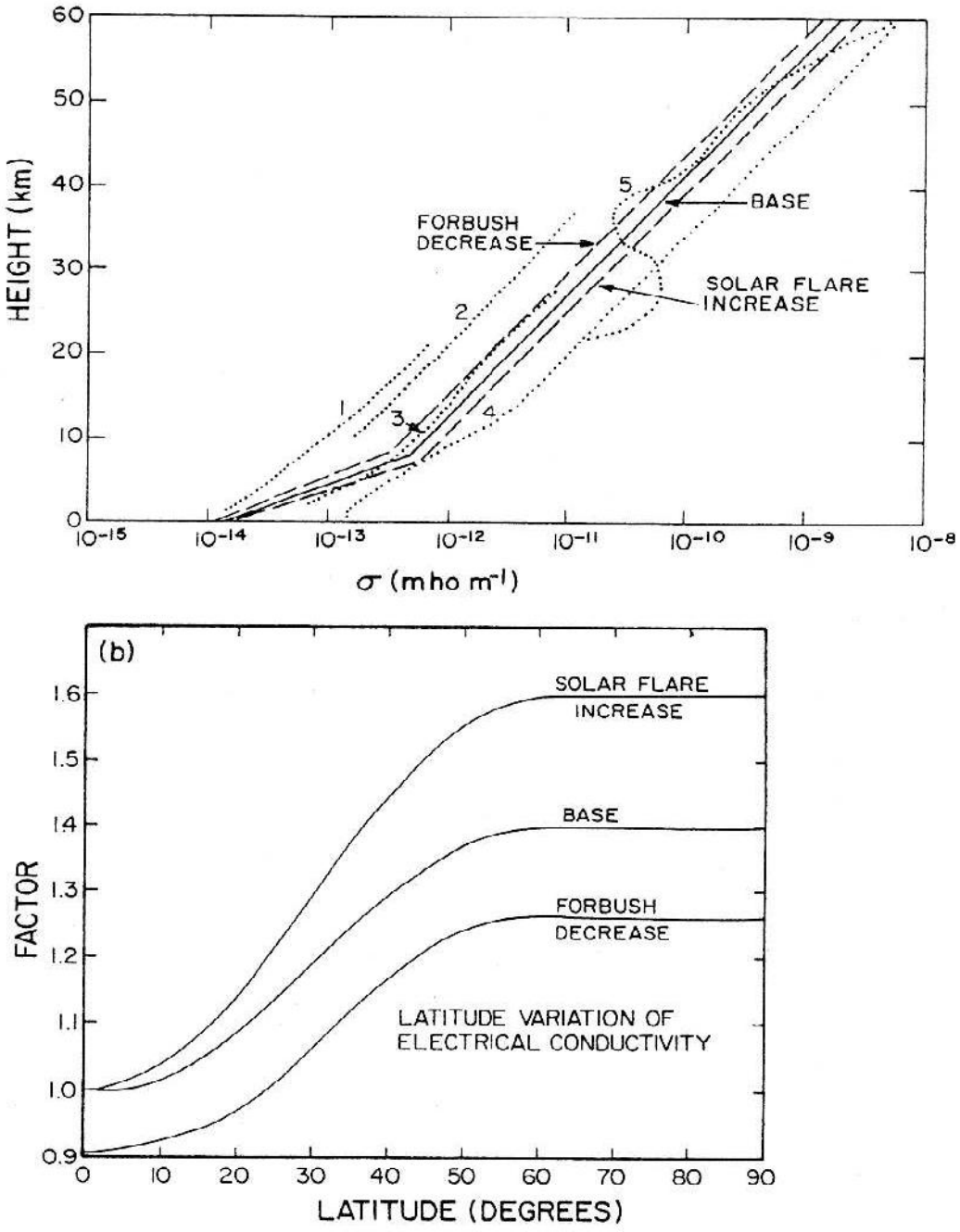

Figure 2.9 The effect of a solar flare and Forbush decrease in air conductivity with (a) altitude and (b) latitude (Hays and Roble, 1979). The numbered lines in (a) represent measured conductivity profiles (see Hays and Roble (1979) for more detail on these observed profiles).

The latitude dependency of the effect of a Forbush decrease and solar flare appears to differ for both magnitude and form. As compared to the natural variation of air conductivity with latitude (base), the model suggests little or no effect of a solar flare in equatorial regions, a larger and more latitude-dependent effect at tropical and extra-tropical regions, and the greatest but latitude-independent effect for high (>60°) latitudes. The reduction in air conductivity due to a Forbush decrease is independent of latitude. It is of note that the approximate 5-6% increase in J_C (and therefore air conductivity via R_C) due to an individual solar flare observed in Hawaii at 20° latitude by Cobb (1967) is in reasonable accordance with the modeled effect of Hays and Roble (1979) for that latitude. Sapkota and Varshneya (1990) produced a more detailed model to investigate the effect of a Forbush decrease on J_C and PG with colatitude. The effect of this decrease was modeled for both altitude dependent and independent assumptions, with a latitudinal dependent change in cosmic ray intensity (between 2-35% global variation) applied to their model, and the effect on surface J_C and PG described. As identified in Figure 2.10 the latitudinal response is quite different for J_C and PG and is more complicated than the earlier model of Hays and Roble (1979) that suggested a latitude-independent decrease of total air conductivity (therefore increase in R_C and decrease in J_C).

The reason for this discrepancy in latitudinal-dependent J_C and PG change between the two models is that the more sophisticated Sapkota and Varshneya (1990) model calculates the perturbation of V_I resulting from the reduction in cosmic ray ionization and the redistribution of R_C with latitude due to the latitude-dependent cosmic ray ionization rate (in turn resulting from the latitudinal variation of the geomagnetic field). For instance, the increase in V_I that results from a Forbush

decrease causes an increased J_C near the equator, as the change in R_C is low (owing to the strong geomagnetic shielding that reduces the cosmic ray intensity). However, at the poles, the increase in R_C outweighs the increase in V_I so causes a decrease in J_C in accordance with Ohm's Law. As PG is a function of both J_C and the local air conductivity (which will also be a function of latitude as the distribution of aerosol is also included in this model) the perturbation with latitude will be different than for J_C alone. More recently, an increase in observed JC after a geomagnetic substorm (such as that initiated by a solar flare) was detected by Belova et al. (2001), even against the background of daily variation. J_C was measured using a long-wire antenna in Sweden during 1998-99. Additionally, the short-period (order minutes) variability of J_C was reported to increase during the geomagnetic storm events in addition to the increase in mean.

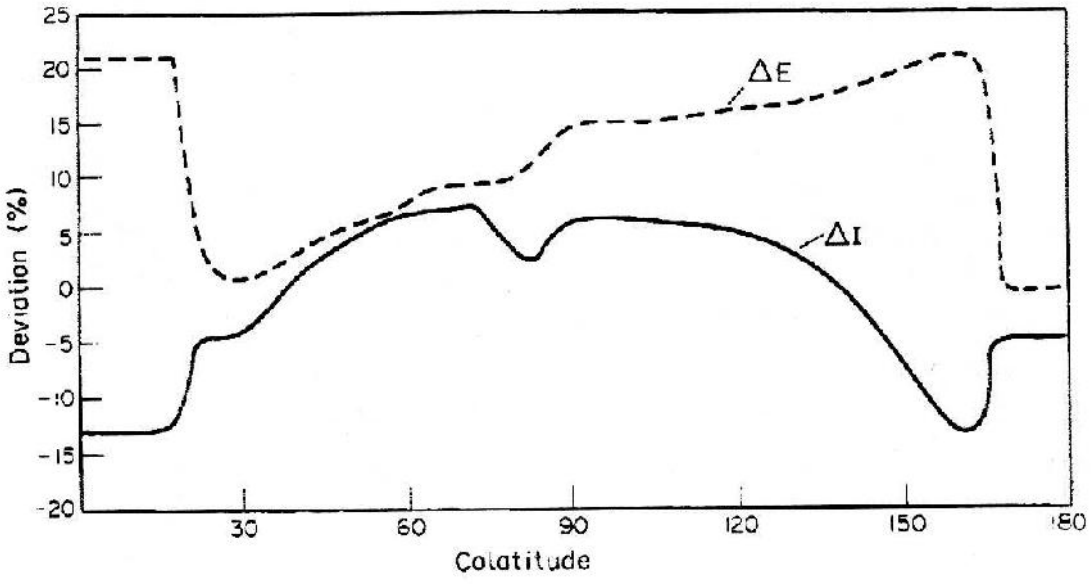

Figure 2.10 Modeled deviation of J_C and PG from the unperturbed condition as a result of the Forbush decrease in cosmic ray ionisation, as a function of colatitude along 72.5°E. (Sapkota and Varshneya, 1990).

Solar influences over long-term (decadal) variation of the global circuit have also been proposed as changes to the solar magnetic field intensity modulate the amount of galactic cosmic rays that enter the Earth's atmosphere, (McCracken et al., 2004) which in turn will modify R_C. This was proposed as a cause of the observed twentieth century secular decrease in the atmospheric electric circuit by Harrison (2002, 2004b) and Märcz and Harrison (2005). However, Harrison (2006a) found no evidence of galactic cosmic ray modulation of more recent surface PG measurements made at Kennedy Space Centre, USA, between 1997 - 2005. As cosmic ray intensity showed little change during this time, the effect may have been unclear in the PG measurements, compared to the longer timescales studied by Harrison (2002, 2004b) and Märcz and Harrison (2005). A change in measured early twentieth-century air conductivity vertical profiles over central Europe was found by Harrison and Bennett (2007a), that was also consistent with a decrease in cosmic ray intensity during this time.

CHAPTER 3

Instrumentation for atmospheric electrical research

3.1 Introduction

The three main atmospheric electrical parameters used for the study of atmospheric electricity at the EGRL are the potential gradient (PG), air-Earth conduction current density (J_C) and total air conductivity (σ). Details of all the instruments used to make these measurements will be given in this chapter. Electrometers used for these instruments designed by us at our electronics laboratory. Of these instruments for the measurement electric potential at a height of one meter, passive antenna system developed by us at EGRL. In this chapter long wire antenna for Maxwell current (long wire antenna), Field Mill (FM) and Electric Field Meter (EFM-100) for electric field, Passive antenna for potential gradient and Gerdian meter for conductivity measurement discussed. Same instruments used at polar station Mairti, Antarctica for this study. Apart from these instruments Wire antenna used for the measurement of air-earth current (conduction current) at Maitri, Antarctica since November 2008.

3.2 Maxwell current (long wire antenna)

There are several methods available for the measurements of atmospheric electrical parameters. An important and the most informative parameter of the global electric circuit is the Maxwell current (Ruhnke, 1965). Ground-based measurements are valuable because they provide continuous long-term recordings. The common ground-based sensors used for current measurements are Wilson plate, the horizontal

long-wire antenna and the spherical shell in the form of two hollow hemispheres. The long-wire antenna is a good alternative since it allows for the suppression of local disturbances by averaging the vertical current over a large area (Tammet *et al.*, 1996). By this technique, the contributions from the convection current can be made minimum. The horizontal long wire antenna, if placed in the atmosphere, will closely follow the electrical current variations of the atmosphere by collecting incoming charges from the atmosphere after the initial net charge on the antenna leaks off. When the antenna is shorted to the ground through a resistor, it will pick up a certain amount of current proportional to the Maxwell current. In the present work we use a long wire antenna of 144 m in length and 3 mm in diameter. The sensor is supported 1 m above the ground by means of masts that are electrically separated by teflon rods as shown in Fig. 3.1.

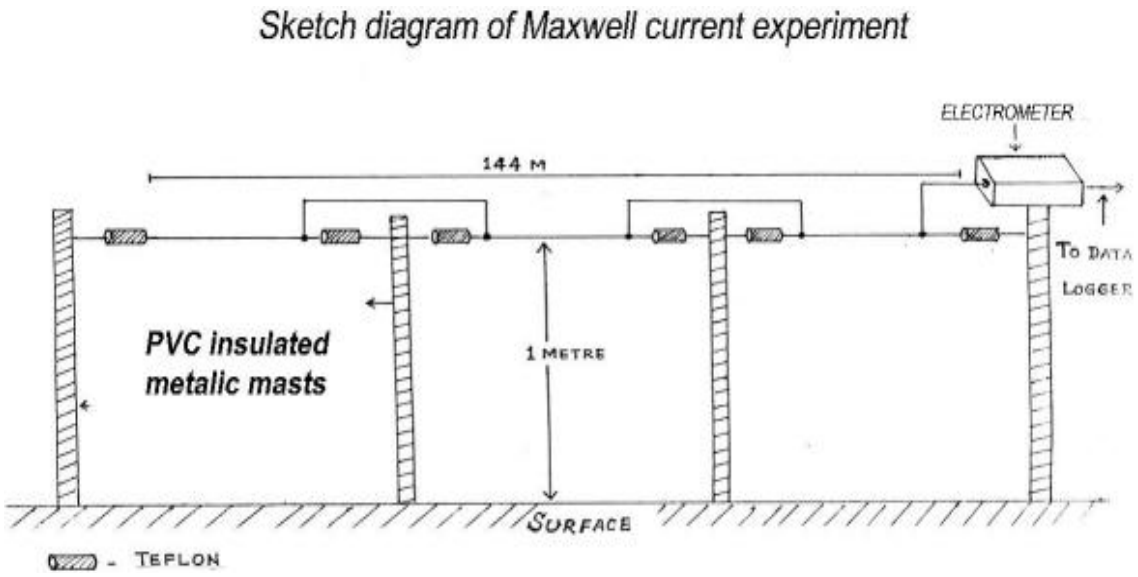

Fig. 3. 1. Sketch of the Maxwell current experiment.

The electrometers were calibrated for their performance at the National Physical Laboratory, New Delhi, India. The calibration curve obtained from this

exercise is shown in Fig. 3. 2. A simple linearity between the input current source and the electrometer output was observed as noticed in Fig. 3.2. The effective area of the present experimental setup using the Kasemir-Ruhnke model (Kasemir and Ruhnke, 1959) is 158.12 m^2 calculated from the formula $(S = hC/\varepsilon_o)$, ε_o being the dielectric constant of air, C is the capacitance of the antenna and h is the height of the antenna above ground. As realized in the recent past, this effective area works well for the displacement current whereas the current flow lines representing the conduction current are not expected to match the electric field lines in the presence of inhomogeneities induced by space charges and convection currents. The static effective area proposed by Tammet *et al.* (1996), which is appropriate for determining conduction current density using long-wire antenna, involves polar conductivity and electric potential.

The sensor is connected to the electrometer (Model AD549) that has high input impedance of the order of 10^9 ohms and permits extremely low input bias current (10^{-14}A). The electrometer converts the current into voltage. The electrometer measures the current in the range of a few picoamperes (pA) to a few nanoamperes (nA) with the high feedback resistance (5×10^9) chosen for this experimental setup. A unity gain operational amplifier (LM308) is connected to the electrometer output signal. The output signals are filtered by a low pass filter with a cut-off period of 1 second (3dB) at the input of an analog-to-digital converter (ADC) that is 100 m away from the preamplifier. The filtered signal is fed to the 12 bit ADC (AD574) with 2.44 mV resolution which is mounted inside the personal computer (PC). The PC records the signal at a sampling interval of one second. The hourly averaging of the data

samples carried out during the analysis stage further eliminates any short-period variations in the measured current.

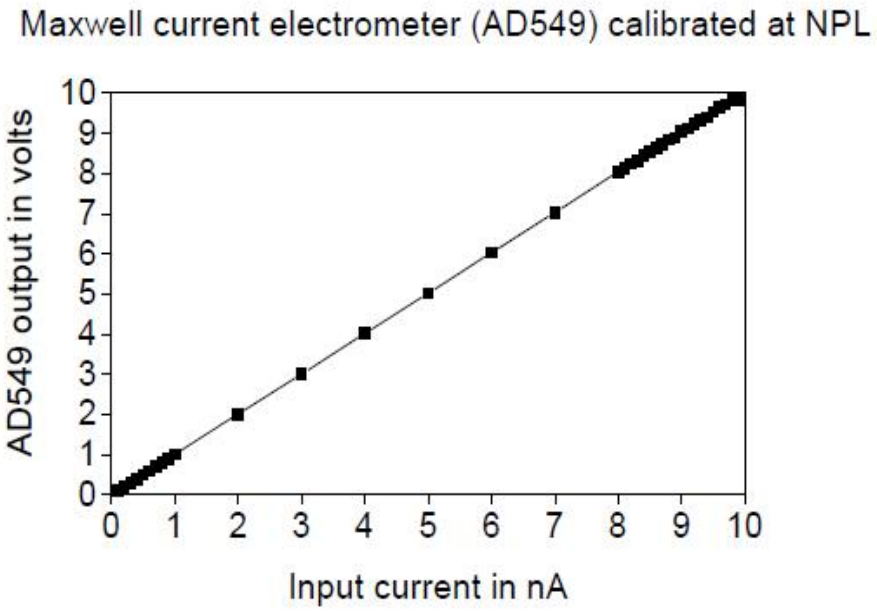

Fig. 3.2 Electrometer model AD 549 calibration curve

3.3 Wilson's plate antenna (Conduction current)

We have developed an experimental set-up to measure the atmospheric air-earth current (conduction current). Data obtained with the continuous measurements of Wilson's plate are used in the study of air-earth current density. There are only a few methods suitable for measuring atmospheric electric currents. The common ground-based

sensors used for current measurements are Wilson's plate, the horizontal long-wire antenna, and the spherical shell in the form of two hollow hemispheres (Raina, 2002). In the case of Wilson's plate set-up, the current collector is in the form of a metal plate flush with the ground and isolated by an insulator supported by Teflon rods. As soon as the charged particles come in contact with the antenna, the electric field is

indicated by an electrometer with AD 549 which converts the current into a voltage. The electrometer measures the current in the range of Pico-amperes to a few nano-amperes with high feedback resistance. A buffer stage (LM308) is connected to the electrometer output. The output signals are filtered by a low pass filter (3 dB) at the input of an analog-to-digital converter (ADC) that is nearly 50 m away from the preamplifier.

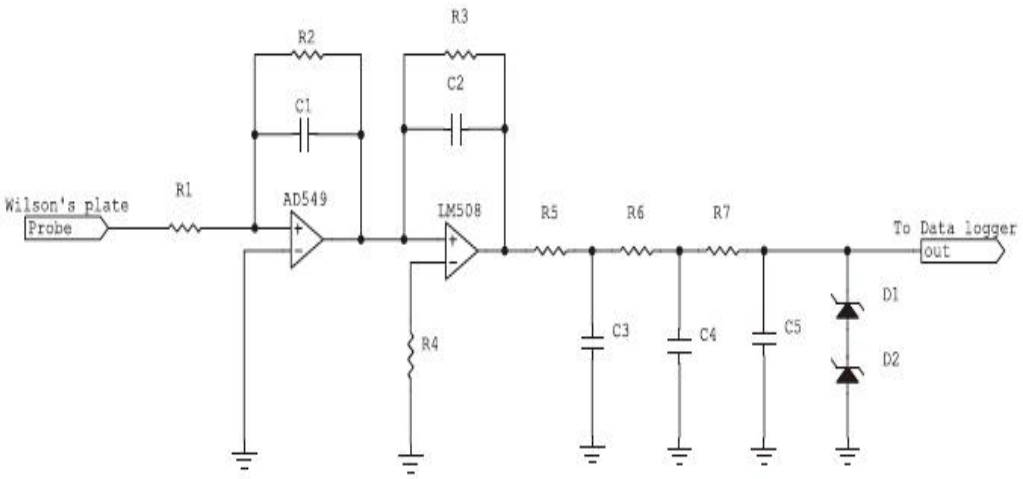

Fig. 3. 3. Circuit diagram of the Wilson's plate experiment.

The filtered signal is fed to a high-resolution Windows based data logging system. Averaging of the data samples were carried out during the analysis stage at 1-min and 30- min intervals, respectively. Wilson's plate is exposed permanently to the atmosphere and kept flush with ground level (zero potential). The charge is accumulated on the plate by the air-earth current. The time-varying component passes through high 50 GΩ resistance ($R2$) and capacitance 18 nF ($C1$) that constitute the feedback loop of the current-to-voltage converter connected as a parallel combination, as shown in Fig. 3.3

The convection current through the surface of an antenna is inherently zero because air cannot pass through this surface. Thus, the total current collected by the plate antenna is the sum of two components (conduction current and displacement current).

Fig. 3. 4. Photograph of Wilson's Plate antenna

To obtain the conduction current component one has to eliminate the displacement current ($\mathbf{J}_d$); this is achieved by making the time constant of the electrometer, in current mode, equal to the relaxation time (ε_o/σ) of the atmosphere. The conductivity is 1.4×10^{-14} to 1.6×10^{-14} mhos/m close to ground level. Therefore, from the above given value, we take the polar conductivity to be half and $\varepsilon_o = 8.85 \times 10^{-12}$ Fm^{-1}. Accordingly, the time constant of the electrometer has been set to nearly the atmospheric relaxation time. A significant contact potential exists between the ground and metal plate. Here, we have nearly 1 V of contact potential in between the Wilson plate and the ground. This potential also varies with the variation in soil moisture and causes a variable error in the measurement of conduction current

density. In order to reduce the error due to the contact potential, the Wilson's plate is made of stainless steel (which is supposed to have a minimum contact potential) which is shown in Fig. 3. 4. The side wall and bottom of the pit are covered with the same stainless steel material and are properly earthed. This helps in suppressing the current from the ground due to radioactive sources.

Another improvement is in the shape and size of the plate. In the air-earth current receiver, a 1×1 m plate or $1m^2$ circular plates are being used as the air-earth current receiver (Price and Rind, 1992). In the improved design installed at EGRL, the plate is 1×4 m. To calculate the conduction current density the measured current has to be divided by the Area of the antenna. The length of the plate is also in the direction of the prevailing wind at the site, which reduces the effect of the convection current carried by the wind to the plate and, consequently, the signal-to-noise ratio is increased. This experiment is conducted during fair weather days and cloudy days and to avoid electrometer damages it is put off on lighting and rainy days. Very much care should be taken regularly for cleaning and maintenance to avoid contact potential and short circuit between ground and antenna.

3.4 Passive antenna for electric field

The vertical atmospheric electric field may be sensed by using a passive antenna, which is charged slowly by exchanging the charges in the atmosphere. The potential of the atmosphere is obtained by the measurement of potential difference between the antenna and earth's surface, which is same as the atmospheric potential. In case of a passive antenna at 1m above the surface, the voltmeter system attached with the antenna system and it is operate over a typical input range of ± 500V. This

voltage is generated by a floating voltage generator. The input bias current used in the system is of the order of nearly 10^{-14}A with input resistance of ~10^{15} Ω. This combination must be considered in this circuit is to provide an appreciably higher resistance than atmospheric resistance. In this passive antenna system a high voltage guard is also desirable. The output is given to the ADC and thus the potential can be measured. This system can be operated at a remote place with minimum power consumption. Damages to the electrometer due to severe electrical storms can be cheaply repaired.

The antenna consists of 20m of 1mm diameter tined copper wire, suspended horizontally between short metal masts. At each end there are porcelain egg insulators, and PTFE fixing under steady compression at the masts. Sketch diagram of passive antenna shown in Fig 3.5. The insulators are regularly cleaned with isopropanol. A guard potential, which is close to the potential on the wire, is applied to the support wires at each end. This is to minimize the leakage through the insulators, which would occur if the support wires were merely grounded. As a precaution against the guard potential influencing the potential sensed by the antenna, the parallel cable that is carrying the guard signal to the far end of the antenna has an earthed screen.

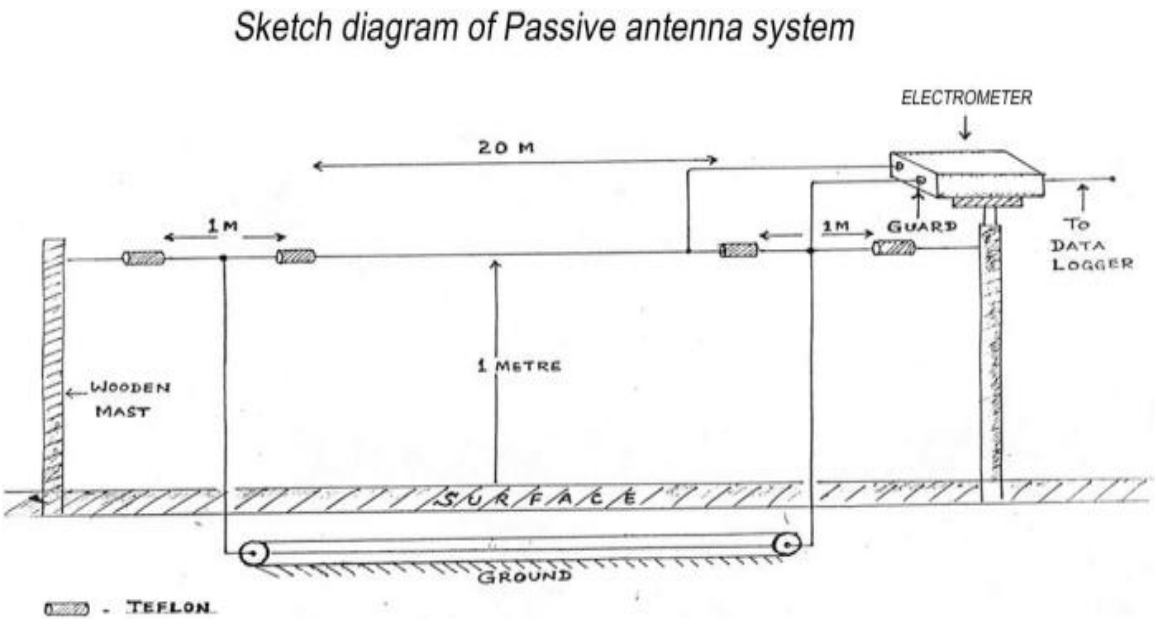

Fig. 3. 5. Sketch of the passive antenna system

The antenna is connected, with a short wire made of same material as that of the antenna, through a UHF male connector to operational amplifier LMC 6042, which is configured as a unity gain follower. LMC 6042 is a low input bias current operational amplifier, which is the input amplifier, and PO-97 is used as driver stage for the source amplifier. The input potential is connected, via a PTFE stand off, to the input of LMC 6042. A 9V battery powers LMC 6042, with the 0V reference set at 1.2 V above the battery negative supply by TC04. This ensures an adequate performance by LMC 6042 around 0 V. The data sheet of the LMC 6042 shows that for positive input voltages, the ultra low bias current is maintained which can otherwise increase for negative input voltage. Thus, by ensuring that the input voltages to LMC 6042 will always be positive at start -up, no large current will be drawn from the high-impedance source, which could otherwise lead to oscillation.

To provide a low impedance output to a voltmeter or logging system the operation potential of LMC 6042 is reduced by a 1/100. 100 MΩ potential divider

(trimmed by high voltage transformer T1), and presented to the input of MAX 430, also a follower stage. MAX 430 is a chopper stabilized amplifier (with a 1pA input bias current) so that any additional dc error is minimized. A low pass filter (C210 and R211) protects MAX 430 from external short circuits. The negative supply of the output amplifier (MAX 430) is taken from a voltage inverter ICL 7661. This work by first accumulating charge in a bucket capacitor connected between pin 2 and 4 and then transfers it into reservoir capacitor connected between pin 5 and ground. A third power supply by-pass capacitor is recommended (0.1 μF to 10 μF).

An isolated, high-tension supply generates approximately ± 500V (designated +-HT), which is supplied to two high-voltage MOSFETS Q1 and Q2 as wired as a source follower, operated at constant current (generated by Q2) to improve the linearity. OP-97 is a unity gain driver stage, which has frequency compensated for phase shifts caused by driving the considerable input capacitances of Q1, and the capacitance of the cable to the antenna support wires (auxillary guard). OP-97 is powered from a transformer derived supply, but shares 0V connection with LMC 6042. At start up, the potential on LMC 6042 and the input of the supply can differ by the full bipolar HT voltage (1kV). This can cause damage to LMC 6042. And hence a series resistor of 100 MΩ is connected to LMC 6042 to restrict the input current under voltage overload. A stable voltage offset is generated by the circuitry around TC04-LM7555 (IC 201). By adjusting the potentiometer T2, the output at pin 1 of LMC 6042 can made to precisely track the input 5. This output can also used to provide a local guard (body of the UHF female connector) potential for LMC 6042 input connection.

The main power for the unit is supplied from two 12V (7AH) rechargeable batteries, from which a 9V (± 4.5) is obtained using a 9V fixed regulator and is given to LM 6042. 10.5V supply is derived from, such as load dump (60V), when the input voltage to the regulator exceed the specified maximum operating voltage (33V type), the regulator will automatically shut down to protect both internal circuits and the load. The LM 2931 cannot be harmed by temperature mirror-image insertion. The output of the output amplifier is connected to a PC based data logger with a 12 bit ADC to record the field variations continuously. From the circuit, the tracks are drawn using software called, PROTEL EASTEDIT 2.0. Print out were taken and from this printout the tracks is taken and from the printout the tracks are transplated into the PCB using screening technique.

The insulators are regularly cleaned with isopropanol. A guard potential, which is close to the potential on the wire, is applied to the support wires at each end. This is to minimize the leakage through the insulators, which would occur if the support were merely grounded. As a precaution against the guard potential influencing the potential sensed by the antenna, the parallel cable that carries the guard signal to the far end of the antenna has an earthed screen. The antenna makes contact with a short wire made of same material as that of the antenna, which is connected to a voltage follower electrometer (LMC 6042) with the unity gain that permits ultra low input bias current of nearly 1 fA. The frequency response of the electrometer is shown in Fig. 3.6. The amplified signals are filtered by the low pass filter at the input of ADC, which is 100 m away from the preamplifier. The filtered signal is fed to the 12 bit ADC. The response of the passive antenna electrometer to specific input voltages is shown in Fig. 3.7.

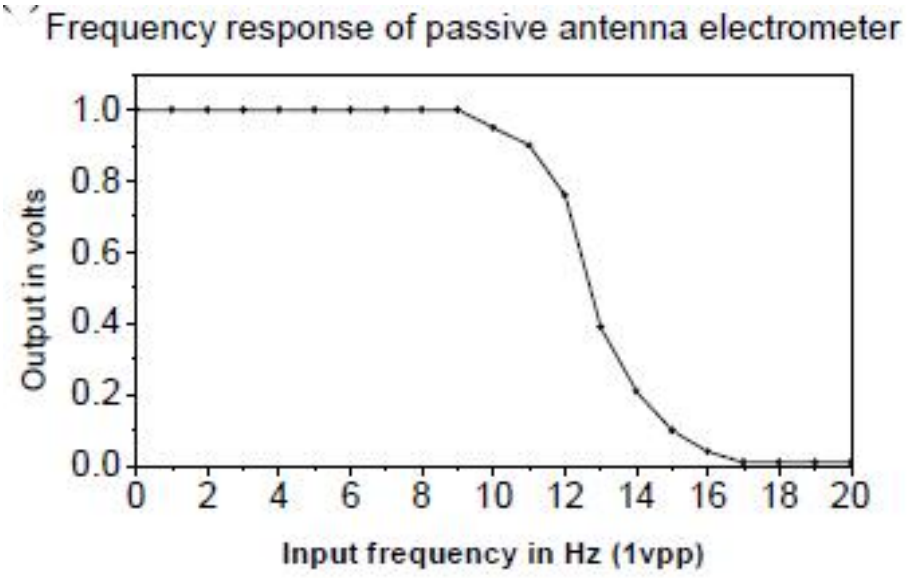

Fig. 3. 6. Passive antenna frequency response curve.

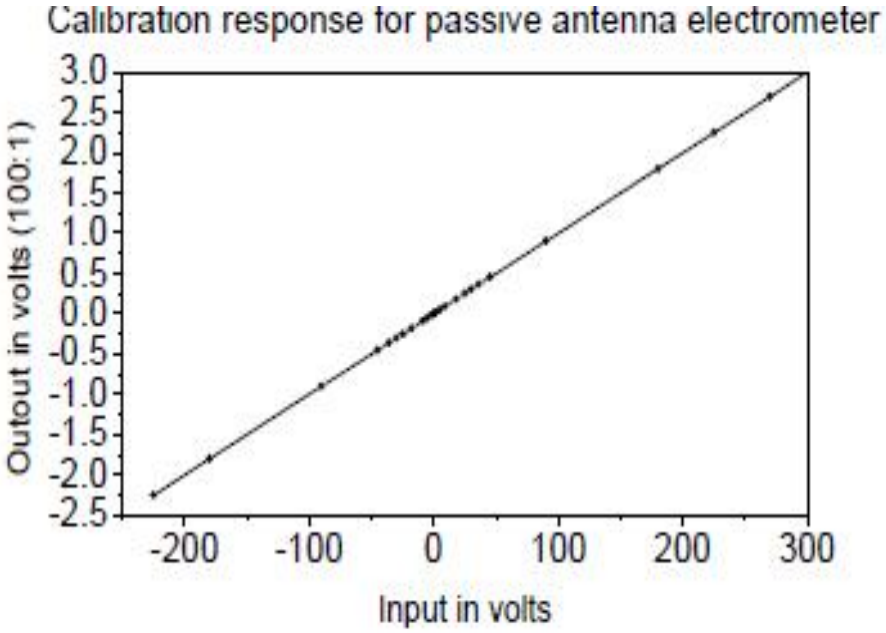

Fig. 3. 7 Passive antenna input output voltage response curve

3.5 Field Mill (FM)

The atmospheric electric field has been measured with a vertical ac field mill made out of nonmagnetic stainless steel to reduce the contact potentials (Willett and Bailey 1983). As constructed the mill consists of an upper rotor plate with four equal sectored plates which alternately cover and uncover two four bladed sets of stator plates. The total capacity between the rotor and stator set is ~500 pf and ~ 90pf. The dynamic capacity between the rotor and each set of stator plates is ~ 6pf. The specific capacitance between the plates is 2.4 X 10^{-8} fm^{-2}. The induced current per plate set is given by

$$I_o = d\varepsilon_o / dt = \varepsilon_o E_o \, dA/dt$$

$$= \varepsilon_o E_o \acute{R} \omega$$

Where Ŕ is geometric function and ω is angular frequency in $radsec^{-1}$. A is the area of the plates. Dynamic range of the mill is 25kV m^{-1}. Calibration constant is 15.5mV/100Vm^{-1} . Non linearity is less than 0.570. Long term uncertainty is zero and the short term uncertainty is less than $3Vm^{-1}$. In addition the field mill will reject common mode signals and D.C. component of non-transient contact potentials and the rejection time is less than 5 milliseconds but it will respond to transients less than 8 milliseconds. Photograph of the Field Mill (FM) shown in Fig. 3. 8.

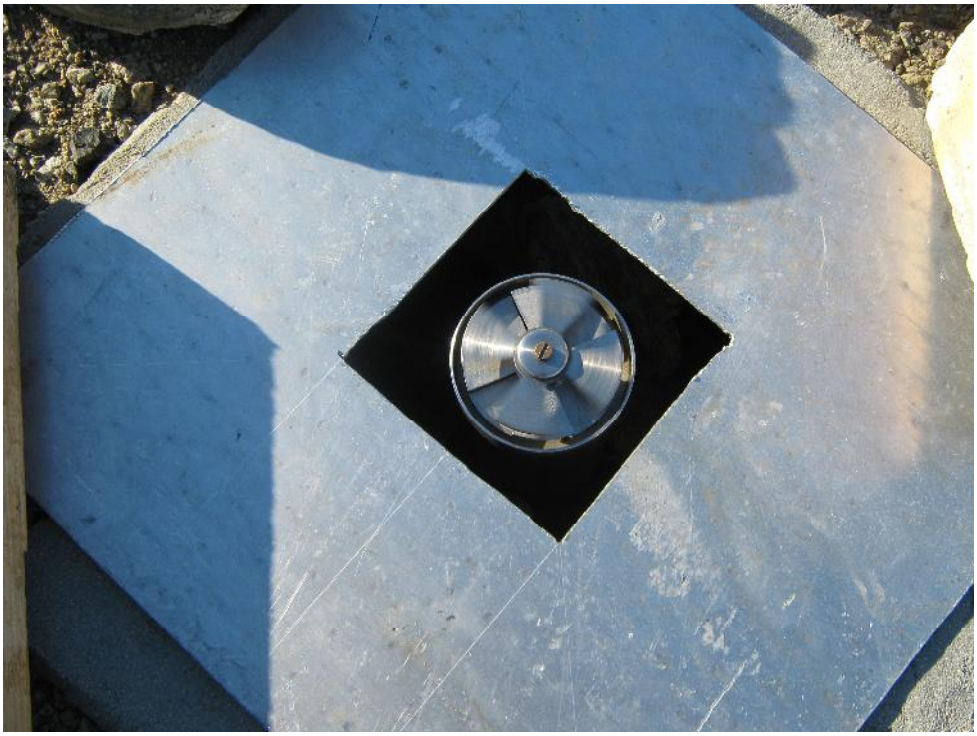

Fig. 3. 8 Photograph of Field Mill installed at Maitri, Antarctica

Atmospheric electric field is measured with a field mill with its sensor plates kept flush with the ground. Field mill consists of two stators which are periodically exposed to and shielded from the atmospheric electric field with a rotor fixed on the shaft of an a. c. synchronous motor of 1400 rpm and 12W power. The diameter of rotor is 12 cm and it is made of nonmagnetic stainless steel. The rotor is grounded using a mercury cup at the other end of motor. Two stators are also made of the same material and of same diameter as the rotor. The stators are separated from each other by a distance of 0.5 cm with Teflon bushes. The stators are connected to the inverting inputs of two operational amplifiers (IC 8007). The magnitude of the charge induced on the stators is directly proportional to the intensity of the atmospheric electric field. The two amplified signals are 180^{o} out of phase with each other. These two signals, after amplification, are fed to a demodulator (IC 1456) for combination into a single wave. The reference signal for the demodulator is generated with a circular plate with

sectors cut of the same shape as that of rotor and fixed at the other end of motor. This circular plate rotates through an opto-separater and generates a square wave signal of same frequency as that of input signals and exactly in phase with one of the two input signals. Neglecting charge separation on splashing, nontransient rain current, as seen by the field mill would depend on the plate area exposed. Since the rotor has constant angular velocity, it would result in the out-of phase triangular voltages at the two current amplifier outputs. The differential action of the demodulator would then give the signal with zero d. c. level. It can measure electric field of ±12.5 kV m^{-1} with response time of 0.1 s. Normally it can sense the lightning-induced electrostatic field changes of an average thunderstorm 20–25 km away from the observatory. The Field mill is calibrated directly by placing it in uniform electric field made by applying known voltages, V, across a parallel plate capacitor, separated by a known distance, d. Batteries are used as a power supply for calibration on the upper plate: the calibration uses the relation E=V/d. The maintenance of the instrument and calibration were carried out regularly. The calibration response curve of the Field Mill is shown in Fig. 3.9.

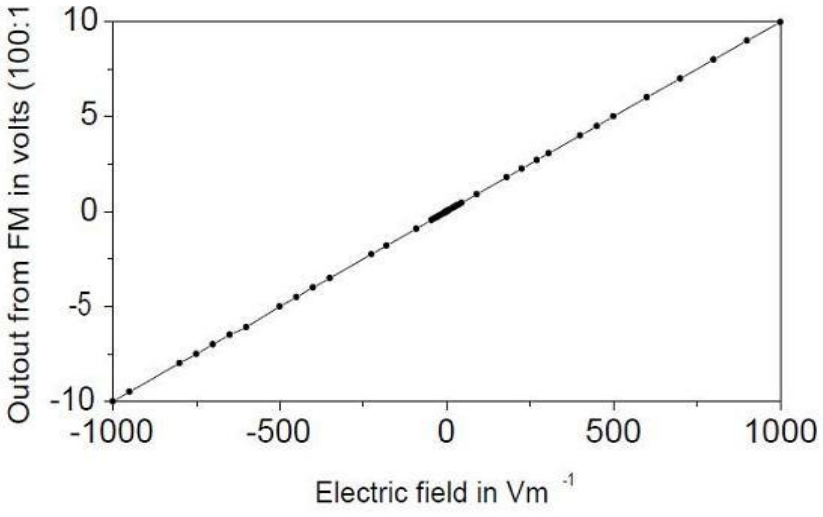

Fig. 3.9 shows the calibration response curve of Field mill

The Field mill is calibrated directly by placing it in uniform electric field made by applying known voltages, V, across a parallel plate capacitor, separated by a known distance, d. Batteries are used as a power supply for calibration on the upper plate: the calibration uses the relation E=V/d. The maintenance of the instrument and calibration were carried out regularly. The calibration response curve of the Field Mill is shown in Fig. 3.9.

3.6 Gerdien conductivity meter

In 1905 Gerdien developed a device which has become the standard instrument for measuring air conductivity. It is made of two coaxial electrodes, a hollow cylinder known as the outer electrode containing a thinner central electrode (which is frequently a solid ire).This configuration has a finite capacitance, which can be theoretically derived from Gauss' Law, and is therefore frequently referred to as a "condenser" (Swann, 1914). If a potential is applied across the electrodes and the tube is ventilated, then air ions of the same sign as the voltage are repelled from the outer electrode and attracted to the central electrode. If they meet it, a small current flows, which is proportional to the ion concentration and electrical conductivity of the atmosphere. Schematic diagram of a Gerdien condenser is shown in Fig. 3.10.

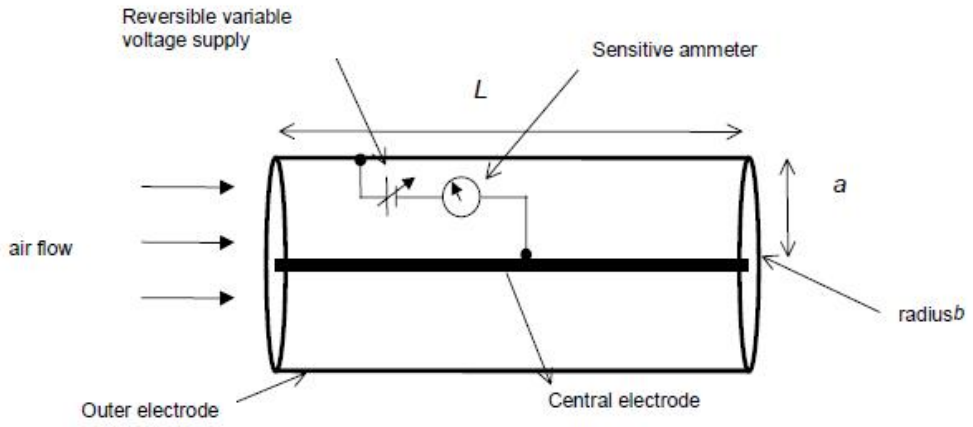

Fig. 3.10 Schematic of a Gerdien condenser (single tube)

Early Gerdiens were substantially proportioned, with linear dimensions of about 8 cm by 50 cm (Torreson, 1949). This was necessary in order for the output current to be large enough to be resolved by contemporary electrometers. In the 1950s smaller tubes were developed for radiosonde measurements, which were typically of order 5 cm in diameter and 30 cm in length. Attaching the Gerdien to a fixed potential, and allowing the voltage to decay through air permits a voltage to be measured rather than the current from the central electrode. This is preferential for conductivity measurement on radiosondes, because it is more straightforward to measure voltage than small currents, and immensely simplifies the issues associated with electrometry. The smaller sized tube was not problematic when ion currents did not have to be directly measured. Recent improvements in electronics have improved measurements of very small currents in the femto ampere range (Harrison, 1997a; Harrison and Aplin, 2000a).

The most common of the varied materials used to make Gerdien condensers has been brass (*e.g*. Higazi and Chalmers, 1966; Brownlee, 1973) probably following successful use of this material by early investigators (*e.g.* Rutherford, 1897). Gerdien

designed for use on radiosondes have necessarily been made of less dense materials such as aluminum or aluminized paper (Hatakayema *et al,* 1958; Venkiteshwaran, 1958). The tube material could be significant for two reasons: firstly that of its durability when used in the field, and secondly that of the effect of contact potential. Wåhlin (1986) discusses the effect of the material of the tube, opining that contact potentials cause offsets in the i-V response. This is credible, as two electrodes touching a fluid containing ions do make an electrochemical cell (*e.g.* Atkins, 1989), even if the electrolyte (air) is dilute. According to Wåhlin (1986), a Gerdien will measure a non-zero current when the bias voltage is zero, due to electrochemical potential at the surface of the tube. Wåhlin (1986) suggests that a steel tube has to be biased at about 0.4 V and the aluminum at 1 V to counteract this. However, he does not explain how the effects of tube material alone were distinguished in his experiments from the many other sources of offset associated with Gerdien condenser measurements. The effect of different tube materials has not been systematically investigated, but Hatakayema *et al* (1958) did apply an offset of -140 mV corresponding to the contact potential for their aluminum tube, though they do not explain how this quantity was obtained.

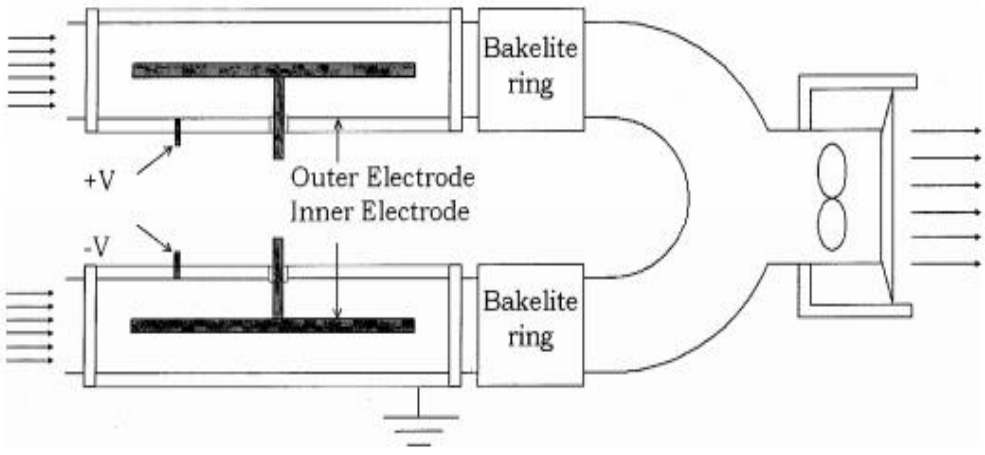

Fig. 3. 11. Diagram of a Gerdien condenser

Atmospheric electrical conductivity of both positive and negative polarities is measured simultaneously with gerdien condenser. The apparatus consists of two identical tubes of 10 cm diameter and 41 cm length joined by U-tube. Each tube has central electrode 20 cm long and 1 cm in diameter. The two central electrodes carry positive voltage of polarity to measure positive negative ions. Air is sucked through them with a single fan fixed at the end of the U-tube as shown in Fig. 3.11. To reduce the intensity of turbulent mixing, the ends of the inner electrodes that face the air stream are rounded smoothly. To reduce the effect of atmospheric wind in the condenser, the inner electrode is placed well inside the outer electrode away from the entrance, allowing the initial atmospheric turbulence to decrease considerably. A voltage of ±35 V is applied to one cylinder, known as the driving electrode, with respect to the other. This driving voltage repels ions of one polarity towards the other electrode, where ions get collected. For voltages that are sufficiently low, the collector current increases in proportion to the driving voltage. The collector current at these voltages is given by the equation

$$i = -\frac{\sigma Q}{\varepsilon_0}$$

Where Q=CV, V (35 V) is the applied driving voltage is the conductivity of the ambient air, ε_o is the permittivity of free space and C is the capacitance of the condenser obtained from

$$C = \frac{2\pi\varepsilon_0 L}{\ln\left(\frac{b}{a}\right)}$$

Where L is the length, a & b are the radii of the inner and outer electrodes, respectively. The collector current, which is proportional to the conductivity which amplified signals from Gerdien's apparatus are fed through Teflon, insulated coaxial cables to a PC-based data acquisition system, which is 20m away from the field. The equipment is operated at a sampling interval of one second. The maintenance of the instruments, especially cleaning of their insulators, was done daily. The zero shifts are checked twice a day and are corrected if the deviations are appreciable (Deshpande and Kamra 2001).

3.6 Conduction current measurement

Wire antenna can be used for the measurement of Maxwell current as well as air-earth current (Conduction current). Maxwell current includes, (1) conduction current, (2) Displacement current, (3) convection current, (4) lightning current, (5) point discharge current and (6) precipitation current, etc., but in Conduction current measurement is has maximum part of conduction current and small portion of displacement current during fair-weather conditions. It depends on the RC (time constant) in the electronic circuit used for the measurement. Close to the ground the atmospheric relaxation time is about 5 to 40 minutes, 4 seconds near 18 km height and 10^{-4} second near 70 km above the earth's surface. Maxwell current has two components which is d.c component as well as a.c. The fluctuation part of the Maxwell current is displacement current (AC part) with time domains of 0.1 seconds to 10 minutes. Conduction current with frequency greater than 1Hz is a pure displacement current and at frequencies less than a millihertz is purely conduction current. For frequencies between 1 Hz to 1mHz the conduction current density contains both components as shown in the below equation.

$$J_M = \Delta \times H = \sigma E + \varepsilon_o \partial E/\partial t$$

Where, J_M is the Maxwell current density, σ is the atmospheric conductivity and E is electric field in the atmosphere. It is of considerable interest to separate displacement current density from conduction current density. The determination of displacement current density will be useful studying global scale a.c., component of Maxwell current density. To separate the purely conduction current density and the displacement current density we have used the wire antenna. The Schematic diagram of the conduction current wire antenna is shown in Figure 3.12.

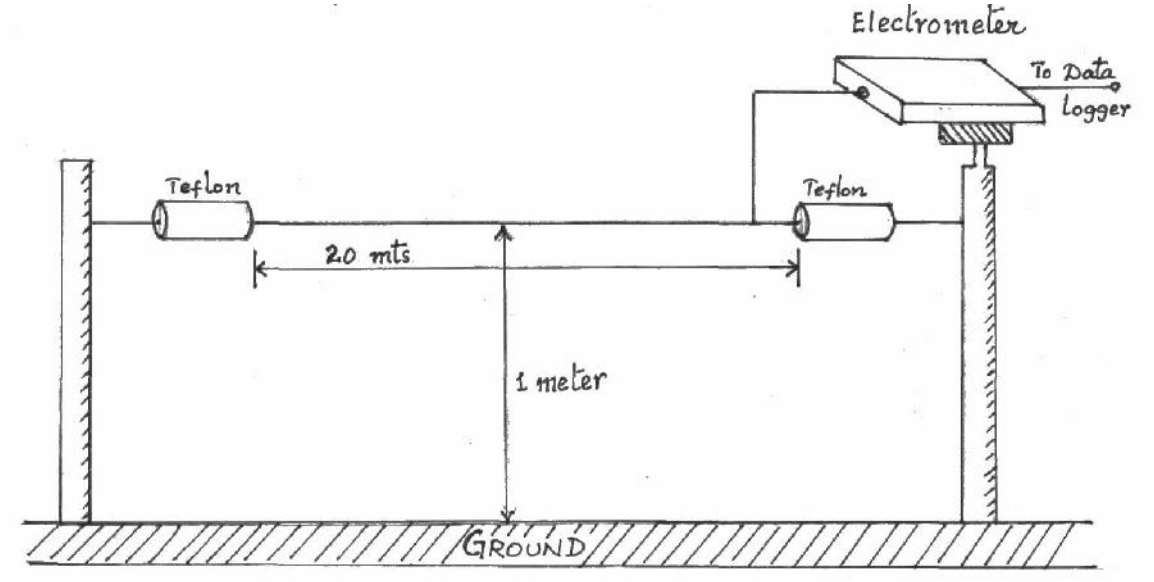

Fig. 3. 12 Schematic diagram of the conduction current wire antenna

The horizontal long wire antenna, if placed in the atmosphere, will closely follow the electrical current variations of the atmosphere after the initial net charge on the antenna leaks off. When the antenna is shorted to the ground through a resistor, it will generate a voltage that is proportional to the air-Earth current. In the present experimental setup, a long wire of length 20 m and thickness 3 mm is kept

horizontally stretched parallel to the ground at a height of 1. The wire is mechanically supported by means of masts. By using Teflon rods at their ends it is ensured that the antenna wire is electrically insulated from the supporting masts. The input is fed through the electrometer (Model AD 549) that has high input impedance and permits extremely low input bias current (10^{-14}A). The electrometer measures the current up to 1 nA (corresponding to the output voltages whose limit is ±5 V) with a feedback resistance of 50 X10^9 Ω. A unity gain operational amplifier (LM308) amplifies the electrometer output signal. The amplified signal is then taken in a shielded cable over a distance of 40 m to the control room where it is fed to a PC-based data logger. The sensitivity of the digitized signal is 2.44 mV that will correspond to a current of 0.5 pA. The data are recorded at a sampling interval of one second (Panneerselvam *et al.*, 2003). The effective area of the experimental setup is 21.9 m2 calculated from the formula (Kasemir and Ruhnke, 1959; Tammet *et al.*, 1996),

$$S_d = \frac{2\pi LH}{\ln(2H / r_o)}$$

L length of the antenna and H the height of the antenna above the ground and r_o is radius of the antenna wire. The current density can be estimated by dividing the measured current by the effective area of the antenna. RC (time constant) used in the electrometer circuit is 1000 seconds to eliminate other than conduction and displacement current.

3.7 Electric Field Meter (EFM-100)

There are different methods to measure atmospheric electric field like Field mill (Deshpande and Kamra 2001), passive antenna (panneerselvam et al., 2007). These instruments cannot be operated during bad weather conditions like heavy rain,

blizzards and etc., The above instruments needs 230 V a.c., and also more care has to taken during the operation conditions. Regular cleaning and maintenance is very much needed. The present one Electric Field Mill (EFM 100) can be operated in any weather conditions and also it can be operated in any remote place with 12 V d.c., where a.c., is not available. It measures the atmospheric electric field intensity of the atmosphere and the data can be operated with the sampling rate of as low as 0.5 seconds. Schematic diagram of EFM -100 is shown in Fig. 3. 13.

Fig. 3. 13. Schematic diagram of EFM -100

Electric fields develop wherever there is a difference in electric potential. Electric field is measured in Volts per meter (1 meter = 3.28 feet.) The electric fields which accompany thunderstorms are normally measured in the thousands of Volts per meter, usually abbreviated to kV/m. Lightning can be detected as a sudden change in

the electric field. The electric charge contained in a thundercloud also generates an electric field. This field can be measured on the ground. For an accurate electric field reading the field mill needs to be mounted flush with the ground. Mounting the field mill flush with the ground is not practical however as water, dirt, insects, etc will collect around the sense electrodes and contaminate the electrode insulators. Mounting the electric field mill above the ground surface will enhance the electric field resulting in an incorrect high reading. Sensitivity Plugs are provided to reduce the sensitivity of our field mill and compensate for the higher field mill readings. The EFM-100's electric field mill senses electric field by repeated exposing and shielding a series of sense electrodes. Field Mill Block Diagram shown in Fig. 3. 14.

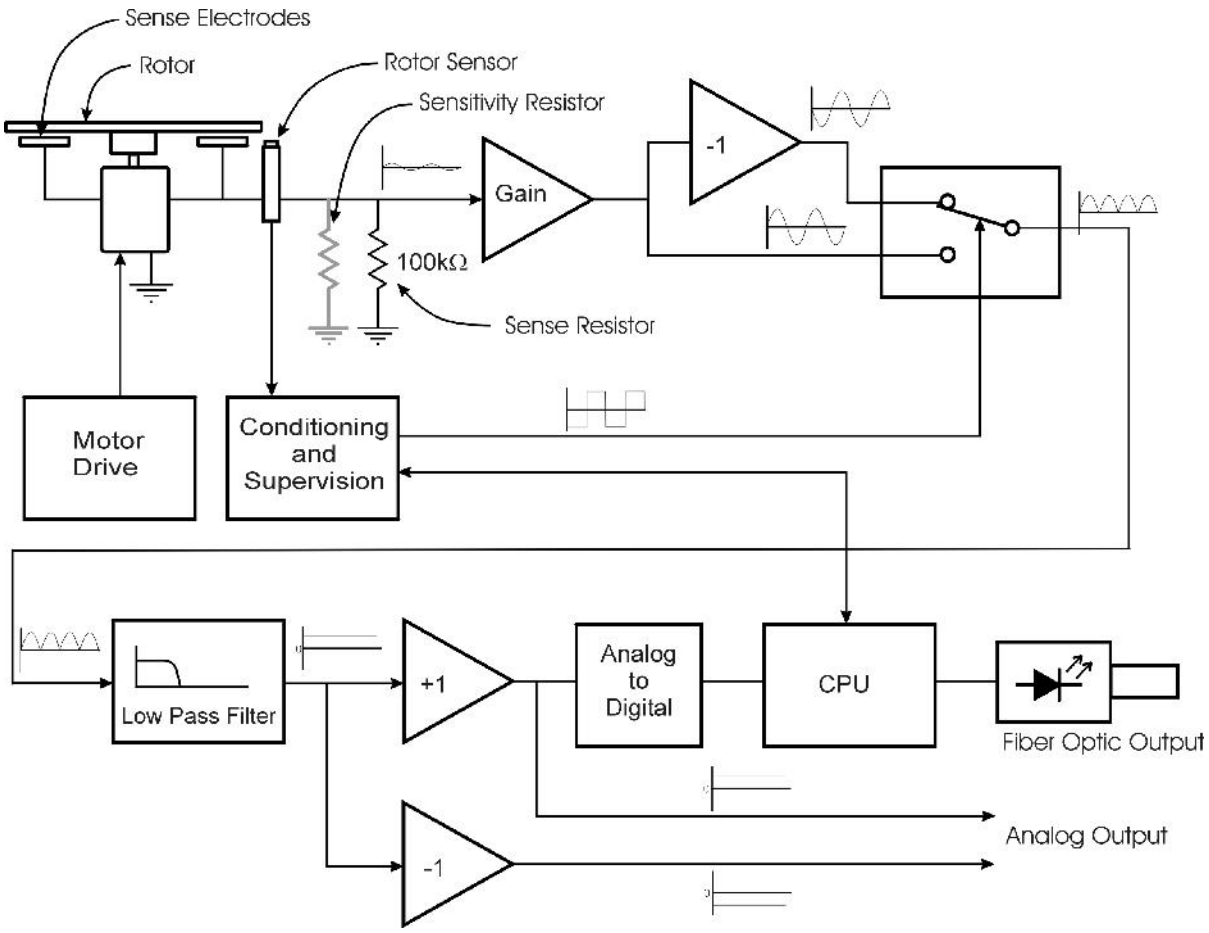

Fig. 3. 14. Electric Field Meter Block Diagram.

An electric field mill uses a mechanical chopper to alternately shield and expose several sense plates to an electric field. When the sense plates are exposed to the electric field an electric charge is drawn from ground to the plates through a sense resistor. When the sense plates are shielded from the field the charge flows back to ground, again through the sense resistor. This moving charge is an electric current which is measured as an AC voltage across the sense resistor. The size of the voltage is proportional to the size of the electric field applied to the plates. Charge flowing onto and off of the sense electrodes will develop a voltage across the sense resistor. This voltage is amplified and then filtered with a low pass filter then, fed into an ADC. Finally the signal cable is connected to the Data logger or PC where the EFM-100 program installed. The signal from the EFM-100 carried by the Fiber optic cables, and to the EFA-10 Fiber Optic Adapter converts the optical data from the field mill to an electrical signal compatible with personal computer. Data is transmitted optically from the field mill at 9600 baud, 8 data bits, 1 stop bit, and no parity. There is a provision for sensitivity selection. Sensitivity plugs reduce the sensitivity to compensate for the enhanced electric field of a field mill mounted above the surface of the ground. Lower numbers represent lower sensitivities. For example, the 0.25X plug will reduce the sensitivity to ¼ of the field mills normal sensitivity. On a clear day simply choose the sensitivity jumper which produces field values closest to the normal fair-weather electric field of 0.1 kVm^{-1}. If electric field readings during thunderstorms routinely exceed 20 kV/m (the limit of the field mill) we should change to a lower value Sensitivity Plug. Grounding of EFM -100 is very important and separate grounding should be provided for the good quality of data collection. There is an option for the data storage in the computer software program, it can be stored in the Hard disk or any external disk with 0.5 seconds sampling rate. The EFM -100

suppliers also supplying the software for detecting the lightning and warning alarm with sound system as well as with different colour option on the graphical display. The EFM has the sensitivity to detect up to 30 kms of the radial distance from the measuring site. There is an option for selecting the range of the measuring electric field. The EFM-100 program creates a file in a day. More details are available in info@boltek.com.

CHAPTER 4

Analysis of local atmospheric electrical parameters

4.1 Introduction

Measurements of the potential gradient (PG), air-Earth conduction current density (J_C) and total conductivity (σ) made at Equatorial Geophysical Research Laboratory (EGRL), Tirunelveli (8.7°N, 77.8°E), which is a regional center of Indian Institute of Geomagnetism, Mumbai under Department of Science and Technology, Government of India. All of these parameters have been recorded simultaneously since 1995 onwards. The environmental and meteorological conditions at the measuring site and the orography relevant observation on atmospheric electricity and data selection reported below and location of atmospheric electrical parameters measuring site shown in Fig. 4.1.

Fig. 4.1 Map showing location of GEC site in India

The experiment site (~30 m above mean sea level) is more than 12 km southeast of the twin towns of Tirunelveli and Palayamkottai. The nearest cement factory is located at a distance of about 15 km to the northwest. It may be noted that moderate-to-intense southwesterly winds blow during one half (April–September) of the year over the region of observation, while moderate north-easterlies blow during the other half (October–March) of the year. The site is about 35 km from the Bay of Bengal, and the nearest hills of Western Ghats are at distances of approximately 45 km to the west and the southwest.

Further, the crustal part of the Earth underneath the site is fixed on solid rocks, and hence does not support dense vegetation. The experiment site receives rainfall normally in the months of October and November during the northeast monsoon, while occasional rains occur during the summer when the southwest monsoon prevails in the Indian subcontinent. Scanty rainfall over most of the year in this region permits a large number of atmospheric electricity measurements to be made. Being in the tropics, this region is under the influence of convection that is expected to be severe around summer period (April–June).

Measurements of atmospheric electrical parameters have been carried out at Tirunelveli since March 1995. After initial test runs for more than 1 year, the Maxwell current data have been available for analysis since May 1996. In the present study type of data set included days on which disturbed local weather conditions, other than fair weather, occurred; these include (1) thunderstorm and showers, (2) fog conditions and (3) Sunrise effects briefly discussed in this chapter.

In 1999, we have started GEC experiments at Maitri, Antarctica with the same instruments which is operational at EGRL. The Indian Antarctic station, Maitri is located in the Schirmacher oasis in the Dronning Maud Land, East Antarctica (117 m above the mean sea level) and location of the site shown in Fig. 4.2. Antarctica has only around 2% of its area that is free from ice. The nearest steep cliff of the east-west trending glacier on the southern side of the station is more than 700 m away from the station and is 300 m in height. The snow-covered surface during summer season was more than half a kilometer away from the station. The instruments were installed on barren land near the station. The surface of the station area is mainly covered by sandy and loamy sand types of soil. The solar zenith angle at Maitri varies from 48◦ to 88◦ during summer months. There was no sunset till the third week of January, but periods of short nights slowly increased during February. The variations in surface meteorological parameters were measured by automatic weather station which is installed during this expedition. The cloud cover over the station occurs mainly under the influence of subpolar low-pressure systems and shows an alternating sequence of the sky changing from overcast to clear as the system moves away (Deshpande and Kamra, 2001). In the present study type of data set days on which disturbed local weather conditions during (1) Effect of Wind Speed, (2) Blizzard and drifting snow and (3) effect of fog conditions also discussed in this chapter.

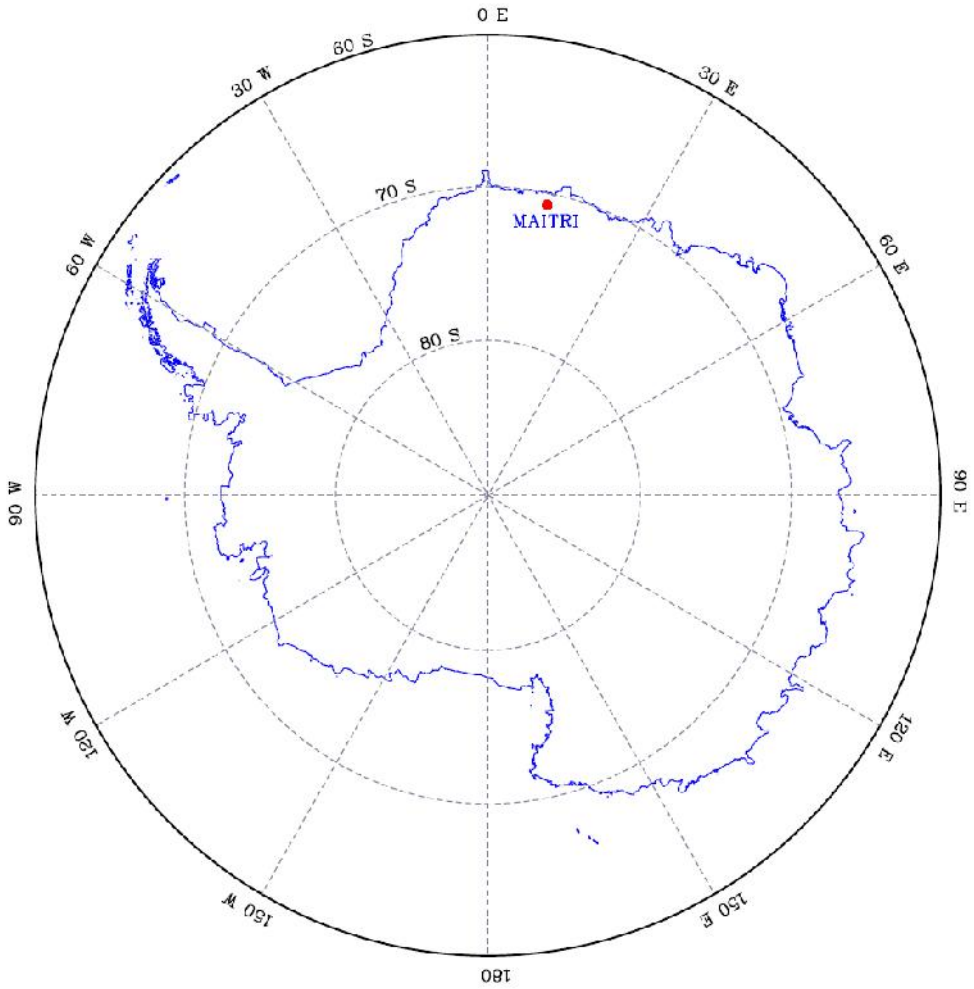

Fig. 4. 2 Map depicting location of Maitri, Antarctica.

From these atmospheric electrical measurements and those of standard meteorological parameters using Automatic Weather Station (AWS) data, it is possible to resent both an electrical "climatology" of the EGRL and a comparison work carried out between electrical and meteorological parameters. Additionally, inter-comparison of electrical parameters will be made and results compared to other instruments which one is measuring the same parameters with some other technique. The variation of PG and J_C during fog, Thunderstorm and shower, blizzard and snowfall conditions investigated from both the place (Equatorial and polar region).

4.2 Analysis of Disturbed Weather Conditions (at EGRL)

4.2.1 Thunderstorm and showers

In this section we have carried out analysis during the disturbed weather conditions like rain, shower and lightning. July 24, 1998 is considered to be a good example of days in which there was rain and thunderstorm activity. On this day, intense convection led to the development of a thunderstorm during the afternoon. For the period of lightning the variation in the current for this day between 09:30 and 11:30 UT is shown in Fig. 4.3. The thunderstorm activity with a few visible lightning strokes took place over the measuring site between 10:15 and 10:45 UT. Severe rains persisted between 10:00 and 11:00 UT. It may be noted in Fig. 4.2 that at times of lightning strokes the current fluctuated between the extremes. The onset of rainfall is clearly marked by the rapid increase in the current that commenced at approximately 09:45 UT. With the traditional view that lightning brings down negative charges and rain positive charges (Israel, 1973), one would expect a downward or upward current trend depending on the incoming charge polarities. A change in the sign of the measured current clearly indicates the dominance of lightning current around these times and conforms to the traditional view that the fairweather electric field changes its direction during thunderstorm activity.

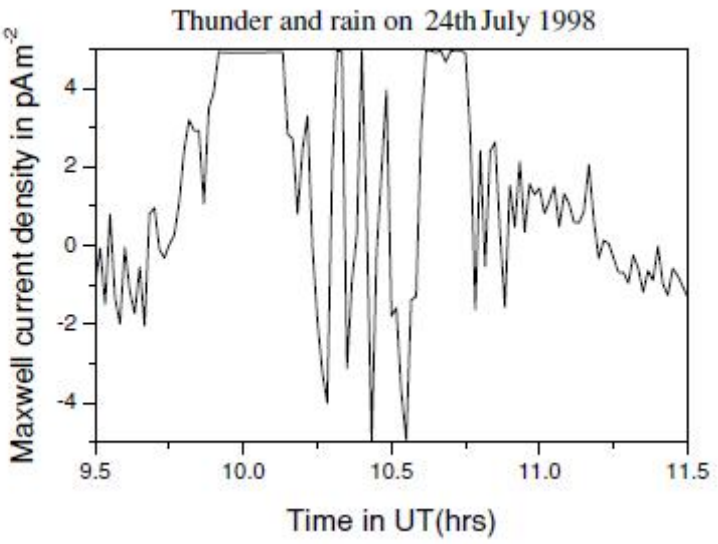

Fig. 4.3. Maxwell current variation on 24 July 1998 in response to thunderstorm and rain.

On the other hand, during the course of rain, the condensed water droplets normally forming near the top of the thundercloud are expected to carry positive charges and, hence, on precipitation near the ground they are expected to cause an increase in the measured current density. Despiau and Houngninou (1996) carried out measurements of electric charges of raindrops, electric field, and Maxwell current during intense storms and showers at a tropical location in West Africa. One of the characteristic features of the storms was the presence of predominantly positive hydrometers with charges between 80 and 240 pC. The observed features described above clearly indicate that the horizontal antenna wires do respond to the electrical disturbances occurring in the near-Earth space environment. At the onset of precipitation the measured current increases, while during intense rainfall, the measurements reveal saturation at their detectable levels. This behavior has been observed at every occurrence of strong downpour is shown in Fig. 4.4.

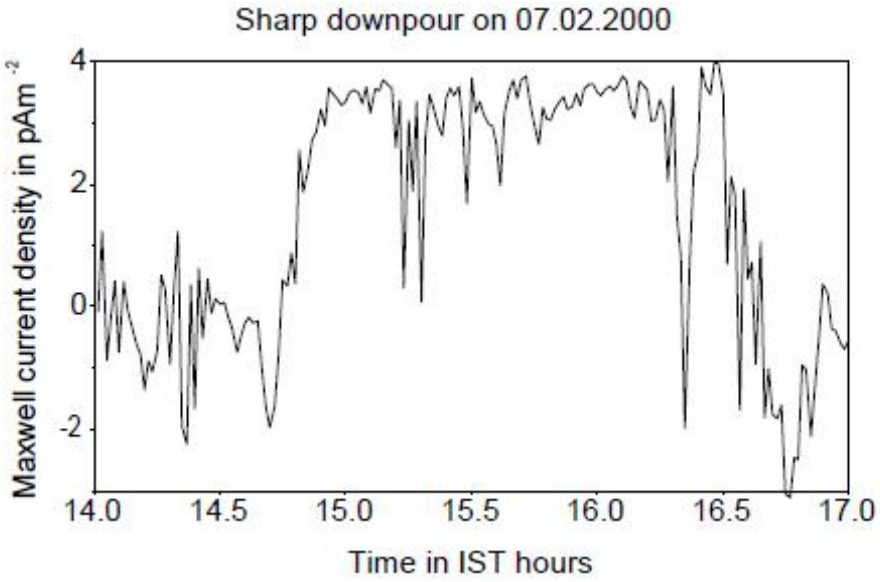

Fig **4.4. Maxwell current variation during sharp downpour at EGRL**

On 7th February 2000 at about 1400 IST there was lighting with light drizzling started and then at about 1445 IST heavy downpour started and continued about 2 hours. During the heavy downpour the measured current density is so high. It is due to the rain drops carries the positive charges. On the other hand, during individual lightning strokes, the current detected by the long-wire antenna fluctuates between extreme values (±1 nA). It is possible that the sign of the current reverses in response to the reversed polarity of the electric field at such instances.

4.2.2 Fog effect

Fog is one of the factors that influence the Maxwell current variation. The necessity of studying the electrical properties of fog is also dictated by a number of practical problems, such as possible means for the fog forecast and control, influence of aerosol and dust systems to the electric field and current in the atmosphere, and the search for mechanisms of solar-terrestrial relationship (Smirnov, 1992). It has been observed that the conductivity of the atmosphere decreases significantly at the onset

time of the fog (Hoppel *et al.*, 1986). An unseasonal rain that occurred over the measuring site on 24 and 25 July 1997 provided an ideal condition for fog development to occur. The variation in the measured current density for this period is depicted in Fig. 4.5.

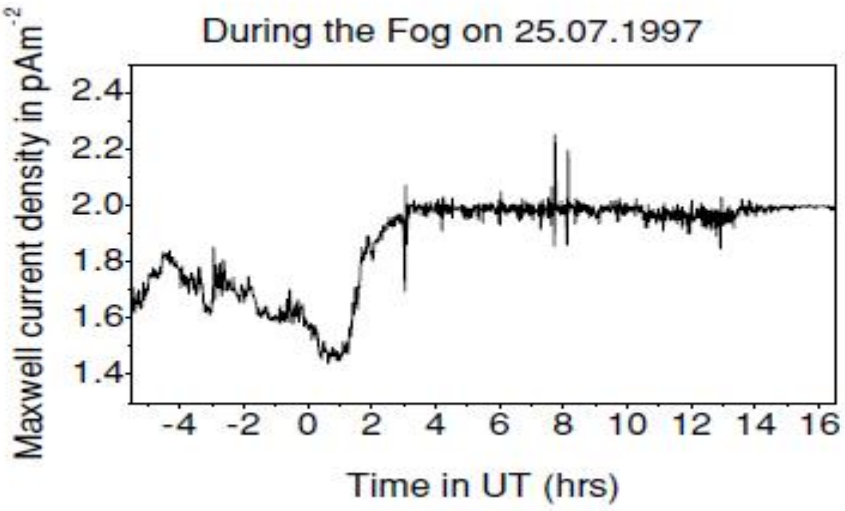

Fig. 4. 5. Maxwell current variation on 24–25 July 1997 in response to fog.

The fog was centered near the sensor complex at approximately 01:30 UT on 25 July, and then drifted towards the east at about 01:40 UT. During this period, the current level decreased to a minimum between 00:30 and 01:30 UT. This observation agrees with the results reported in earlier works by Dolezalek (1963) and Serbu and Trent (1958). Prospero (1984) showed that before fog visibly forms, the growing droplets capture atmospheric ions, thereby increasing the resistivity of air and leading to a rapid reduction in the current density. When the droplets begin to fall, the thickness of the fog layer decreases and, consequently the columnar resistance of the air decreases. This is expected to cause an increase in the measured current density. The present experiment is thus shown to be consistent with these previous observations.

Studying the electrical properties of fog requires the development of modeling with consideration for the microphysics of particle charging and the availability of external sources of ionization and the electric field in the atmosphere (Sorokin, 2001; Anisimov *et al.*, 2003; Mareev and Anisimov, 2003). The fog developed due to radiation cooling of the air in the surface layer; in the morning, the advection of the warmer moist air took place. A characteristic feature of the fog typically causes the current density to decrease (Anisimov *et al.*, 2005). At times of fog development, the current tends to diminish in its magnitude, recovering later as the fog disappears. This feature is explained based on the reasoning that as the fog thickens, the growing droplets reduce the conductivity and, hence, the current flowing to the sensor. As the fog dissipates, the evaporation of water drops leads to a slow recovery of the conductivity, and the current returns to the initial values. Burke and Few (1978) observed a similar fog effect on the air–Earth current density measured at Houston.

4.2.3 Sunrise effect

In order to examine the sunrise effect in more detail we have used the one-minute averaged data that are shown in Fig. 4.6. These data are plotted in Indian Standard Time (IST) which is 5.5 hours ahead of UT. It is seen that Electric field (E) and Current (I) begin to rise 30 minutes before ground sunrise (sunrise time at Tirunelveli is 0631 IST (the local time is 18.8 minutes behind IST) for this month). The increase in the measured parameters before ground sunrise is perhaps related to the process at some height in the atmosphere that will see an earlier sunrise. A time difference of nearly 30 min between the rise time of the electrical parameters and the ground sunrise time reveals that such height could be somewhere in the region between stratopause and the ionosphere. The maximum that occurred at 1900 UT in

Figs. 4.6 and 4.7 is believed to be associated with the global thunderstorm activity. The other local processes that contaminate the global signal are due to dew and mist that may be present in the morning hours on some days. The space charges that exist at the time of evaporation from dew or mist may contribute to the observed variations in electrical parameters (Karasnogorskaya and Pokhmelnik, 1983, for example).

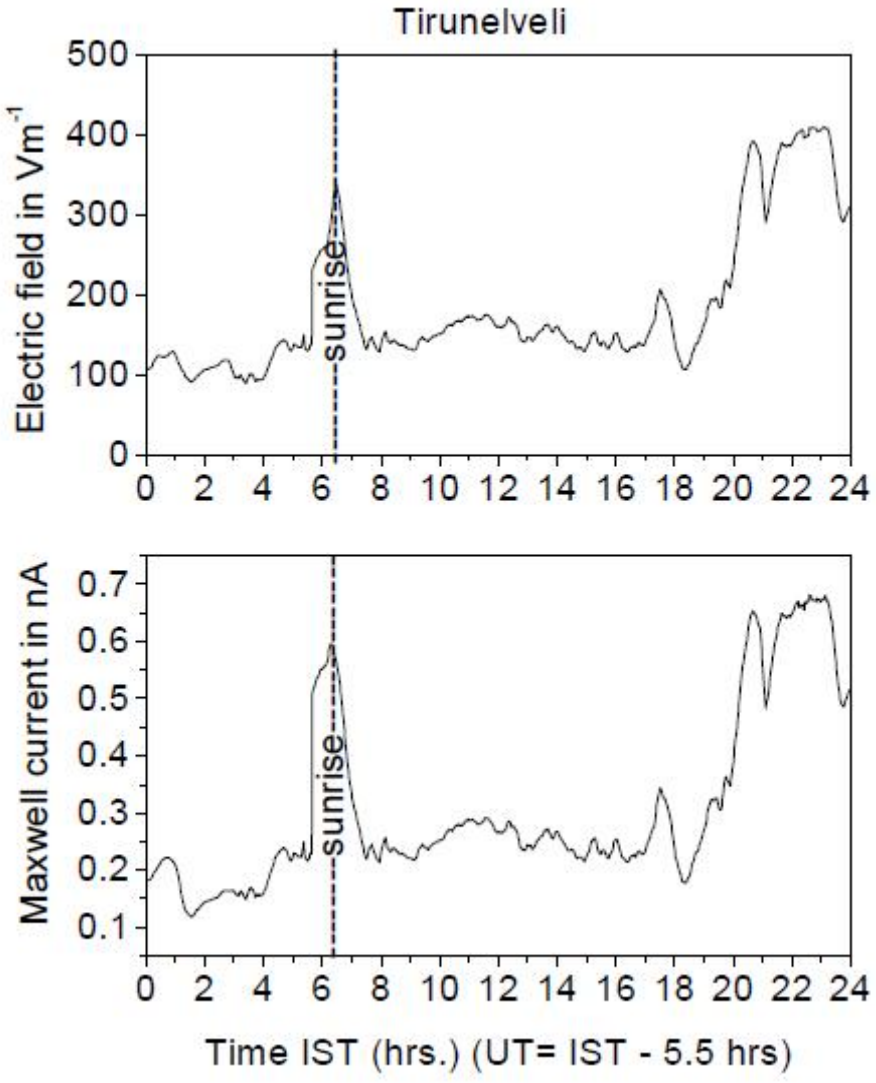

Fig. 4. 6 Diurnal variations of Maxwell current and electric field (one-minute data) on 20 January 2002

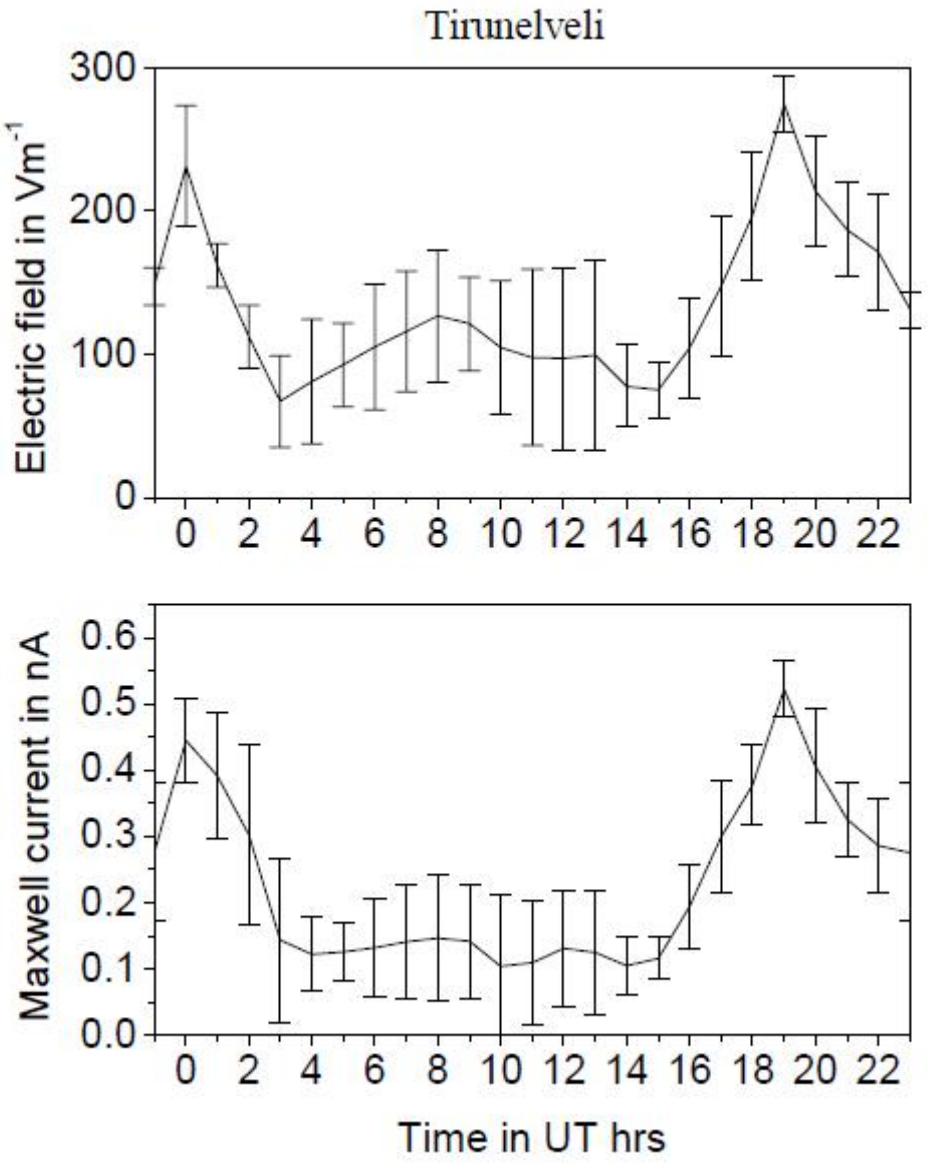

Fig. 4. 7 Diurnal variations of Maxwell current and electric field at Tirunelveli averaged over 8 fair weather days during January/February 2002.

The variations observed in I and E at this low latitude station differ markedly from those reported from other low and middle latitudes (Israel, 1973; Burke and Few, 1978; Reiter, 1985; Adlerman and Williams, 1996). Israel (1973) found no characteristic fundamental behavior among the measurements from ten continental stations. This can be realized if one considers the relationship between the field intensity (E), current (I), and column resistivity (R), given by $E = wV/R = w.I$, where

w is the resistivity at the observation point, *V* is the total potential difference between the earth's surface and the atmospheric electric equalization layer, and *I* is the current. Though the field intensity depends strongly on the meteorological processes through its dependence on the local resistivity *w*, the current, given by $I = V/R$, is less sensitive to local changes in conductivity. However, changes in the columnar resistance, induced by the atmospheric suspension content and its vertical transport, may be expected to dominate the vertical current and its variations. Thus the behavior of I depends on whether the percentage changes in *V* or *R* dominate. Over the continental stations one can expect that the changes associated with *R* are larger than those associated with *V* (Israel, 1973). Gringel *et al.* (1986) showed that the first two km of the atmosphere contribute about 50 percent to the total columnar resistance and the first 13 km about 95 percent. With observations conducted at Weissnau, Germany, Gringel *et al.* (1986) measured a variation in *R* of about 30 percent, and attributed the variation to a changing ionization near ground and by varying aerosol concentrations in the lower troposphere. Muir (1975, 1977) tried to explain it on the basis of sunrise effect at the height of electrosphere leading to build up of a potential through dynamic motion associated with tides.

During the course of this investigation pre-sunrise effect is most noticeable. Muir (1975, 1977) has suggested that the processes of ionization in the ionosphere and polarization in the electrosphere at sunrise would result in an increase in the potential of that part of the electrosphere experiencing sunrise. This would be possibly detected as an increase in the atmospheric electrical parameters at the ground. This pre-sunrise effect would be caused by a tidal sunrise effect at the height

of the electrosphere (where sunrise occurs earlier than sunrise at the ground). Further studies are needed to be sure of the cause of the pre-sunrise effect.

4.3 Analysis of Disturbed Weather Conditions (at Maitri, Antarctica)

4.3.1 Effect of Wind Speed on atmospheric electrical parameters

The surface atmospheric electrical parameters at a place can be influenced by wind speed if some space Charge is either advected or locally generated by wind. There is known anthropogenic source of space charge upwind of our instruments. The local generation of space charge can be neglected during periods of low wind speeds However, when wind speeds are high, the blowing snow or raising of dust particles may generate and introduce some space charge in the atmosphere During the period of our observations the ground at Maitri is not covered with snow, and there was no incidence of blowing snow. However, when wind speeds are very strong (say > l 0 ms^{-1}) some dust is observed to be blown off ground. The dust particles so stripped off from the ground may be highly charged and influence the local GEC parameters. If the wind speeds higher than10ms^{-1} may lower the GEC parameters is shown in Fig. 4.8.

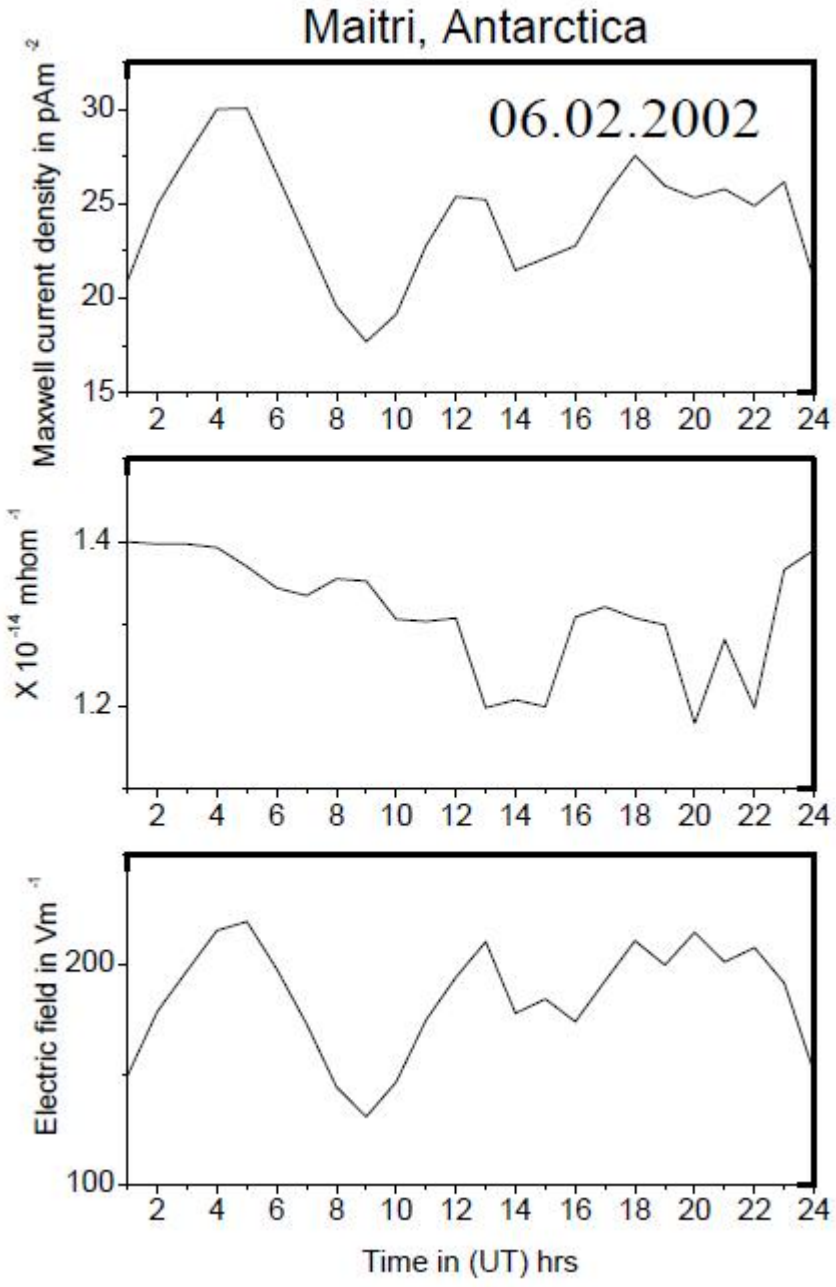

Fig. 4. 8. GEC parameter variation on clear sky data with high wind

On February 6, 2002 the whole day the sky is clear and shinny, but the wind speed is high more than 10ms^{-1}. This may well be because of the presence of the negative space charge formed by the negatively charged dust particles in the lower atmosphere which are blown off the ground with high wind speeds [Kamra, 1969, 1972]. Wind speed may also be caused by the blowing off of the space charge caused by the electrode effect or convection currents. Such electrode effect / convection

current caused deviations in atmospheric electrical parameters. In fair weather, gamma radiation from the ground and from space ionizes air, separating charge and creating an electric field at the Earth's surface. The field is extremely variable, averaging 120 V m^{-1} at 1m height (Iribarne and Cho, 1980). The atmospheric electric field reverses direction and its magnitude increases in the region occupied by blowing particles, indicating excess negative charge density above the surface (Schonland, 1953). Electric field strength diminishes with increasing height in the transport region (Schmidt and Dent, 1994), as expected if excess charge density is associated with the distribution of moving particles. During clear sky days the conductivity is more or less stable, so as per the ohms law if the electric field varies and the conductivity is stable the current should vary according to the field which is seen in Fig. 4.8

4.3.2 Effect of Blizzard

Blizzards are generally described by low temperatures, strong winds, large quantities of snow (Bostwick 1916; Breton 1928; Huschke 1959; Bozman 1970; Hank 1976; McLeod and Hanks 1982; Whittow 1984; Barnhart and Barnhart 1984; Gretz 1986; Sinclair 1992) and with long duration (Funk 1956). While the words 'blizzardy', 'blizzardly', 'blizzarded' and 'blizzardous' (adjectives) are terms to describe a blizzard tending to occur or to produce a blizzard (Gove 1961; Klein 1971; Barnhart and Barnhart 1984; Schwarz 1989; Simpson and Weiner 1989; Schwarz 1993). Sometimes a blizzard is called a 'white-out' where blizzard conditions occur with a total snow cover. Under these conditions it is extremely difficult to find one's direction. The impression is of being swathed in a white opacity (Monkhouse 1970). White-outs are common in polar region and leads to loss of balance and sense of balance (Whittow 1970). Today, in general terms the word means a severe snowstorm

in nearly every English-speaking country (Tufty 1987). According to Barnhart and Barnhart (1984) a similar storm of wind-blown sand or dust is also called a blizzard.

In Antarctica, blizzards are associated with winds spilling over the edge of the ice plateau at an average velocity of 160 km/hr (Anonymous 1915; Monkhouse 1970; Monkhouse and Small 1976; Hudson 1979; Gretz 1986). In the USA, the US Weather Bureau in 1958 defined a blizzard as one characterized by winds of 56 km/hr or more, a temperature of -7 °C or less and driving snow to limit visibility to 150 m, while a severe blizzard is one where winds exceed 72 km/hr, visibility near zero and temperatures of -12 °C or lower (Huschke 1959; Considine 1976; Gretz 1986; Tufty 1987; Ahrens 1991; Meteorological Office 1991). The Canadian Weather Service describe a blizzard as winds of 42 km/hr (Force 6) or above; visibility 0.8 km or less; temperatures 22 °F (-7 °C) or less and to last six hours or more (Hudson 1979). The blizzard duration is likely to be dependent upon the scale and shape of cyclones. The number of severe blizzards is not controlled by ‘‘in situ’’ annual mean meteorological conditions, but by the number of strong cyclones having time scales of several days coming from the lower latitude region.

Antarctica is the windiest continent on the earth. The land mass is scoured by a regime of persistent and powerful katabatic or gravity winds which are the result of cold dense air rolling down the continental slope from the high plateau. The term katabatic is defined as a wind that flows downslope (due to negatively buoyant air being acted upon by gravity) with a vertical profile that possesses a near-surface jet, such that the wind speed measured at some level near the surface is greater than the wind speed at the adjacent level above. Generally, a katabatic wind’s low-level wind

maximum is located within the lowest 100 m of the atmosphere. These katabatic winds interact with warmer air from the ocean to produce clouds, fog and extremely strong blizzards in association with moving low pressure systems. The local winds are strengthened with the passage of low pressure systems and wind speed of 88 knots gusting to more than 100 knots. A combination of two moderately strong cyclones is also important in the formation of severe blizzards.

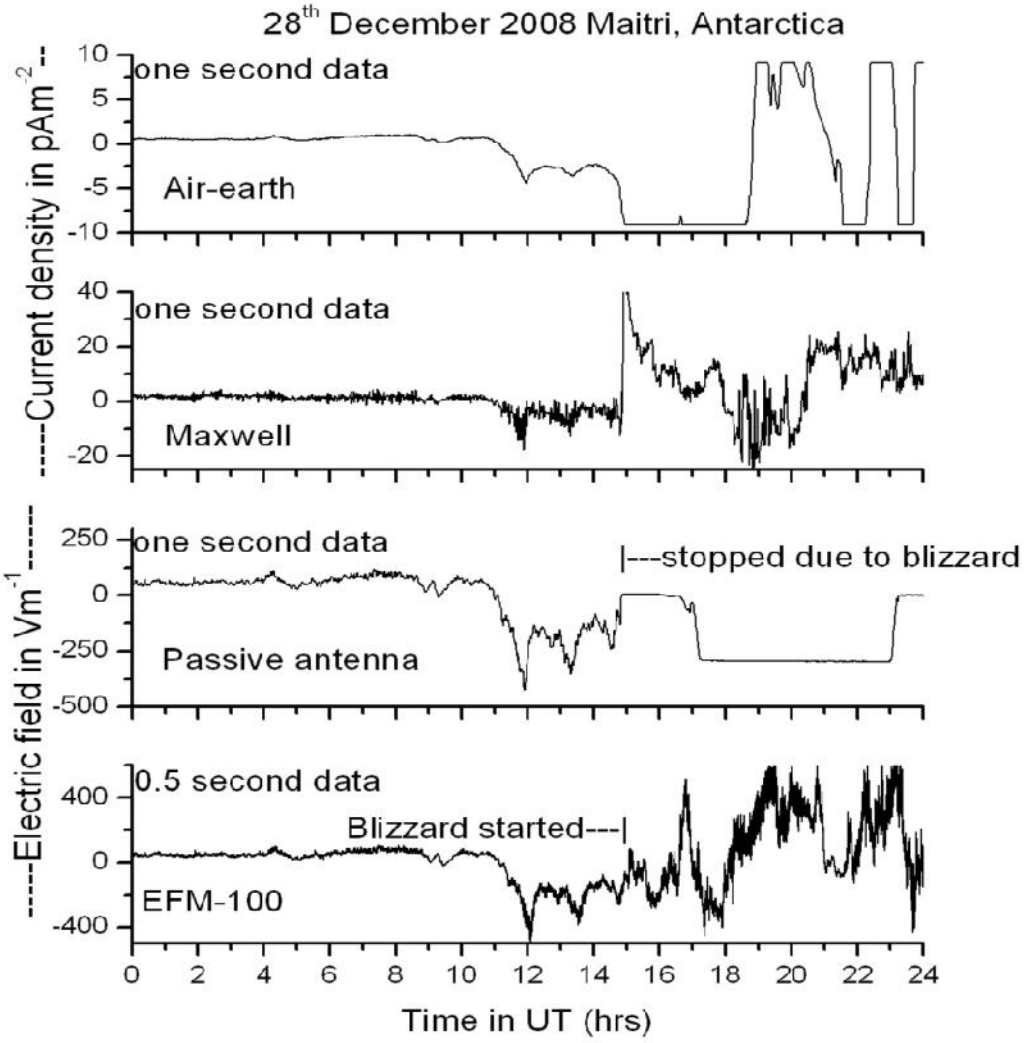

Fig. 4.9 Variation of GEC parameters during blizzard day.

Simpson [1919] observed that blizzards are intensely electrified and produce high positive potential gradients on the ground. In our observations we observe that whenever high winds are accompanied with some snowfall, i.e., atmospheric Maxwell current, Air-earth-current , electric field of all the three categories begin to decrease about 3 – 4 hours before the appearance of blizzard. For example, on December 28, 2008, winds begin to strengthen at 1200 UT and blizzard started from 1500 UT shown in Fig 4.9. Devendraa Siingh, Vimlesh Pant and A K Kamra made similar observations at the same place in summer 2005 on atmospheric air-earth current density, temperature are below freezing point, positive ion concentration of all four categories begin to decrease 3-4 hours before the onset of blizzard. The decrease observed in all types atmospheric electrical parameters during snowfall indicates that snow particles effectively scavenge the ions. The fact that the air-earth current density and electric field almost reduces to zero value indicates that scavenging of atmospheric ions is almost total at that time. The observations that the decrease in different ion categories is not always parallel to each other are likely to result from the non-uniform rate of scavenging of the ions of different sizes. This observation can be used as a forecasting for the convoy persons and other activities around Maitri for human safety and preliminary percussions. The detailed mechanisms underlying the formation of severe blizzards are not yet well understood and form one of the interesting topics for future polar research.

4.3.3 Effect of Fog

The fog was formed due to advection of southeasterly winds by high moisture containing northwesterly winds, blowing from the ocean over the cold ice shelf,

which leads to the condensation of moisture, thereby forming fog at Maitri, Antarctica. Stratiform clouds are common near the Antarctic coast. Fog is essentially a dense cloud of water droplets, or cloud that is close to the ground. Fog is also an important alternative source of moisture for plants. Virtually no higher plant life-form exists on the Antarctic continent. However, minute organisms survive in small pockets of ice-free areas. In the driest and coldest habitats, especially where fog and dew are the major water sources, desiccation-tolerant algae or cyanobacteria, bryophytes and lichens may form the only vegetation (M.A., Lazzara et al., 2003). Fog is the biggest forecast problem related to flights aborted due to bad weather and few studies have been undertaken on the Antarctic fog. Fog and haze at Maitri, Antarctica have been rarely recorded.

Fog is defined as a cloud that touches the ground and reduces the visibility to 1 km or less. There is no physical difference between a fog and a stratus cloud, other than altitude. Unlike thick, rain-producing clouds which are characteristically formed by the expansion and cooling of rising air, the cooling of humid surface air below its dew point temperature usually causes fog. This cooling can result from radiational processes, from the mixing of warm and cool air masses, or from warm moist air moving over a cooler surface. The induction of warm, marine oceanic air to the interior causes low-level cloud over the Maitri.

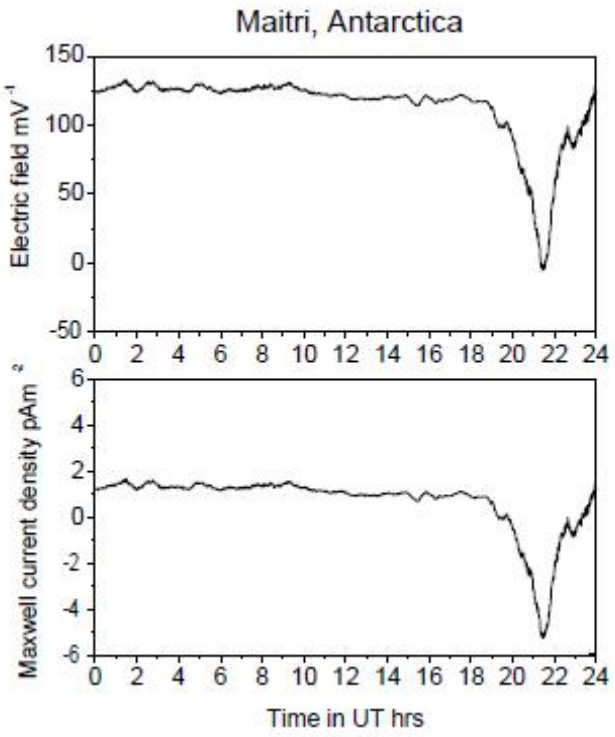

Fig. 4.10 Fog on 10th February 2004 at Maitri, Antarctica

On February 10, 2004, the PBL dynamics revealed unique sodar facsimile features shown in Fig. 4.10. The fog was seen between 1600 – 2345 UT and the Maitri region was under the influence of thick fog. The fog layer ultimately diminished, as the flow of northerly air weakened and was taken over by the gravity-driven flow (katabatic wind) around 2400 h on 11 February 2004. During this period the electric field and Maxwell current went well below zero and become negative. However, further investigation on the wind direction gives us an idea of how the fog was formed. The direction of the surface wind on 10 February 2004 remained basically from the NE sectors for most of the time during the foggy period. It is pertinent to mention here that the wind directions over Maitri are dominated by the ESE direction; these are mostly katabatic winds flowing from the interior of the continent. Thus, the present case of winds from the northern quadrants is clearly

oceanic in nature. The above results therefore suggest that the slow wind from the NE quadrant brought moisture-containing air masses from the ocean, which is about 70 km from the oasis. Visual observations suggested that the condensation of fog was considerable and the ground was wet during this episode. The dissipation of fog was only after the katabatic wind started flowing from the interior of the continent. Therefore, this type of fog can be regarded as advection fog(Petterssen, S.,1958). However, in Maitri, the number of days with fog is generally low throughout the year. In Maitri, there is little or no rainfall, and thus the localized fogs contributed atmospheric moisture to the few microbiotic crusts as their sole water source. It is also likely that due to changing climate over Antarctica, frequent fog may occur in the near future.

CHAPTER 5

Observation of the global atmospheric electric circuit

5.1 Introduction

Measurements of PG and J_C provide an opportunity to monitor the intensity of global thunderstorm activity from one point on the Earth's surface, through the global electric circuit. However, variability in these measurements cannot usually be attributed only to the global circuit, but also to changing meteorological conditions, such as those that affect the aerosol number concentration vertical profile. These local sources of variability in J_C and PG often dominate measurements made at urban sites, as identified in chapter 4. To observe variability attributed to more global sources, a site with low variability in meteorological conditions known to affect surface J_C, σ and PG must be used. As the aerosol number concentration is often the dominating source of local variability (Alderman and Williams (1996), Harrison and Ingram (2005)), a globally-representative site is usually one of consistently low air pollution (and therefore low variability) such as oceanic, arctic or mountain observatories (Chalmers, 1967). The low-pollution site used for this investigation will be EGRL, India (equatorial station). This site has a record of hourly J_C, σ and PG measurements over decade since 1995. Air pollution is low due to its remote location away from any large settlements and nearly 35 kms away from the Bay of Bengal and Indian Ocean. , making it ideal for investigation of global sources of surface electrical parameters variability at EGRL. In addition to analysis of data from the low-pollution site of EGRL, an attempt will be made to retrieve the diurnal cycle of ionospheric potential

(i.e. the global circuit). We have the data since 1999 from Maitri, Antarctica (polar station). J_C is considered as the parameter measured at the surface that is most representative of the global circuit (e.g. Chalmers (1967), Dolezalek (1978)). This is because fair-weather J_C is a function only of R_C and V_I (the latter being the intensity of the global circuit), where as PG has the additional dependence on local σ. The hypothesis that J_C is a more globally-representative parameter than surface PG will be investigated, including whether PG at an urban site can be used to represent global circuit variability at all.

The global circuital path links the lower troposphere, the ionosphere and the magnetosphere form a circuit is called Global Electric circuit (GEC), the measurements of atmospheric electrical parameters will be handy in any integrated approach that involve all these regions. Long term measurements would be considered useful for addressing some of the problems associated with global change. The hourly averaging procedure is most suited for the identification of the signatures of global electric circuit. Since the charge generated by a thunderstorm somewhere on the globe is distributed in the equalizing layer (ionosphere) within 10–15 minutes, mean values of measurements over at least 30 minute duration would be required if the global thunderstorm activity is to be adequately represented (Reiter, 1992). One-hour averages are considered in the present work for examining the diurnal variation in the measured parameters. We define a fair weather day when there is no rainfall at the measuring site, high clouds less than 3 octas throughout the day, and wind speed less than or equal to 10 ms−1.

5.2 GEC models

The classical model of atmospheric global electric circuit proposed by Wilson considers the earth's surface and the ionosphere (~ 70km) to form two plates of an electrical condenser in which ionosphere (outer plate) is maintained at a uniform positive electrical potential of a few hundred kilovolts with respect to the earth (inner plate)by the worldwide thunderstorm activity. The classical GEC model Schematic diagram is shown in Fig. 5.1. In this Figure the resistance R = 230 Ω and the total charging current I = 1000 A. Separately depicted are mesoscale convective systems with the horizontal scale length 150 ± 200 km. Typical respective resistances of the above and below cloud regions are $R_1 = 10^4$ and $R_2 = 10^5$ Ω. GCR: Galactic Cosmic Rays.

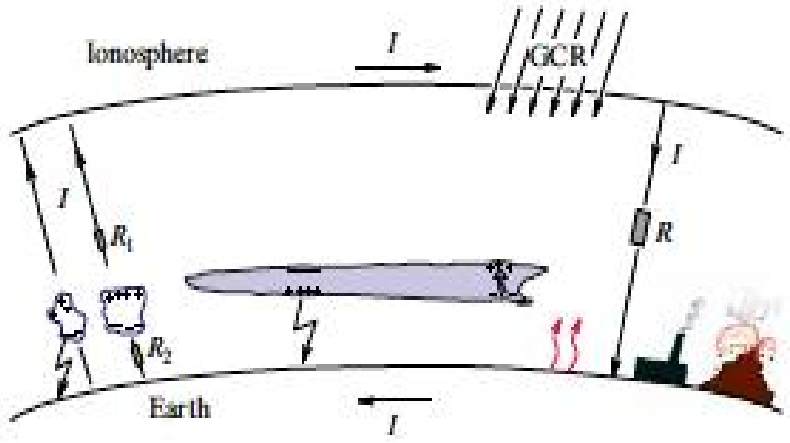

Fig. 5.1. Schematic representation of the classical GEC

The atmosphere acts as a leaky dielectric between these two conductors. The basis for the formulation of this classical model was the observations that the vertical electric field had globally uniform diurnal variations similar to that of global thunderstorm activity. This model considers the thunderstorms as the only generator

and neglects all other sources. It also hypothesized that the thunderstorm electric field cannot go beyond the ionosphere. Over the past few decades, with the advent of satellites and the availability of modern sophisticated instruments, there has been very fast advancement in GEC studies and it links the other sources contributing to the atmospheric electrical parameters which is called modern GEC model.

The new discoveries earlier make it clear that electric field and current do not feel the artificial boundaries encompassing the regions for the lower atmosphere, or the ionosphere or magnetosphere. Hence the mutual coupling and interconnections between these regions, which have been traditionally studied separately so far, are essential to understand the complexities of our planets electrical environment. Such approach would yield new light in identifying the physical causes of solar-terrestrial-weather relationships. New GEC circuit schematic model is shown in Fig. 5.2.

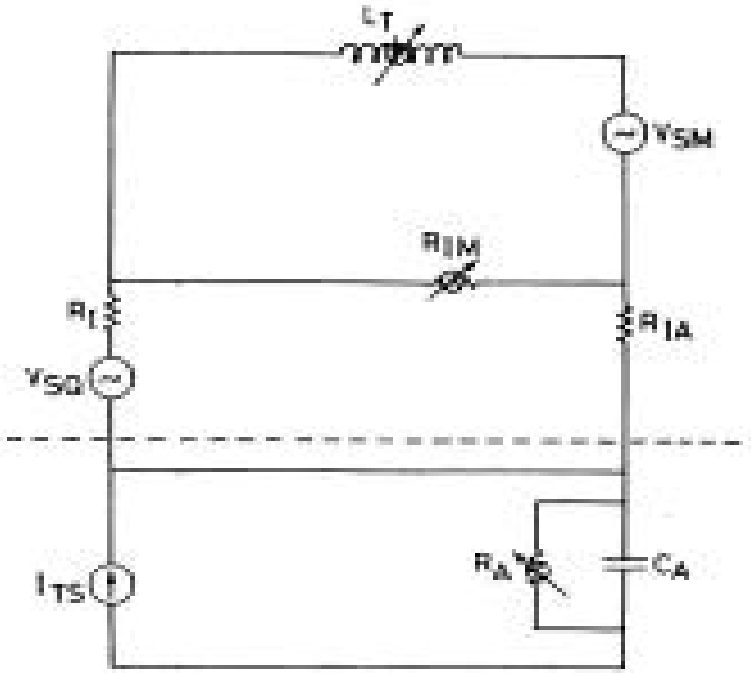

Fig. 5. 2 Modern GEC model diagram

Here the portion below the dotted line in figure 5.2 is the usual classical GEC, where thunderstorm and other generators in the lower atmosphere are plugged together as a current source I_{TS}. Here R_A represents atmospheric resistance and C_A is atmospheric capacitance with in lower atmosphere (up to 60 kms). The ionospheric electrical generator is denoted by V_{SQ}, and the magnetosphere generator by V_{SM}. The variable resistor R_{IM} represents the ionosphere-magnetosphere coupling, and L_T represents the energy stored in magnetotail. According to the new global electric circuit model there are three main generators that operate the GEC: (1) thunderstorms, (2) the ionosphere wind dynamo, and (3) the solar wind/ magnetosphere dynamo. In this thunderstorm is the major contributor to GEC compared to the other two generators. The ionospheric and upper atmospheric generators contribution to the global electric circuit and separation of different atmospheric current density is discussed briefly in chapter 6.

5.3. Diurnal variations of GEC parameters (EGRL, Tirunelveli)

5.3.1 Over a month of days

The hourly averaging procedure is most suited for the identification of the signatures of global electric circuit. Since the charge generated by a thunderstorm somewhere on the globe is distributed in the equalizing layer (ionosphere) within 10–15 minutes, mean values of measurements over at least 30 minute duration would be required if the global thunderstorm activity is to be adequately represented (Reiter, 1992). One-hour averages are considered in the present work for examining the diurnal variation in the measured parameters. The diurnal variations of the electric field ($E = V/h$ where V is potential and h is in meters) and Maxwell current (J_M)

averaged for the selected fair weather days during January/February 2002 are depicted in Fig. 5.3.

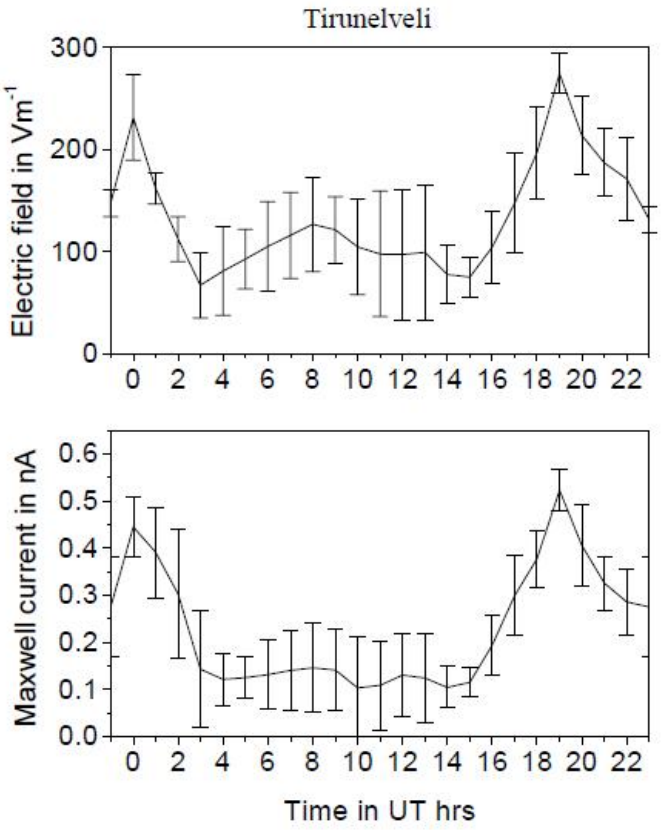

Fig. 5.3 Diurnal variations of Maxwell current and electric field at Tirunelveli averaged over 8 fair weather days during January/February 2002.

In this figure we have included average values corresponding to one hour before 0000 UT to see when the sunrise effect occurs. The diurnal variations show a local morning and a local evening maximum feature during this period. There are peaks at 0000 UT 1900 UT. The global UT variation in atmospheric electrical parameters is expected to show a maximum at 1900 UT and a minimum at 0300 UT. The present data on electric field and current do show a maximum at 0000 UT and 1900 UT. The local sunrise effect obscures global signature minimum. The maximum that occurred at 1900 UT in Figs. 5.3 is believed to be associated with the global

thunderstorm activity. The correlation between Maxwell current and the electric field variations are shown in Fig. 5.4.

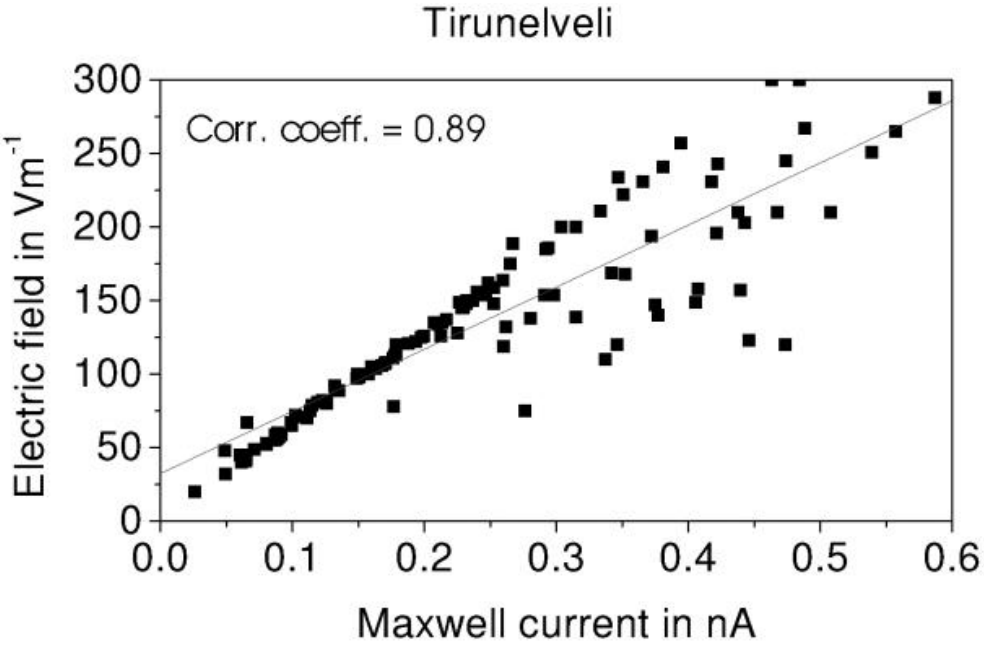

Fig. 5. 4 Maxwell current Vs electric field at Tirunelveli for 8 fair weather days during January/February 2002.

The correlation coefficient for these measured parameters has a high value (more than 0.8) during the fairweather days. From the slope of the curve the conductivity was calculated and its value is 1.0 X 10^{-14}S/m. The morning sunrise enhancement observed on the fair weather days is a local effect whereas the 1900 UT maximum in the measured electrical parameters are attributed to the global thunderstorm activity that is expected to peak at these hours. Measurements from this setup confirm our analysis of local and global effects in the data obtained from the continental site. These results supports that this site is free from local pollution and is suitable for long-term measurements of atmospheric electrical parameters. Diurnal variation of atmospheric electrical parameters is similar like "Carniege curve" and also with earlier reported by (Israel, 1970, 1973, Adlerman and Williams, 1996).

The electric field strength or potential gradient is closely related to the air-earth current and atmospheric conductivity. The field can undergo considerable fluctuations near the ground owing to conductivity variations and local generators. Here, the measured value of air-earth current density was compared with that of the potential gradient measured with a horizontal wire-passive antenna. Resemblances were observed in Fig. 5.5.

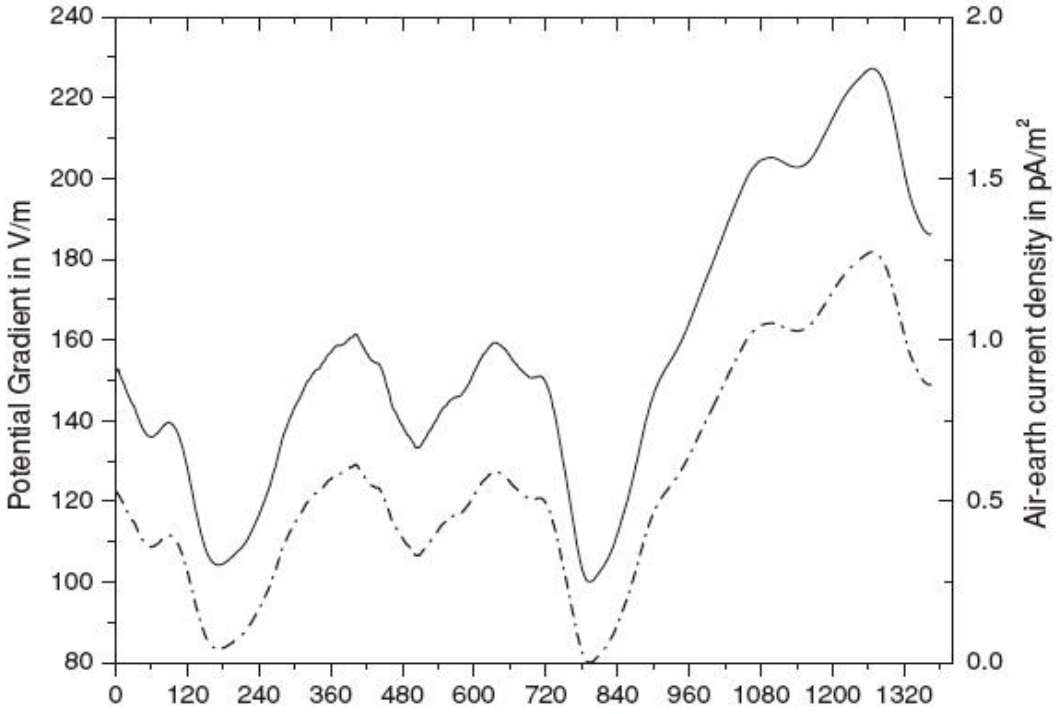

Fig. 5. 5 Plot of 1-min average of the air-earth current values of Wilson's plate (dotted line). The continuous plot shows the potential gradient values of passive antenna at measuring site Tirunelveli on the 25 April 2007.

When the diurnal variations of atmospheric electrical signatures were compared, implying that the columnar resistance remains almost steady at the measuring site. On the other hand, the measuring site is less polluted. Thus, the variations in Fig. 5.5 can be seen as (1) partially a world-wide variation associated

with the variation of V, the potential of the electrosphere (or ionosphere), and (2) partially a local variation related to the variation in R_C, the local columnar resistance. The above relation is used to predict the spatial variation of air-earth currents from the known variation of V with universal time and assumed variation R_C with local time. The present data on electric field and current do shows two minimum at 0300 & at 1300 UT and a maximum at 1900 UT. The 0300 UT minimum and 1900 UT maximum is due to the global thunderstorm activity contributing to the global electric circuit. The second minimum at 1300 UT is due to the local activity or may be on that day the European continent thunderstorm activity is low (it is 12:00–14:00 UT). On the other hand the measured electric field and current shows similar variation and hence the conductivity during that period is constant. The minimum in the measured electric field and current parameters between 1200 - 1400 UT probably due to low thunderstorm activity in European continent on that day.

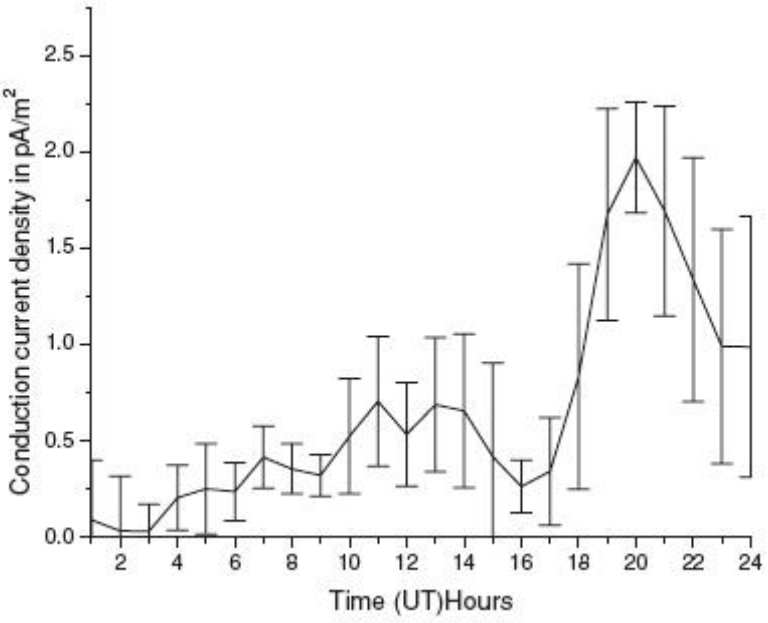

Fig. 5.6 Plot of average of 42 fair-weather days during the observation period.

Figure 5.6 illustrates the average picture for 42 fair-weather day observations. A general characteristic is that the minimum value lies at 03:00 UT and a broad maximum lies near 19:00–20:00 UT. An air-earth current sensor placed over the continents other than the polar/ocean region may show the variation with respect to local and regional origin. Since the observed site here is a tropical site, the sunrise effect and other diurnal variations are statistically removed in graph shown in Fig. 5.6, with the vertical bar showing the standard deviation. The observations can be compared with the classical Carnegie expedition curve (Whipple and Scrase, 1936). As a result of the global distribution of lightning, there are three main centers of lightning activity over the three tropical continental landmasses. In addition to the tropical lightning, extra tropical lightning activity plays a major role in the summer season in the northern hemisphere (Whipple and Scrase, 1936), resulting in global lightning activity being a maximum in June–August. Since the lightning activity in the tropics maximizes late in the local afternoon (14:00–16:00 IST), the combination of the spatial and temporal activity produces the well-defined diurnal cycle in measurements of the global electric circuit, with the ionospheric potential agreeing well with the 'Carnigie curve', thereby confirming that lightning plays a major role in the global electric circuit. There is a good agreement between the fluctuating component of the global circuit and global lightning activity (Tinsley and Heelis, 1993). All of these studies show that the global electric circuit has a maximum at approximately 18:00 UT and a minimum at 03:00 UT. This variation has been widely observed elsewhere and, according to classical theory, this is attributed to the variation with time of day of the thunderstorm activity across the globe.

5.3.2 Long –term (over a decade)

In the present work, vertical Maxwell current data for years 1996 – 2005 analyzed for the long term GEC studies. Hourly average adopted for this study to avoid short period variations on the measured atmospheric electric parameters. We have explored the possibility of identifying the signature of the DC global circuit in our Maxwell current data. For this purpose only, the fairweather days each month are considered and the diurnal variations are closely examined. The number of fairweather days for each month during the years 1996–2005 is given in Table 5. 1.

YEAR	JAN	FEB	MAR	APR	MAY	JUN	JUL	AUG	SEP	OCT	NOV	DEC
1996	N	N	N	N	N	Y	Y	Y	Y	Y (6)	Y	Y
1997	Y (6)	Y (0)	Y (13)	Y (2)	Y (0)	Y (0)	Y (0)	Y (0)	Y	N	N	N
1998	N	N	N	N	N	Y (0)	Y (14)	Y (0)	Y (0)	Y (0)	Y (15)	Y (12)
1999	Y (9)	Y (7)	Y (10)	Y (0)	N	N	Y (4)	N	Y	Y	Y (11)	Y (17)
2000	Y (12)	Y (13)	Y (5)	Y (0)	Y (0)	Y (12)	Y (3)	Y (0)	Y (0)	Y (2)	Y (10)	Y (6)
2001	Y (11)	Y (18)	Y (19)	N	N	N	Y (12)	Y (17)	Y (4)	N	Y (6)	Y (6)
2002	Y (21)	Y (2)	Y (7)	Y (5)	Y (0)	Y (8)	Y (16)	Y (12)	Y (7)	Y (6)	Y (8)	N
2003	Y (5)	Y (11)	Y (15)	Y (16)	Y (8)	Y (5)	Y (12)	Y (10)	Y (19)	N	N	N
2004	N	N	Y	Y	Y	N	N	N	N	N	N	N
2005	Y (19)	Y (12)	Y (17)	N (0)	Y (18)	Y (20)	Y (11)	Y (4)	Y (7)	Y (5)	Y (0)	Y (5)

Table. 1. Y-Data available, N-No data. No of fair weather days yearwise: 1997-21, 1998-41, 1999-58, 2000-63, 2001-93, 2002-92, 2003-101, 2004-0, 2005-118. Total No of fair weather days: 587.

A total of 587 fairweather days were observed during this period. The overall average diurnal variation of the Maxwell current for the period 1997–2005 is shown in Fig. 5.7(a). The error bars indicate the standard deviation representing the variation in the observed current density. The diurnal variation has a minimum at about 04:00 UT and two maximums, one at 01:00 UT and the second at approximately 20:00 UT.

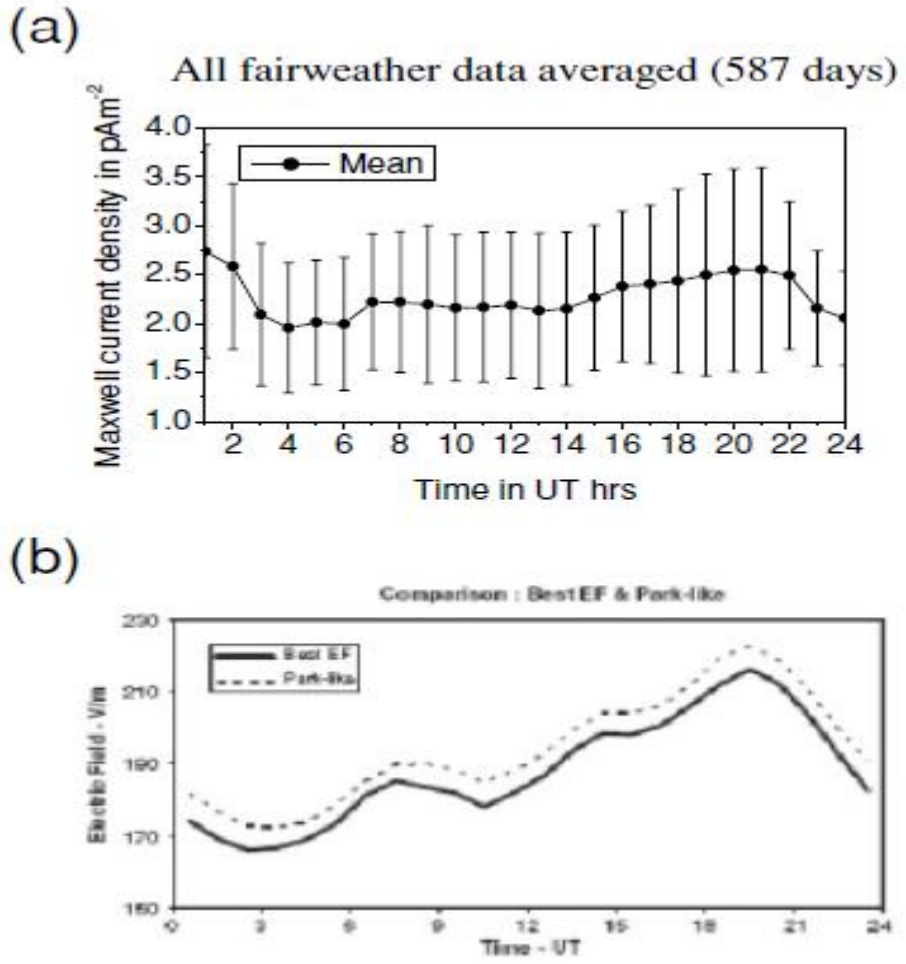

Fig. 5. 7. (a) The overall average diurnal variation of the Maxwell current during the period 1997–2005. (b) Average diurnal curves of vertical electric field, Vostok (from Burns *et al.*, 2006).

The first maximum is the local sunrise effect, and the second maximum in the pre-midnight (Local Time = UT +5.30 h) hours is possibly associated with the global peak in thunderstorm activity. The normal daytime value is reached in less than 2 h after the sunrise. This feature is often referred to as the 'sunrise effect' (Muir, 1975; Panneerselvam *et al.*, 2003). This effect is not detected on mornings when there is rain, haze, or dense cloudiness. The maximum that occurred in the premidnight hours for each fairweather day might be associated with the global thunderstorm activity. Excluding the sunrise enhancement, the diurnal variation of the measured Maxwell

current at Tirunelveli resembles the Carnegie curve discussed often in the literature (Roble, 1985). The measured Maxwell current density compared with the past reports of electric field measured at Vostok, Antarctica is shown in Fig. 5.7(b).

Continuous ground based measurements of atmospheric electrical parameters are valuable for establishing the regional electrical climate. They are also necessary for understanding what processes control and maintain the global electrical circuit. For this purpose, long-term measurements need to be made under fairweather conditions at sites remotely located from anthropogenic influences. It was believed in the past that sensors located within the planetary boundary layer in a tropical site would essentially measure electrical parameters influenced by boundary layer processes like convection and turbulence. On the other hand, equipment installed on a mountain top above the boundary layer, on a remote island, or on an ocean surface are expected to measure the atmospheric electrical parameter signals associated with the thunderstorm activity, presuming that Wilson's classical hypothesis is true. In this scenario, the measurements of Maxwell current measurements reported herein from a remote tropical location are considered to be important. Having established the sensitive nature of the long-wire antenna to the changing electrical environment, the diurnal behavior of the measured current at Tirunelveli during fair-weather conditions was examined. The prominent features in the diurnal behavior are the sunrise effect and the minimum and the pre-midnight maximum in the Maxwell current. In Fig. 5.7(a) we have removed the sunrise effect data points for comparing the tropical station Maxwell current, density with the polar station atmospheric electrical parameters. Excluding the local sunrise effect in the measured Maxwell current, the diurnal behavior is remarkably similar with the past reports of electric field measured

at Vostok, Antarctica. The Maxwell current data from Tirunelveli do in fact reflect the global changes in the atmospheric electrical parameters, and they are not contaminated by local disturbances during fair-weather conditions. The local pre-midnight maximum in the measured Maxwell current occurring at approximately 20:00 UT in the present work is possibly associated with the DC component of the global electric circuit.

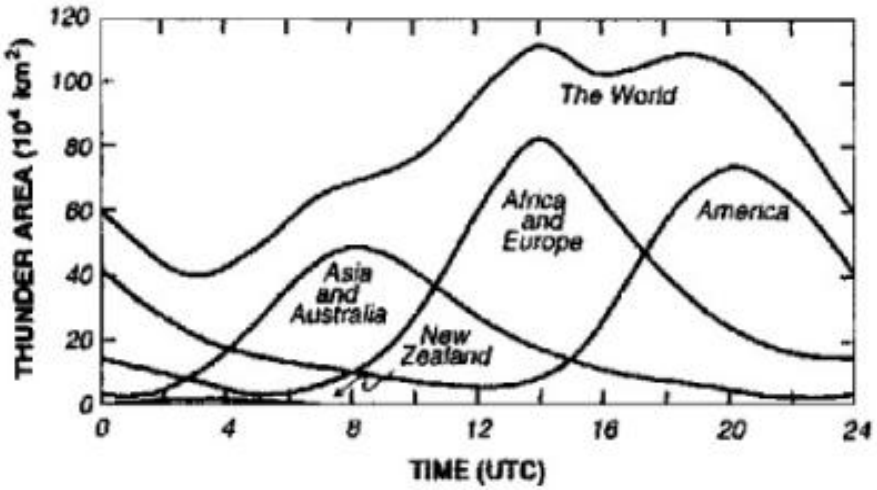

Fig. 5.8 Diurnal variation of worldwide areas of thunder over land. Individual curves are labeled to indicate the continental regions whose thunderstorm activity is plotted (from Whipple and Scrase, 1936).

The day-to-day variability in the measured Maxwell current density (diurnal variation) is attributed to the different thunderstorm regions active at different times worldwide, as shown in Fig. 5.8. The thunderstorm processes over the Malaysian Archipelago and the adjoining maritime continent extending from South Asia across the Philippines, Indonesia, and Borneo into Northern Australia, are active around 1000 UT. The sub- Saharan African region is active around 16:00 UT and the Americas principally, the Amazon basin in South America is active around 22:00 UT. The other mechanisms that might influence the occurrence of this maximum are the

ionospheric wind dynamo process and the solar wind-magnetosphere interaction. Both these processes lead to a large potential drop within the upper atmosphere, thereby contributing to significant changes in the spatial and temporal behavior of the global air–Earth current (Roble, 1985). According to the modern GEC theory, one also has to include the magnetospheric /ionospheric contributions. A detailed study is currently being carried out and is discussed in next chapter.

5.4 Diurnal variations of GEC parameters (Maitri, Antarctica)

For this study we have analyzed the data of atmospheric electric field and Maxwell current data during fair-weather days considered for the month of January / February 2001, which is collected at Maitri, Antarctica. Hourly average adopted for analysis to avoid short period variations which is shown in Fig 5.9.

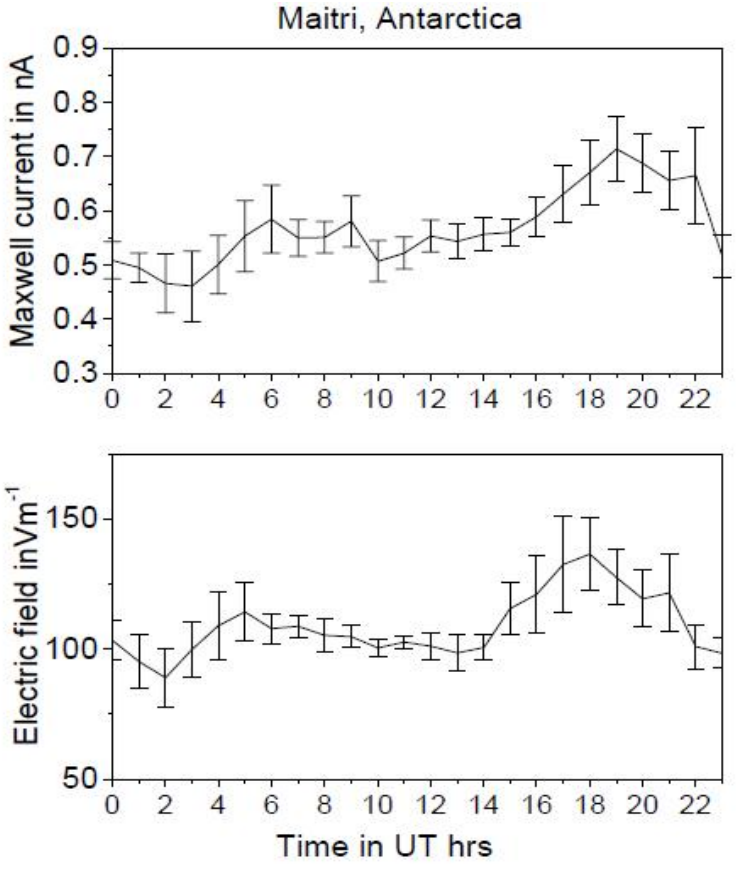

Fig. 5. 9 Diurnal variations of Maxwell current and vertical electric field

The diurnal pattern shows single maxima at about 1900 UT and minimum near about 0300 UT which is following the famous "Carnegie curve". The data from Antarctica show that the sunrise effect is not present at this station. Since the observation is made during the austral summer there is no any significant change in the sunlight as the sun is visible round the clock. The error bar indicates the large day to day variability of the measured atmospheric electrical parameters. The measurement made during high sunspot activity and hence more geomagnetic disturbance that has the influence to the ground electric field and current. The solar sunspot cycle is shown in Fig 5. 10. (for reference)

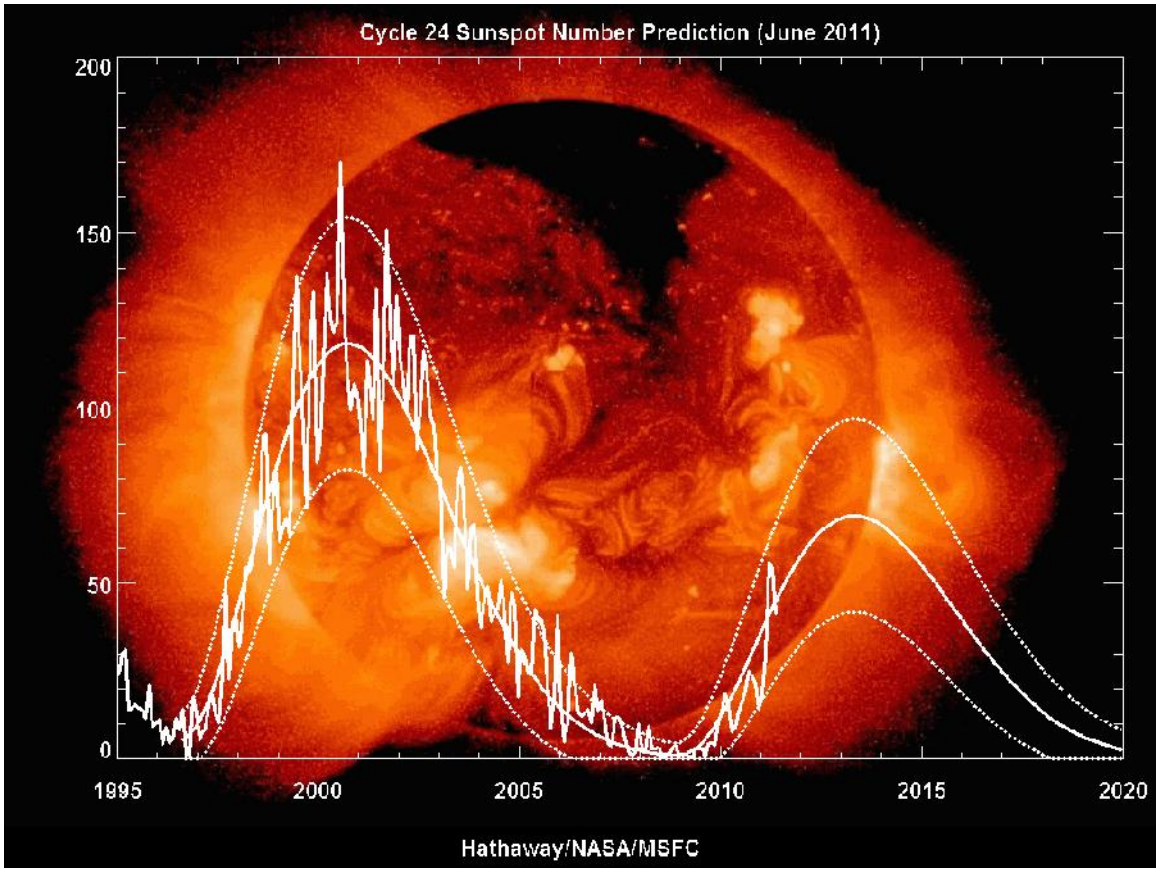

Fig 5.10 The sunspot cycle from 1995 to the present. The jagged curve traces actual sunspot counts. Smooth curves are fits to the data and one forecaster's predictions of future activity. Credit: David Hathaway, NASA/MSFC

During our observation period the mean sunspot number is nearly 150 and one can expect more magnetic disturbance at polar region. Part of the day-to-day variations may be ascribed to the solar wind/magnetospheric and ionospheric contribution because our station is outside the region of auroral oval during the magnetically quiet times and is encompassed by the auroral oval under magnetically disturbed conditions. The measured atmospheric electrical parameters have the influence of upper atmospheric contribution during this period. The Maxwell current is plotted against the electric field in Fig. 5. 11 and as noted the correlation coefficient for these measured parameters has a high value (more than 0.8) during these fair weather days. The estimated atmospheric conductivity is 2.0 X 10^{-14}S/m.

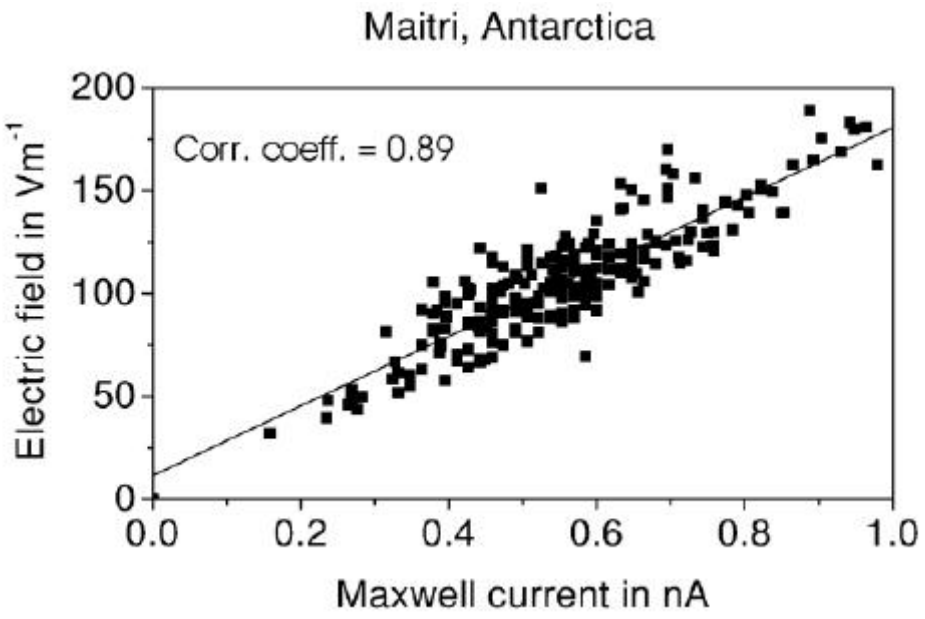

Fig. 5. 11 Scatter plot for Maxwell current and electric field at Maitri, Antarctica for 10 fairweather days during January/February 2001.

Measurements from the southern continent, Antarctica, with a similar experimental setup at equatorial station, Tirunelveli confirm our analysis of local and

global effects in the data obtained from the continental site. Above results support our view that our equatorial station site is free from local pollution and is suitable for long-term measurements of atmospheric electrical parameters. The Antarctic data have shown the capability of providing high quality and high resolution data for monitoring the global electric circuit (Panneerselvam *et al.*, 2007), to study the long-term climate and short period weather coupling processes. With continuous measurements of atmospheric electrical parameters and the geomagnetic field variations there is scope for addressing to the problems related to the modulation of global electric circuit by upper atmospheric effects.

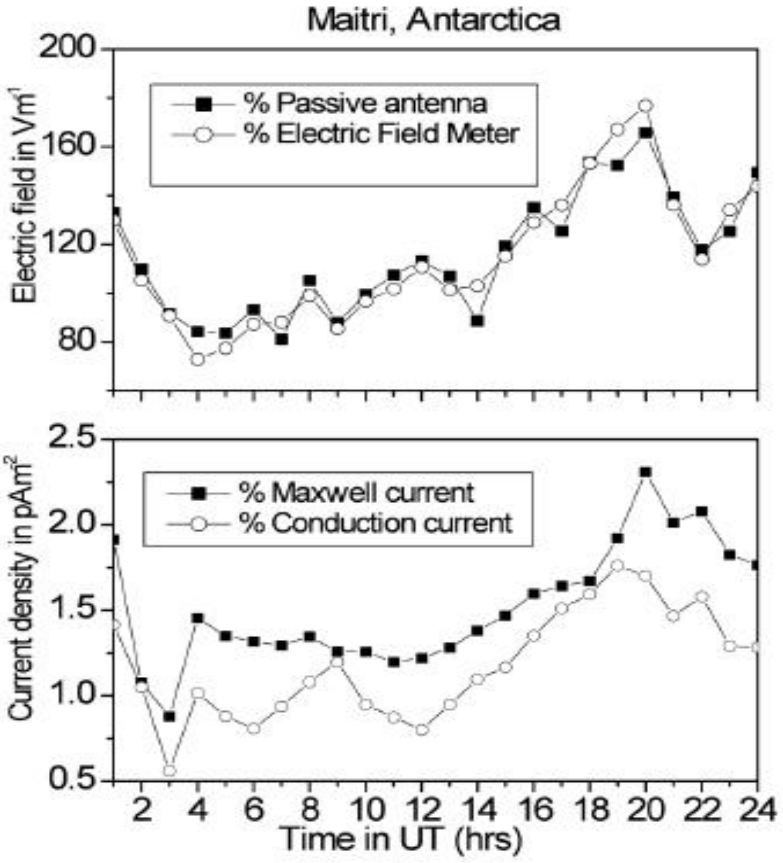

Fig . 5. 12 Diurnal variation of atmospheric electrical parameters during summer 2008/2009.

The diurnal variation of the hourly averaged values of the atmospheric electric field and current density for the period of November 2008 – February 2009 is depicted in Fig. 5. 12. The diurnal variation of curve of electric field using passive antenna and Electric Field Mill (EFM-100) during fairweather days has a single period with a minimum at 04:00 UT and a maximum at 19:00 UT. The atmospheric current variation has minimum 03:00 UT and has a maximum for Maxwell current at 20:00 UT and 19:00 UT for the conduction current, which is very similar to the Carnegie curve. This variation has been widely observed, and according to classical theory, it is generally attributed to the variation with time of day of the number of thunderstorms across the globe (Roble, 1985). Day-to-day variations may be ascribed to the solar wind/magnetospheric and ionospheric contribution because our station is outside the region of polar currents during the magnetically quiet conditions. Electric fields are generated in the ionosphere by the dynamo action and by the interaction of the magnetosphere with the solar wind and its frozen-in Interplanetary Magnetic Field (IMF). This part corresponds to mainly horizontal potentials of the order of tens of kilovolts. This horizontal potential will have effect on the measured atmospheric electrical parameters.

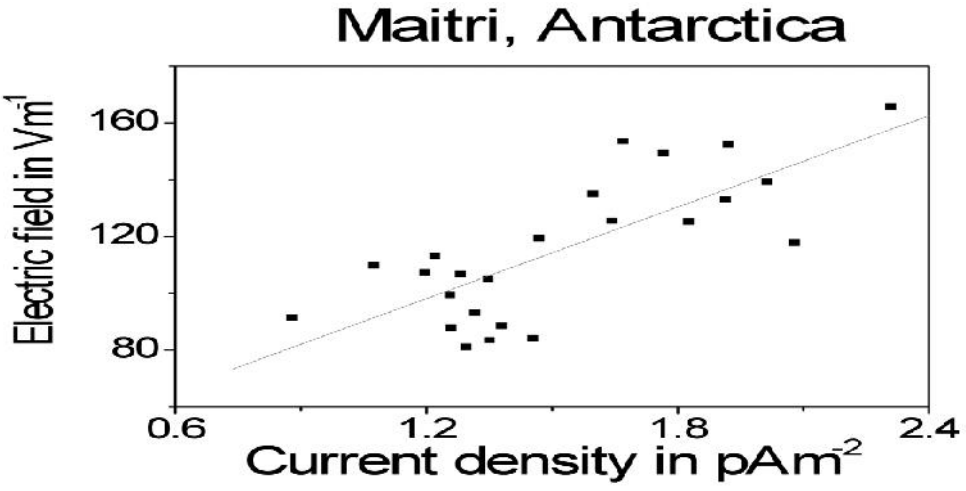

Fig. 5. 13 Conduction current *V*s electric field during summer 2008/2009.

The observations made during the sunspot minimum period more are less no sunspot during this period, the details available in www.spaceweather.com. One would expect the upper atmospheric contribution less compared to active sunspot days. Further we have selected the days during magnetic quiet day to reduce upper atmospheric contribution the measured atmospheric electrical parameters. Hourly average value of the measured conduction current density plotted against the measured electric field variations using Electric field meter are shown in Fig. 5. 13. The correlation coefficient for these parameters more than 0.9 during fairweather days and hence, during fair weather the conductivity is more or less stable. During fairweather days the electric field and current variations are similar but during meteorologically disturbed days the variation of field and current always not similar because of atmospheric conductivity variations.

Observations of the atmospheric Maxwell current and electric field made at Maitri during fairweather days for the period 2001–2004 Fig. 5. 14. The error bar indicates the standard deviation from the mean. The diurnal variation has a single periodic variation with a minimum at 03:00 UT and a maximum at 19:00 UT. Both the current and electric field variations are similar because the conductivity during fairweather conditions is nearly constant. This variation has been widely observed elsewhere and, according to classical theory, is generally attributed to the variation with time of day of the thunderstorm activity across the globe (Roble, 1985). The other mechanisms that might influence the occurrence of this maximum are the ionospheric wind dynamo process and the solar wind-magnetosphere interaction.

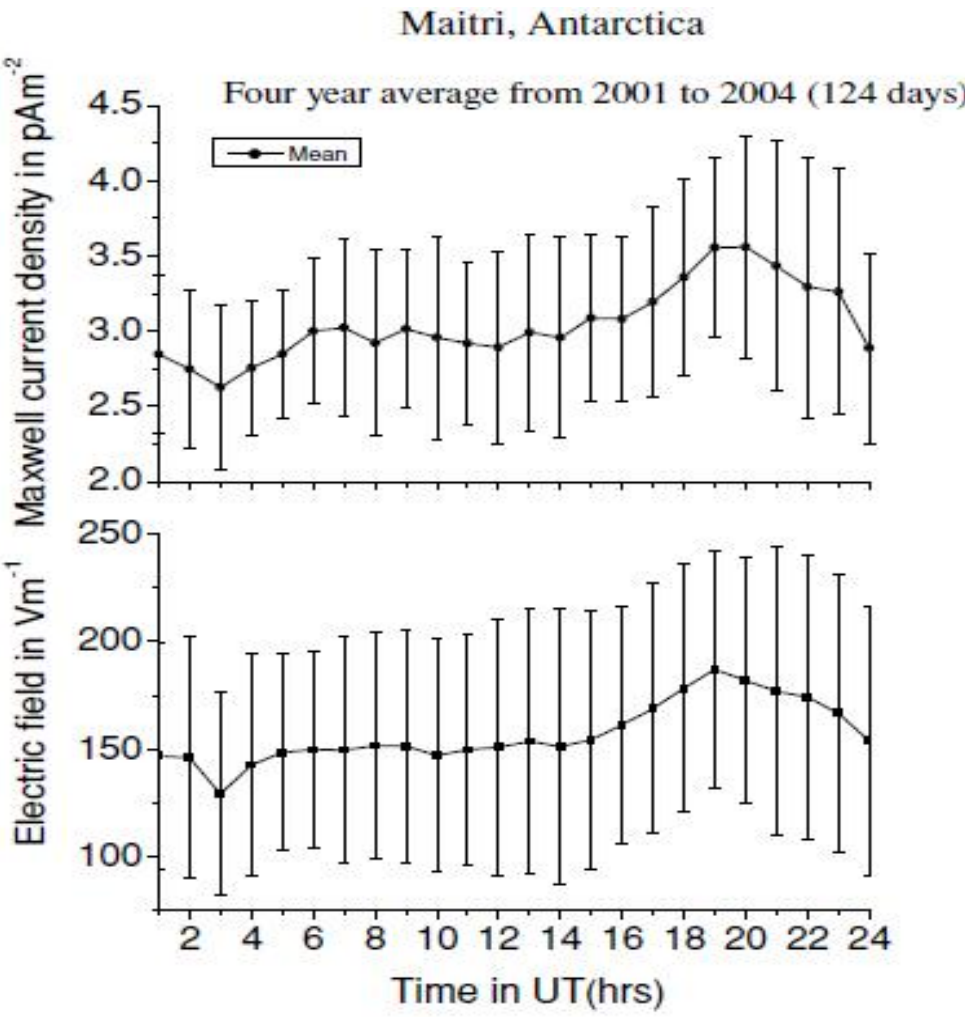

Fig. 5. 14 Diurnal variation of the electric field and Maxwell current during the period 2001–2004.

Both these processes lead to a large potential drop within the upper atmosphere, thereby contributing to significant changes in the spatial and temporal behavior of the global air–Earth current (Roble, 1985). Figure 2(a) indicated that the Maxwell current and electric field data from Maitri, Antarctica are in good agreement with earlier measurements made over oceans (Whipple and Scrase, 1936). The diurnal trend in the measured parameters is consistent with the familiar "Carnegie curve" variation. Again the day-to-day variations are so high it is because of the observations

made during maximum solar activity period. Studies on ionospheric/magnetospheric contribution to measured atmospheric electrical parameters during different geomagnetic conditions at a polar station discussed in chapter 6. The long-term operation of various atmospheric electrical sensors in Antarctica will enable a comprehensive study on the processes that control the global electric circuit as well as provide useful information about the influence of ionosphere-magnetosphere interactions occurring in the polar cap region on the global electric circuit.

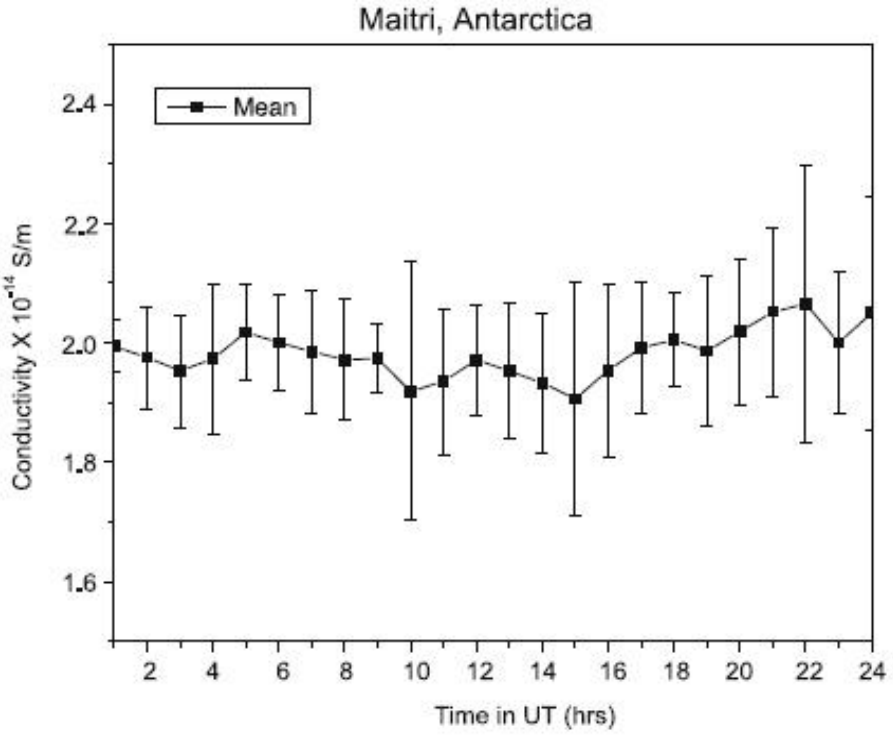

Fig. 5. 15 Diurnal variation of electrical conductivity averaged over 28 fairweather days in 2004

The electrical conductivity of both polarities has been measured at at Maitri, Antarctic with Gerdien's apparatus, which is shown in Figure 5. 15. The measured conductivity is similar with the estimated conductivity which is 2.0 X 10^{-14}S/m (Ohm's law).

CHAPTER 6

Influence of upper atmospheric electric generators on GEC and separation of different atmospheric currents

6.1 Introduction

According to the modern Global Electric Circuit (GEC) there are three main generators that operate in the Earth's global electric circuit: (1) thunderstorms, (2) the ionosphere wind dynamo, and (3) the solar wind /magnetospherice dynamo. About the above main three generators discussed below.

6.1.1 Thunderstorms generators

The major source of dc electric field is the thunderstorm in the lower atmosphere. Source of electric field in this region comprises of troposphere-stratosphere and mesosphere. Troposphere: extends from the surface of the earth to about 10 km. Galactic Cosmic Rays (GCR) and radioactivity of the earth are the main sources of ionization in this region. Temperature decreases with height and attains a minimum at the tropopause. Stratosphere: It starts from above the tropopause (~ 10 km) and extends up to stratopause (~50 km), where the temperature profile attains maximum. GCR are the prime source of ionization, in addition solar proton events provide a sporadic and intense source of ionization at high latitudes. The conductivity which is roughly of the order of 10^{-14} $mhom^{-1}$ at the earth's surface increases exponentially with altitude in the troposphere-stratosphere: main charge carriers are the small positive and negative ions. Mesosphere: this is the region of second decrease of temperature profile as seen in Figure 6.1. It extends from about 50 km to 85 km in

altitude. The major sources of ionization are the solar Layman – alpha radiation, X-ray radiation and intense auroral particle precipitation. The conductivity increases rather sharply in this region. The main charge carriers are electrons, positive ions and negative ions.

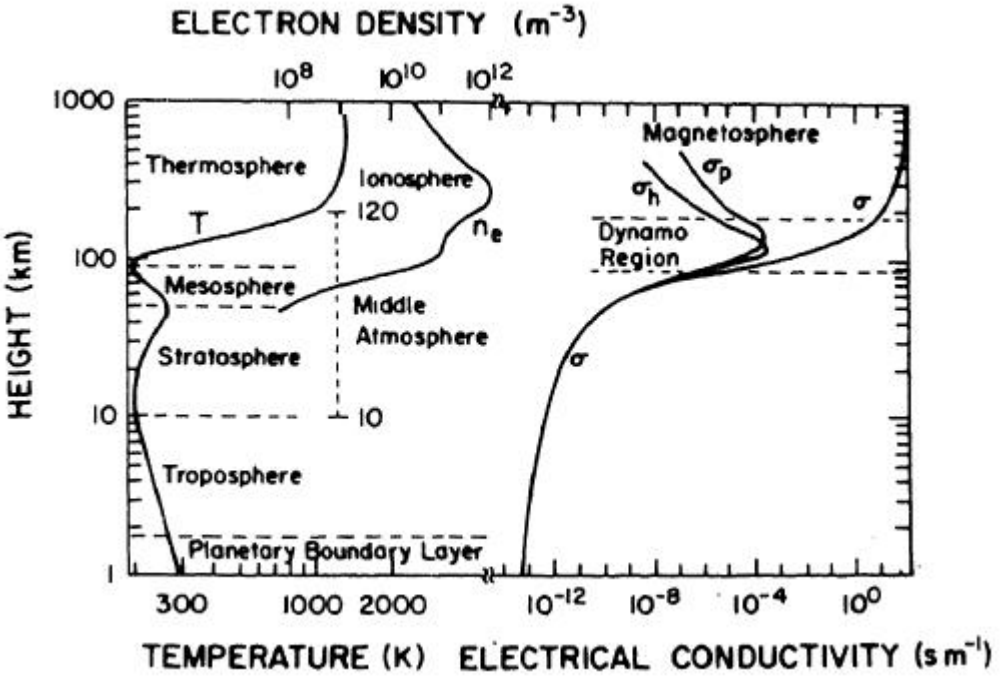

Fig. 6. 1 Divisions of Earth's atmosphere based on the profiles of the distribution of temperature, conductivity, and electron density through atmosphere

Below the cloud, a net negative charge is transferred from the thundercloud to the earth and above it positive charge is transferred to the conducting upper atmosphere/ionosphere making it at positive potential. Charge separation inside thunderstorms leads to the development of huge electric potentials and associated energized charge particle beam, which is known to radiate wide spectrum of electromagnetic waves such as optical emissions, X-rays and gamma rays (Fishman et al., 1994; Rodger, 1999; Milikh and Valdivia 1999).

Lightning activity is mainly concentrated in three distinct zones - East Asia, Central Africa and America. Lightning is more prevalent in the northern hemisphere than the southern hemisphere and mostly occurs over the land surface. The variation of lightning activity with latitude as observed from space shows that two of every three lightning flashes occur in tropical region (Williams, 1992). In addition to the tropical lightning, extra-tropical lightning activity plays a major role in the summer season in the northern hemisphere, resulting in the global lightning activity having a maximum from June to August. The diurnal variation of the electric field over the oceans and of the worldwide thunderstorm activity supports the hypothesis that thunderstorms are the main electrical generators in the GEC. About 200 thunderstorms are active at any time, which are mainly concentrated over the tropical land masses during the local afternoons and cover about 10% of the earth's surface (Markson, 1978). On the remaining 90% of the earth's surface return current ~1000A (~ 2 pAm^{-2}) from the ionosphere to the earth's surface flows, which is also known as fair weather current. We have the voltage supply of nearly 300 kV between the base ionosphere (60 km0 and earth, with power of 700 megawatts. The vertical electric field maximum at about 1900 UT and is minimum at about 0400 UT corresponding to the global thunderstorm activity.

6.1.2 The ionosphere wind dynamo generator

The D-region of the ionosphere extends from about 60 km to 90 km. The ionosphere proper (i.e E and F regions) starts from above the mesosphere, and extends to about 500 km. the upper boundary is not well defined. The so-called thermosphere is included in the ionosphere. The major sources of ionization in the ionosphere are EUV and X-ray radiation from the sun and energetic particle precipitation from the

magnetosphere into the auroral ionosphere. The current carries are electrons and the positive ions. Electrical conductivity becomes anisotropic in this region.

The regular tidal wind system drives ionospheric plasma at dynamo layer heights and pushes it against the geomagnetic field. Ions and electrons are affected differently by these winds. While the ions being massive still move essentially with the neutrals, the geomagnetic field already controls the motion of the electrons. The differential motion of ions and electrons is responsible for horizontally flowing electric currents. Moreover, charge separation causes an electric polarization field, which is constrained by the condition of source free currents (Volland, 1987) and has been observed indirectly from backscatter measurements (Richmond, 1976). Lunar variations are usually less than 10 % of magnitude of solar variation (Matsushita, 1967). They depend not only on latitude, solar time, season and solar cycle, but also on lunar phase. Global analyses of geomagnetic lunar effects have also found significant longitudinal variations. The seasonal variations of the lunar magnetic perturbation tend to be greater than those for the solar perturbation. The lunar current system finds its origin in the ionosphere dynamo and lies close to the dynamo height along with Sq current system. The dynamo electric field associated with the wind drives a current, which tends to converge in some regions of space and cause an accumulation of positive charge, while in other regions of space it would diverge and cause negative charge to accumulate. These charges would create an electric field, which would cause current to flow tending to drain the charges. An equilibrium state would be attained when the electric-field driven current drained charge at precisely the rate it was being accumulated by the wind driven current. A net current flows in

the ionosphere owing to the combined action of the wind and electric field (Takeda and Maeda, 1980).

A large-scale vortex current at middle and low-latitudes flows counter clockwise in the northern hemisphere and clockwise vortex flow in the southern hemisphere. Traditionally these vortices are known as the Sq current system because of the nature of the ground-level magnetic field variations that they produce. Currents and electric fields produced by the ionospheric wind dynamo are relatively weak in comparison with those of the solar wind/magnetospheric dynamo at high latitudes. Electric field in the equatorial lower ionosphere has a localized strong enhancement of the vertical component associated with the strong anisotropy of the conductivity in the dynamo region. This enhanced electric field drives an eastward daytime current along the magnetic equator called equatorial electrojet (Forbes, 1981; Richmond, 1986). Efforts are being made to understand the changes in equatorial electrojet in response to the electrodynamic processes involved in the coupling between the solar wind, magnetosphere and ionosphere. This is due to dynamo region electric fields being communicated to higher latitudes along the geomagnetic field lines. Monitoring the upper atmosphere by coherent and incoherent backscatter radar observations has confirmed that the distributions in the dynamo region electric fields at equatorial latitudes originate in the corresponding electrodynamics disturbances at high latitudes (Somayajulu et al., 1985). Studies based on the surface magnetic data have shown consistent and near instantaneous response of equatorial electrojet variations to geomagnetic disturbances at high latitudes (Rastogi and Patel, 1975). Ionospheric dynamo is also affected by the absorption of ozone at the lower altitudes (30-60 km) and presence of stronger winds at higher altitudes (> 130 kms). The ionospheric wind

dynamo produces potential drops on the order of 5 – 10 kV with total current flow of 10^5 A. primarily on the dayside of the Earth. The electric filed associated with this potential pattern also map downward to the Earth's surface (horizontal potential difference). The maximum occurs in the early morning hours at the low latitude and the minimum occurs in the evening hours. The large scale features of this potential pattern map directly to the ground where a symmetric diurnal variation of a few per cent is superimposed upon the GEC.

6.1.3 The solar wind/magnetosphere dynamo

The stresses applied to the outer magnetosphere by the solar wind and dynamical processes in the tail, is ultimately applied to the terrestrial ionosphere and upper atmosphere. As a consequence of the high thermal energy of the plasma the drift motion causes charge separation and hence polarization electric field is setup directed from dawn to dusk. The currents flow along the geomagnetic field lines down into the ionosphere on the dawn side and up from the ionosphere on the dusk side, both foot points being electrically connected via the dynamo region. This process can be considered similar to a huge hydromagnetic generator situated in to the magnetosphere (in which kinetic energy of the solar wind plasma is converted in to electric energy) and the load in the ionosphere; linked to each other via field-aligned currents (Strangeway and Raeder, 2001). The work done by these currents in the ionosphere overcomes the drag on the flow over the polar cap away from the sun and on the flow back towards the sun at lower latitudes. The force on the plasma moving anti-sunward across the polar cap is supplied by the solar wind, predominantly by reconnection with the magneto-sheath magnetic field (Russel and Fleishman, 2002).

Mass, momentum and energy transfer from the solar wind via the magneto-sheath can occur through the cusps as a result of a number of processes, of which magnetic reconnection is the most important. Lester and Cowley (2000) have discussed the role played by reconnection in the magnetospheric convection and its importance for space weather. There are two processes by which the solar wind plasma can cross the magnetopause, (i) direct entry due to flow along reconnected open field lines (Dungey, 1961; Gonzalez et al., 1994) and (ii) cross field transport due to scattering across closed magnetopause field lines (Lee et al., 1994). The first process is more likely to be important when the interplanetary magnetic field (IMF) is directed southward. In this case, the solar wind and magnetospheric field lines are anti-parallel; the magnetic reconnection can occur easily leading to 5 to 10% solar wind energy imported into the earth's magnetosphere (Weiss et al., 1992) during sub-storms and storms. During northward IMF intervals, the energy injection due to magnetic reconnection is considerably reduced and cross-field transport becomes important. Tsurutani and Gonzalez (1995) have estimated that about 0.1 to 0.3% of the solar wind energy gets transferred to the magnetosphere during northward IMF. Several other processes, like impulsive penetration of the magneto-sheath plasma elements with an excess momentum density (Owon and Cowley, 1991), plasma entry due to solar wind irregularities (Schindler, 1979), the Kelvin Helmholtz instability (Miura, 1987) and plasma percolation due to overlapping of a large number of tearing islands at the magnetopause (Galeev et al., 1986) have been suggested for the plasma transport across the magnetopause. The finite dawn-dusk electric field imposed by the solar wind magnetosphere interaction in the whole cavity accelerates the ions and to a lesser extent the electrons in the central part of the plasma sheet, where the magnetic field almost vanishes.

The plasma in the plasma sheet has very large ratio □between the kinetic and the magnetic pressure, this makes the system extremely unstable; very fast developing time variations called sub-storms, do develop in the plasma sheet. Prior to a sub-storm, the plasma sheet extends to a large space where the vertical component of the magnetic field becomes significant. The plasma is pushed earthward by E X □B convection (E being essentially dawn to dusk) and the tail current increases. As plasma is convected inward, it faces increased magnetic field. The conservation of the adiabatic invariants leads to the energization of plasma by Fermi and betatron mechanism. The small-scale fluctuations that develop within the magnetospheric boundaries/discontinuities also play a significant role in accelerating electrons along field lines. Energetic particles, especially electrons precipitate from the magnetosphere due to wave-particle interaction in to the upper atmosphere and produce the visible emissions called the aurora borealis (in the north) or the aurora austral is (in the south). This energetic particle precipitation also causes significant ionization, heating and dissociation in the thermosphere. Further, the energized plasma also has an important influence on the flow of the electric currents and on the distribution of electric fields *(*Spiro and Wolf, 1984*)*. Energetic particles drift in the Earth's magnetic field, electrons towards the east and positive ions towards the west, so that a westward ring current flows which exerts an electromagnetic force on the plasma directed away from the Earth; thus tending to oppose the earthward convection. Charge separation associated with the ring current tends to create an eastward electric field component, opposite to the night side westward convection electric field, largely canceling the convection electric field in the inner magnetosphere. The overall pattern of the magnetospheric convection tends to map along the magnetic field line in to the ionosphere even though this mapping is

imperfect because of net electric field that tends to develop within the non-uniform energetic plasma. In the upper ionosphere,

$$E_{Plasma} = 0 = E + \mathbf{V_s} \times B$$

where E is the electric field in the Earth fixed frame of reference, Vs is velocity of solar wind plasma with respect to the Earth and B is geomagnetic field vector. The electric fields due to solar wind /magnetosphere dynamo map down to the auroral ionosphere and produced potential difference across the polar cap of the order of 50 kV to more than 200kV depending on geomagnetic conditions. This generator can produce perturbations of 20% in the air-earth current and ground electric field at high latitude during geomagnetic quiet times, and larger during the geomagnetic storm periods.

We have already discussed about the diurnal variation of atmospheric current and electric field in the earlier chapter. Earlier exercise we have considered only for the fair-weather days and we have not considered the geomagnetic conditions (Geomagnetic quiet and disturbed days). Because of upper atmospheric contribution to the ground atmospheric electrical parameters during magnetic disturbed days is so large compared to quiet days. To look in to the day-to-day variation in this section we have selected the days which satisfies the geomagnetic quiet day conditions.

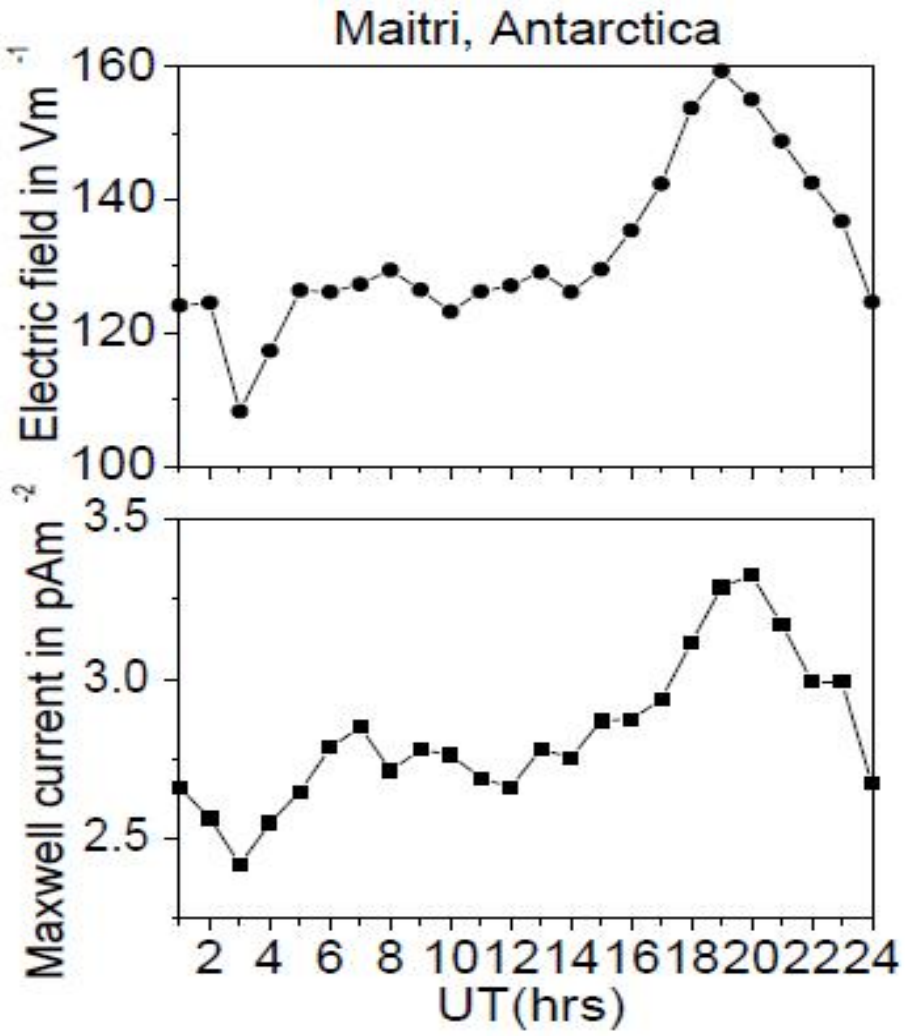

Fig. 6. 2 Diurnal variations of Maxwell current density and electric field averaged for 37 fairweather days at Maitri.

In this chapter we are discussing the global thunderstorms contribution to global electric circuit in the absence of upper atmospheric influence (we can say very less contribution). For this exercise, atmospheric electrical parameters Maxwell current and electric field measured at Maitri, Antarctica, during austral summer have been analyzed for the years 2001 to 2004. A total of 69 days were selected which satisfied the 'fairweather' conditions, i.e., days with absence of high winds, drifting or falling snow, clouds, and fog effects throughout the day. From 69 fair weather days we have 37 fair weather days with geomagnetic quiet days. The diurnal variation of

37 fair weather days (geomagnetic quiet) plotted in Fig. 6.2. The diurnal variation curve of electric field and vertical current averaged for 37 fairweather days is a single periodic with a minimum at 03:00UT and a maximum near 19:00UT, which is very similar to the Carnegie curve.

6.2 Influence of upper atmospheric contribution to GEC

In this study we have selected days which is a fairweather days on which different geomagnetic conditions like magnetic quiet days, moderate and disturbed days (geomagnetic storm days) were considered. Geomagnetic storm is defined in general, by the existence of a main phase during which the magnetic field at earth's surface is depressed and this depression is caused by a westward ring current in the magnetosphere. The main phase of geomagnetic storm is characterized by the 'frequent' occurrence of intense substorms. It is believed that the magnetospheric substorm results when the energy stored in the magneto-tail is explosively released towards the inner magnetosphere and finally deposited as heat energy in the upper atmosphere. During substorm activity some of the ionized particles drift around the Earth and enhance the ring current as well as energy. Field aligned current intensity and particle precipitation are increased. Dramatic increases are observed in ionospheric current which flows across the night side auroral ionosphere. The brightening and expansion of the auroral forms are observed when viewed from the ground. The electric field due to solarwind/magnetosphere dynamo map down to auroral ionosphere and produced potential difference across the polar cap of the order of tens of kilovolts depending on the geomagnetic conditions. It will also have measurable effects on the vertical electric field and current. The auroral or magnetic substorm activity lasts from about one hour to a few hours. Such studies help in the

investigation of the influence of high latitude upper atmospheric contribution to the measured electrical parameters.

Part of the day-to-day variations may be ascribed to the solar wind/ magnetospheric and the ionospheric contribution because our station is outside the region of auroral oval during the magnetically quiet times and is encompassed by the auroral oval under magnetically disturbed conditions. According to the modern GEC theory one has to include the magnetospheric / ionospheric contributions also. Electric fields are generated in the ionosphere by the dynamo action and by the interaction of the magnetosphere with the solar wind and its frozen-in interplanetary magnetic field (IMF). This part corresponds to mainly horizontal potentials of the order of tens of kilovolts. This horizontal potential will have effect on the measured atmospheric electrical parameters. Through the observations made during the sunspot maximum year, one would expect more magnetic storms that may produce large day-to-day variation in electric field and Maxwell current density.

An attempt has been made to identify the geomagnetic influences on the Maxwell current density and electric field associated with dawn-dusk potential difference across the polar cap. The dawn-to-dusk horizontal potential difference (up to 100 kV) across the polar cap arising from the interaction of the solar wind with the magnetosphere, which causes the two-cell convection pattern in the polar region, one side it is clockwise and the other is anti-clockwise. This enhanced clockwise cell would map to increased upward vertical electric field and current at the ground. The anti-clockwise cell dawn convection would map to decrease the atmospheric vertical electric field and current. Our data (69 fairweather days) were classified into three sets

according to the geomagnetic conditions: geomagnetically quiet, moderately disturbed and disturbed days. The international quiet and disturbed days are downloaded from the website "World Data Center for Geomagnetism, Kyoto". The selection of the quietest days (Q-days) and most disturbed days (D-days) of each month is deduced from the *Kp* indices on the basis of three criteria for each day: Geomagnetic disturbances can be monitored by ground-based magnetic observatories recording the three magnetic field components. The global *Kp* index is obtained as the mean value of the disturbance levels in the two horizontal field components, observed at 13 selected stations. The sum of the eight *Kp* values.

1. The sum of squares of the eight *Kp* values.
2. The maximum of the eight *Kp* values.

According to each of these criteria, a relative *order number* is assigned to each day of the month, the three order numbers are averaged and the days with the lowest and the highest mean order numbers are selected as the five (respectively ten) quietest and the five most disturbed days. The normalized Maxwell current density and electric field diurnal variations for magnetically quiet, moderate and disturbed days are shown in figure 6.3.

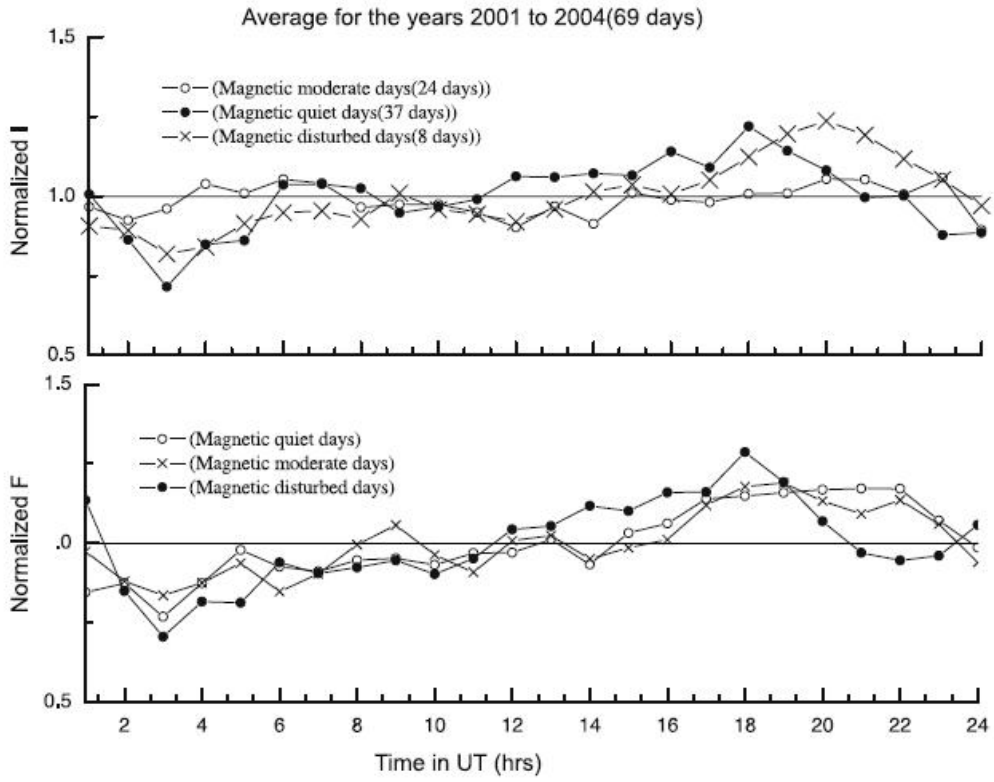

Fig. 6. 3 Normalized electric field and Maxwell current density during different geomagnetic conditions.

We had 37 quiet days, 24 moderately disturbed days and 8 disturbed days among the selected 69 fairweather days. During magnetically quiet and moderately disturbed days the variation of the Maxwell current density and electric field follows the global thunderstorm variation like the famous 'Carnegie curve'. During magnetically disturbed days the measured electrical parameters show greater variation deviated with a modification upon the UT pattern. Our station is under the influence of auroral oval during the geomagnetic disturbed period (Rajaram *et al* 2001). During magnetically quiet days the variation of atmospheric electrical parameters follows the famous 'Carnegie curve' a minimum at 03:00UT and a maximum at 19:00UT. During moderately disturbed days, the UT pattern is modified and follows the maximum at about 19:00UT but during disturbed days the diurnal pattern is modified due to the

magnetospheric/ ionospheric contribution to the measured parameters. With the continuous measurements of atmospheric electrical parameters and geomagnetic field variations, there is scope for addressing the problems related to the modulation of GEC by the influence of magnetosphere–ionosphere coupling processes on the near-surface electrical parameters in the polar caps. In this section we are concerned with the variation of the atmospheric electric field and the air– earth current due to the excessive power generated by the solar wind-magnetosphere dynamo during geomagnetic storms, recorded at Maitri in Antarctica during 2004. A major part of the power generated by the solar wind-magnetosphere dynamo is used in the formation of the ring current and the rest is utilized for Joule heating and auroral particle precipitation. The method adopted by Frank-Kamenetsky et al. [Frank-Kamenetsky A.V., Troshichev O.A., Burns G.B., Papitashvili V.O., 2001. Variations of atmospheric electric field in the near-pole region related to the interplanetary magnetic field. J. Geophys. Res. 106, A1, 179–190.] was utilized to delineate the variations due to the signatures of tropical thunderstorm activity from the geoelectric data; while statistical methods used in our earlier studies were used to delimit variation due to the constant buffeting of the solar wind. We find that the solar wind-magnetosphere energy coupling function (ε) to be well correlated with the atmospheric electric parameters during the onset of geomagnetic disturbances. However the correlation breaks down during minor storms and sub-storm events.

The polar region is one where the geomagnetic field lines are open and get reconnected rather easily when the Interplanetary Magnetic Field (IMF) points southwards and maps down to the auroral ionosphere and produces potential differences of the order of 50–120 kV across the polar cap (Tinsley, 1996; Frank-

Kamenetsky et al., 2001; Devendra Siingh et al., 2007). Though this dawn-dusk potential difference may not play a dominant role over Maitri, Antarctica (70.75° S, 11.75° E) during magnetically quiet times the plasma convection pattern expands and the station comes under the auroral oval during magnetic disturbances. As a result, the potential gradient at this station varies with respect to over-head ionospheric potentials. To gain insight into this phenomenon, we analyzed the energy coupling function (ε) with the recent data of atmospheric electrical measurements made during geomagnetic storm periods. We therefore investigate the developments in the vertical electric field (E) and air–earth current density (J) measurements made close to the earth's surface at Maitri, during the time of Coronal Mass Ejections (CMEs) associated with major magnetic disturbances during 2004. The diurnal variations were statistically removed by the method of Frank-Kamenetsky et al. (2001). The energy coupling function (Akasofu's (1981) computed from ACE satellite data during 2004. Variations in the atmospheric near surface vertical electric field and air–earth current density in Maitri in 2004 were analyzed in conjunction with changes of the magnetospheric energy coupling function. A total of 36 days were selected which satisfied the 'fairweather' conditions. Out of these 36 days, 20 were highly magnetically disturbed days with Coronal Mass Ejections (CMEs). The solar ejections consisted of hot electrons, protons and helium ions embedded in a magnetic field of various intensities that propagated with supersonic velocities. When directed towards the earth they caused geomagnetic disturbances and atmospheric ionic excitation or relativistic electron impact excitation. We measured conjugate data of atmospheric electrical measurements at the aurora oval, after expansion (at Maitri), to investigate the electrical process during, before and after CMEs associated variation (during a fair weather period) in atmospheric electric field and air–earth current, with the aid of the

energy coupling function. It has been proven by Perreault and Akasofu (1978) and Akasofu (1981) that the main phase of a geomagnetic storm is primarily controlled by the solar wind parameter (ε) given by

$$\varepsilon = \frac{4\pi}{\mu_0} VB^2 \sin^4 \frac{\theta}{2} l_0^2 \text{ J/s}$$

where μ_0 is the permeability of free space, V (m/s) is the solar wind speed, B (Tesla) is the magnitude of the IMF, θ is the polar angle of the IMF projected onto the Y–Z plane and l0 (m) is seven earth radii. Later Kan et al. (1981) identified this parameter (ε) as the power generated by the solar wind magnetosphere dynamo. Using numerical methods we computed (ε) in each case and compared it with air–earth currents and vertical electrical fields. To quantify the solar wind magnetosphere interaction under various interplanetary magnetic field conditions, we conducted a study on the influence of azimuthal and vertical components of IMF on atmospheric electrical parameters at Maitri, Antarctica during 2004 and the results are presented in Anil Kumar et al. (2006). This is necessary for estimating the efficiency of the solar wind-magnetosphere dynamo, and mass and energy transferred to the magnetosphere. We have to remove global thunderstorm activity which results in a diurnal curve with peak near 19:00 UT and a minimum near 03:00 UT (Carnegie curve). The measured hourly electric field values of the non stormy days, say E (days, h) were scaled first. Then the hourly average of electric field values during magnetic stormy days $\bar{E}$ (days) equaled the hourly average of the entire magnetic storm days minus the daily hourly average of the scaled values, i.e., the scaling is described as,

$$\bar{E}(\text{day}) = \bar{E}(\text{total day}) - E(\text{days}, \text{h})$$

Similar work carried out for the air–earth current density is described as,

$$\bar{J}(\text{day}) = \bar{J}(\text{total day}) - J(\text{days, h})$$

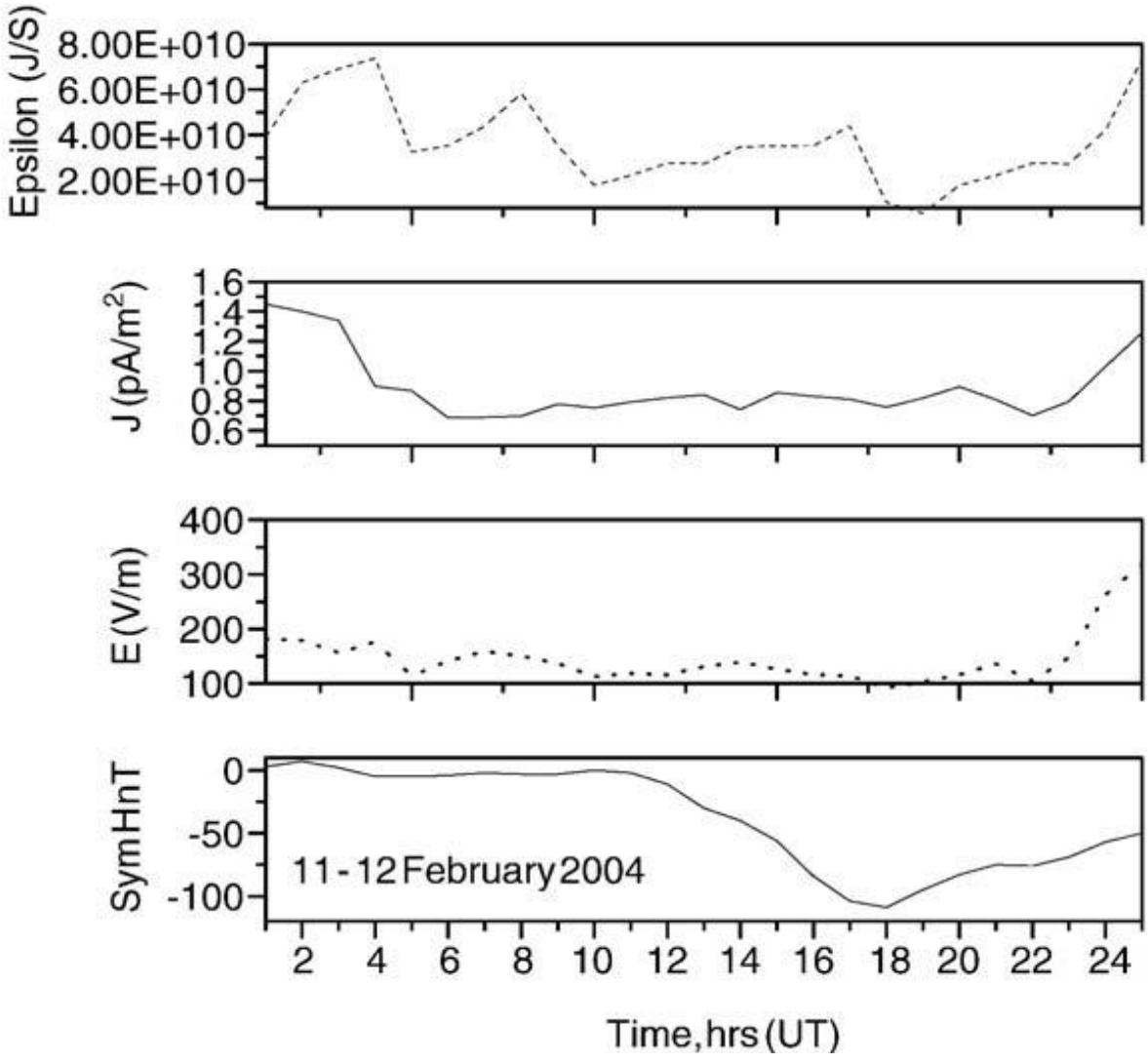

Fig. 6.4 The figure depicts CME associated changes in four panels that are compared respectively from top to bottom. The top panel shows the hourly means of energy coupling function; the second one depicts conduction current density (J_C) and the third panel illustrates the vertical electrical field (E) and the last panel shows the magnetic disturbances observed in terms of Sym-H for the storm of 11–12 February, 2004.

Fig. 6.4 represents the energy coupling function in association with the measurements of air–earth current and vertical electric field during a CME associated magnetic disturbance on the 11–12th February, 2004. A substantial increase in current is noted during 01:23 to 03:21 UT on the 11th February. During magnetic storms there is usually a decrease in cosmic ray flux, which is actually an increase in the column resistance, Tinsley and Zhou (2006). On the next day, the 12th February, an increase in both field and current is noted in conjunction with an increase in the energy coupling function. It is expected that incoming protons may be cogent agents for modulating the atmospheric electric conductivity under a favorable orientation of the IMF.

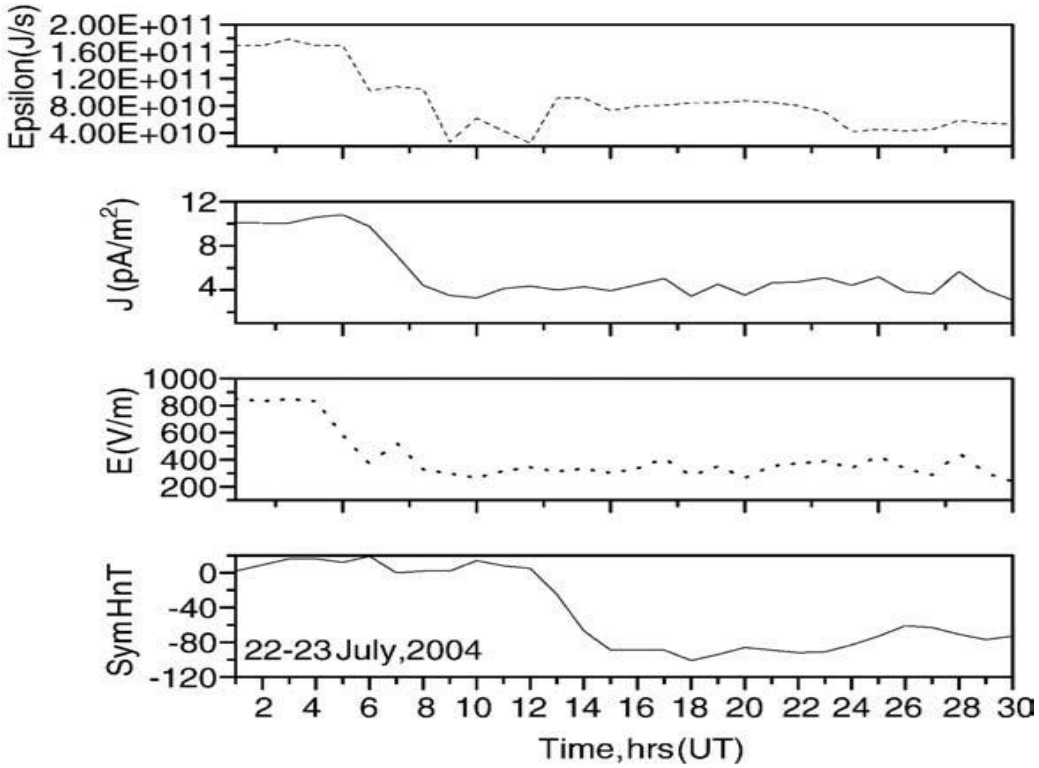

Fig. 6.5 The figure shows CME associated changes in four panels that are compared respectively from top to bottom. The top panel shows the hourly mean values of the energy coupling function; the second one depicts the conduction current density (J_C) while the third panel illustrates vertical electrical field (E) and the last panel depicts the magnetic disturbances observed in terms of Sym-H for the storm of 22nd–24th July, 2004.

Fig. 6.5 illustrates the data of global electrical parameters, viz., vertical electric field and current, which were observed during magnetically disturbed (high Kp) days, the 22nd -24th July, 2004. The results depicted above again provide strong support to the idea that the energy coupling function (ε) influences both E and J at high latitudes. The magnetic field near the earth is so strong that it is not easy for the incoming multi-ion plasma to distort the constraint. This implies that, all particles in a dipolar field line must, more or less simultaneously, move together to another field line. Convection of plasma is thus mapped between the magnetosphere and ionosphere along the field lines. Hence mapping of the point is very clear, one foot of the magnetic field line is connected to the earth's surface and the other extends into interplanetary space. This process can be considered similar to a huge hydromagnetic generator, in which a major part of the kinetic energy of the solar wind plasma is converted into electrical energy. Fig 6.6 represents the measurements of current and electric fields in support of the above suggestion. Both the GEC parameters show an increase with respect to energy coupling function during the initial phase on the 24 July 05:31 UT spanning over 21 hours. The accumulation of ions affects the conductivity profile from high to low altitude, and due enhancement in air–earth current is expected. The same trend is not repeated during 27th July 22;00 UT to 28th July 08:12 UT. This is the reason why the initial and main phases of the geomagnetic storm are considered as a time invariant enhancing mechanism in the high latitude atmospheric electrical environment, even though we have considered the station Maitri in a rotating frame of reference.

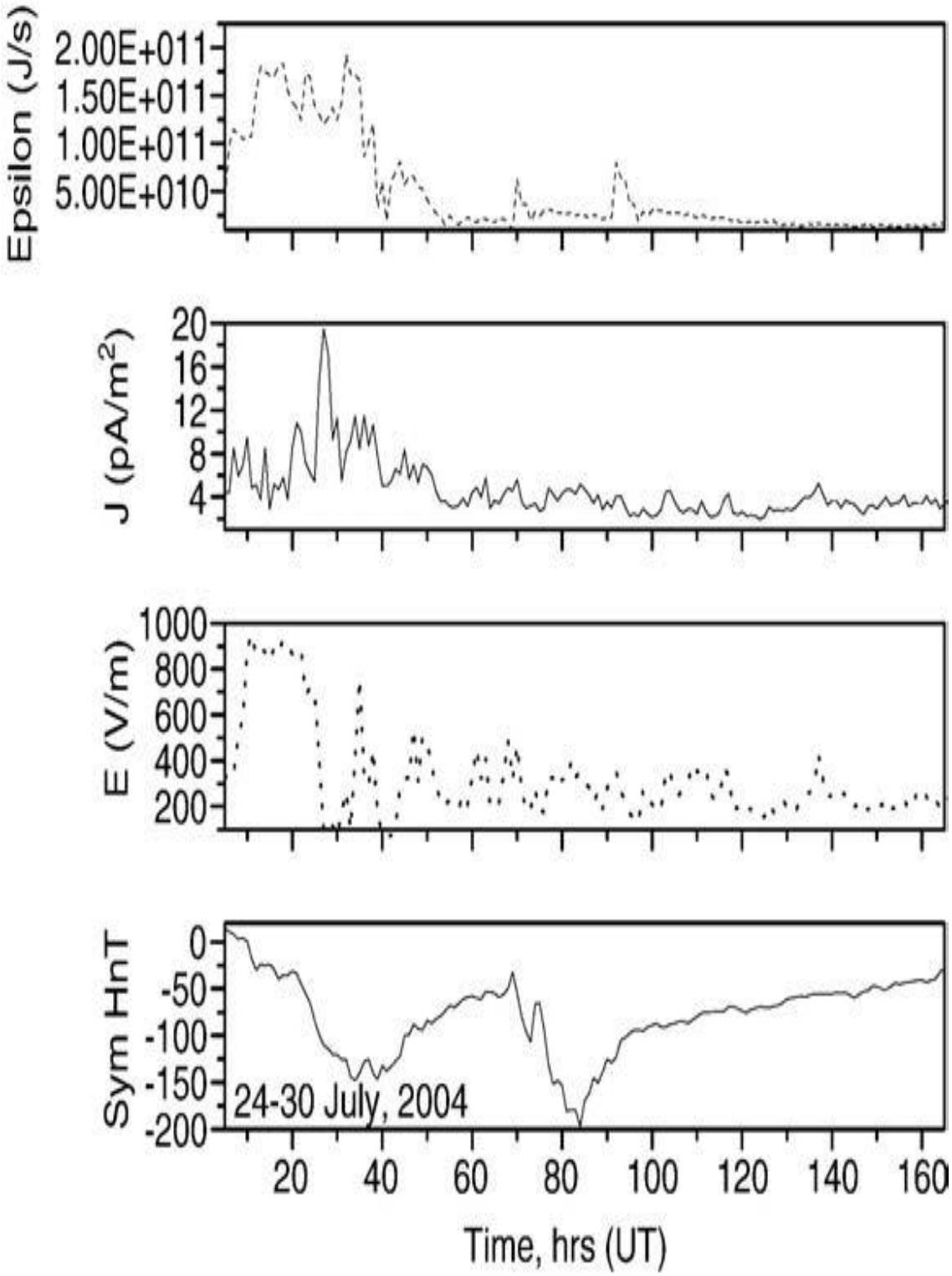

Fig. 6. 6 Same as Fig 6.5 but for 24–30th July 2004.

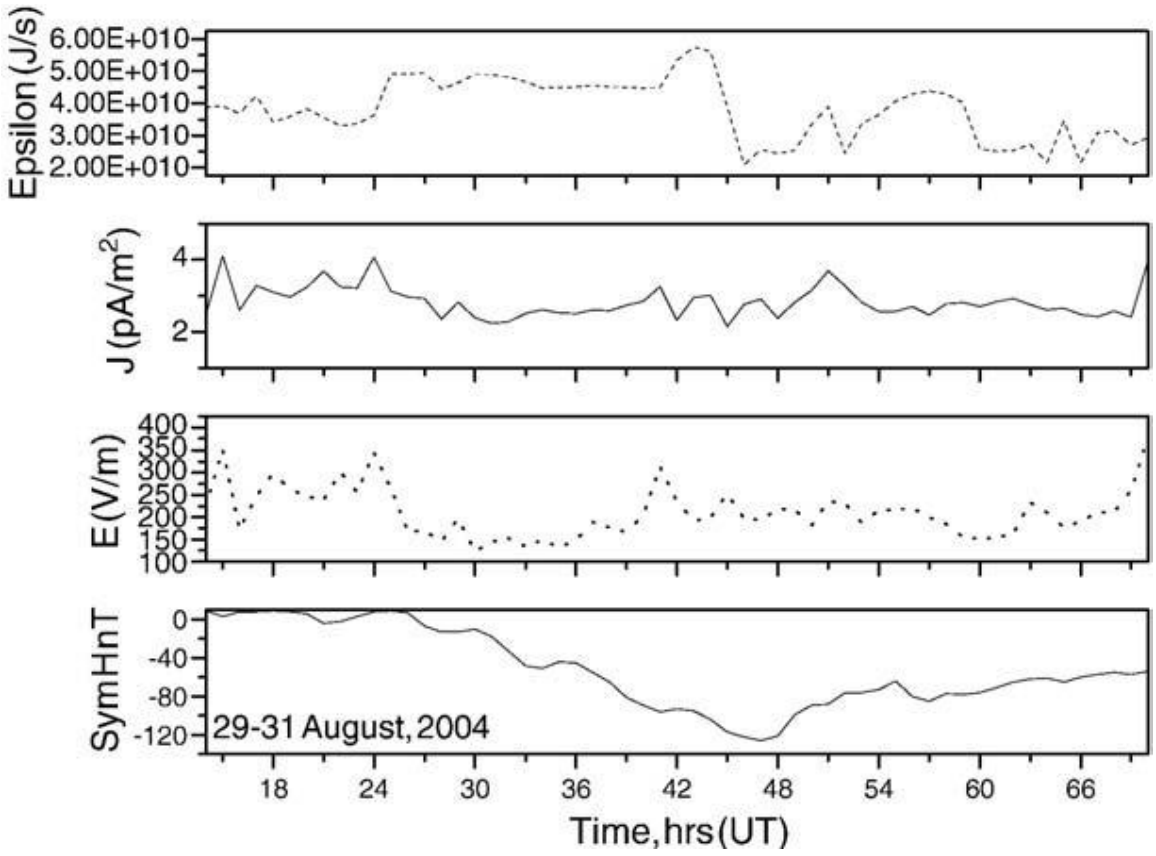

Fig. 6.7 same as Fig. 6. 5 but, for 29th to 31st August, 2004.

Fig. 6. 7 Depicts the CME associated magnetic disturbance on 29th to 31st August, 2004. The magnetic storm started at 14:32 UT. The B_Z turned southward (not shown in this figure) till 20:00 UT on the 30th August. The solar wind velocity increased during this period. The potential gradient also showed an enhancement during the first day. But on subsequent days the field did not vary, though the energy coupling function varied. It would be appropriate and interesting at this stage to conclude that the energy coupling function is a cogent mechanism that modulates the near-earth electrical environment during the initial and main phases of the storm.

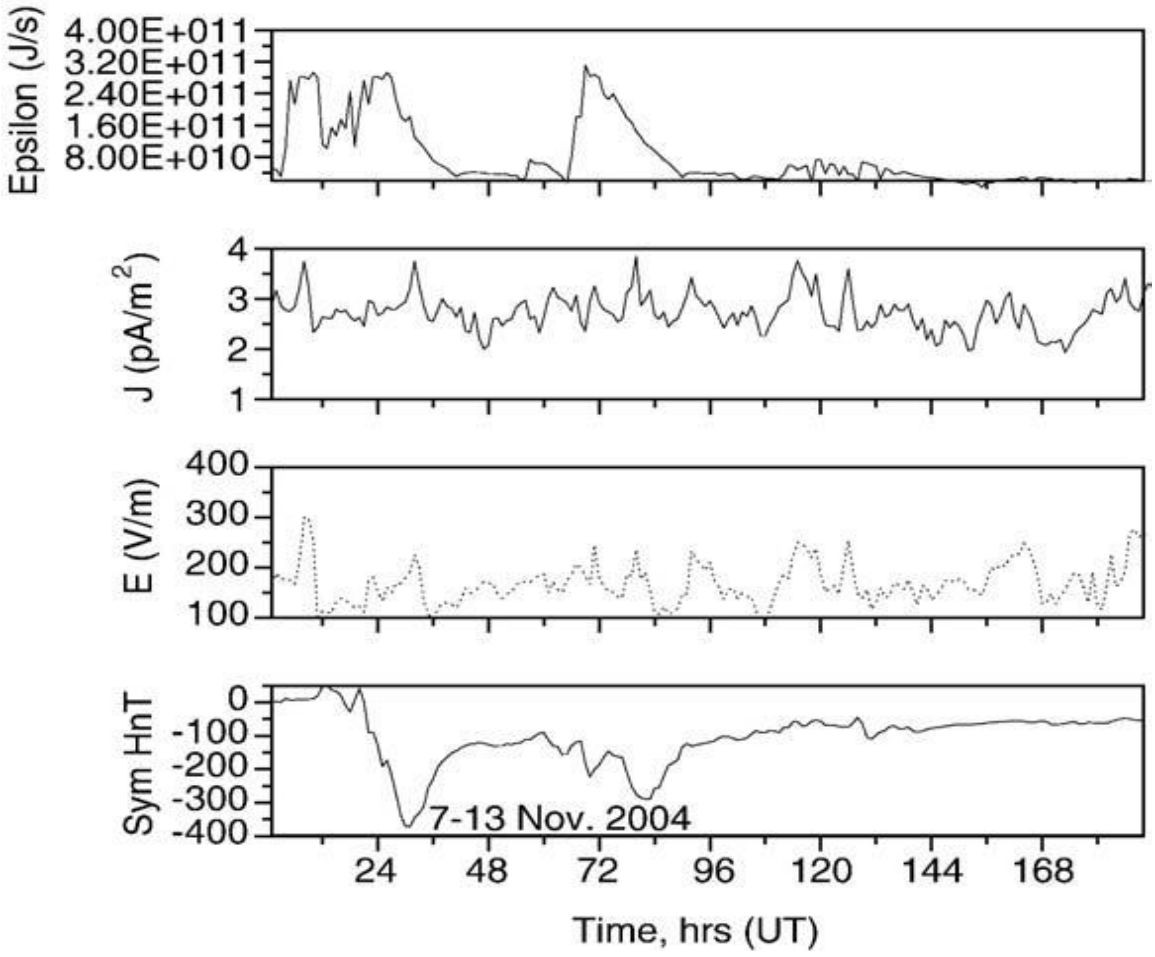

Fig. 6. 8 Same as Fig. 6.5 but, for 7th–14th November, 2004.

In Fig. 6. 8 we have illustrated another major magnetic disturbance due to CME on 7th November which lasted up to the 14th November, 2004. It caused a severe sub-storm during 11th November at 22:34 UT. After elimination of the diurnal variation say (ΔE), as in above figures, we can make out that CME associated terrestrial magnetic coupling is an enhancing mechanism to GEC at least during the initial phase. The correlation coefficient for the measured parameters has a high value (0.77 to 0.87), as shown in Fig. 6. 9 a, b, and c and its magnitude of modulation depends on the velocity, direction and density of the incoming solar stream. We also studied the effect of the sub-storm during this period. The sub-storm correlation showed a level of 0.33 on GEC parameters and is small. In all magnetic storms a

linear regression analysis was carried out to associate the geoelectric field with the energy coupling function in order to emphasise the energy coupling function's influence on GEC parameters. Since the interaction of the IMF and the earth's magnetic field results in anti sunward plasma flow at high latitudes that varies with the location of a station, the magnitude of the diurnal variation was removed by using Eqs.(2) and (3) in all the data sets. The hours for which ΔE and ΔI are significantly correlated are the initial and main phases of a storm. A comparative study of ΔE and ΔI with the energy coupling function of a minor storm and sub-storm yielded no significant correlation.

Principal Component Analysis, (discussed later in next section) to separate the thunderstorm, ionospheric/magnetospheric contribution during magnetically quiet and disturbed days. The quiet day curve is similar to the Carnegie curve and the first component gives information about the thunderstorm's contribution to GEC. The second and higher components give information about the ionospheric and magnetospheric contributions. But during magnetically disturbed days the ionospheric and magnetospheric contribution modifies the diurnal pattern. It is generally agreed that the major part of the energy transferred from the solar wind to the magnetosphere is stored in the ring current.

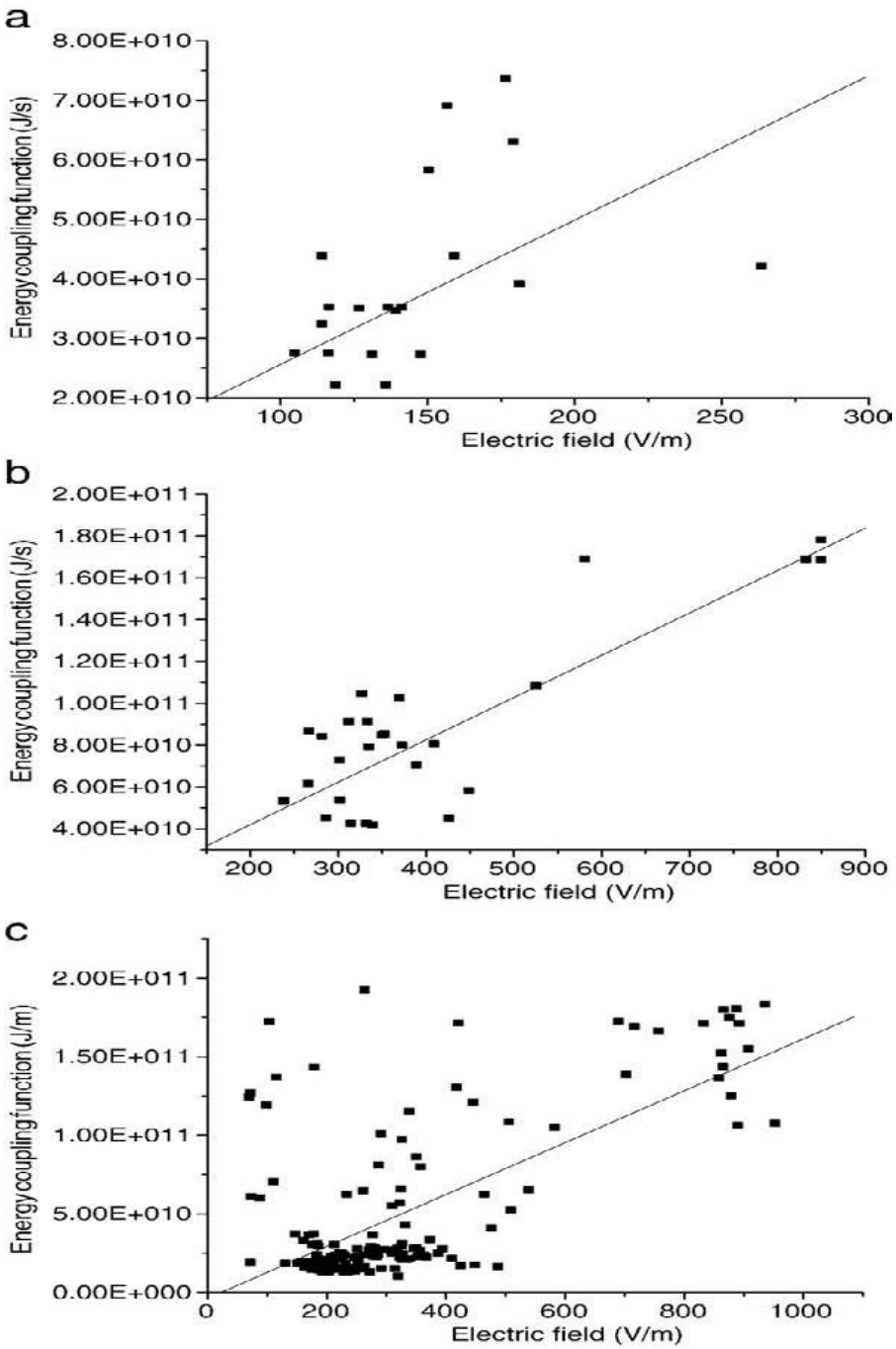

Fig. 6. 9 (a, b, c) Electric field plotted against energy coupling function for magnetically disturbed days.

Akasofu's (1981) solar wind magnetosphere energy coupling function (ε) explains the flow of solar wind across the open geomagnetic field lines. Since the magnitude of the field produced by the solar wind magnetosphere dynamo is given by, E = Vsw × B, the auroral ionosphere acquires an addition potential difference. As

a result, potential gradient and air–earth current at a station varies with respect to over-head ionospheric potential made at the high latitude Indian Antarctic Research Station, Maitri (70.45° S, 11.44° E) we have investigated the influence of the geoelectrical coupling during, before and after magnetic storms and sub storms. The study provides evidence of solar wind-magnetosphere energy coupling function (ε) to be well correlated with the atmospheric electric parameters during the onset and main phase of geomagnetic disturbances. However the solar wind-magnetosphere energy coupling function exerts only a minor influence during minor and sub-storm events.

We have tried to compare some results of geomagnetic and atmospheric electric field measurements obtained at Maitri during January 2005. The results are shown in Fig. 6. 10. for the selected fair-weather days during magnetic quiet conditions. The mean variation of both parameters shows similar variation and the correlation coefficient between these measured parameters has a high value (more than 0.5) for the selected fair-weather days. The preliminary results obtained at Maitri need to be examined further with statistical treatment of the obtained results, comprising spectral analyses and properties of polarization of the geomagnetic field and its influence on atmospheric electric field If these investigations yield more corroborated data on the behavior of geomagnetic disturbances in the atmosphere below the ionosphere, we may expect to get additional information exceed.. The expected information would concern the effective ionospheric boundary conditions for the magnetospheric disturbances and may also be useful for a better understanding of physical nature of geomagnetic pulsations.

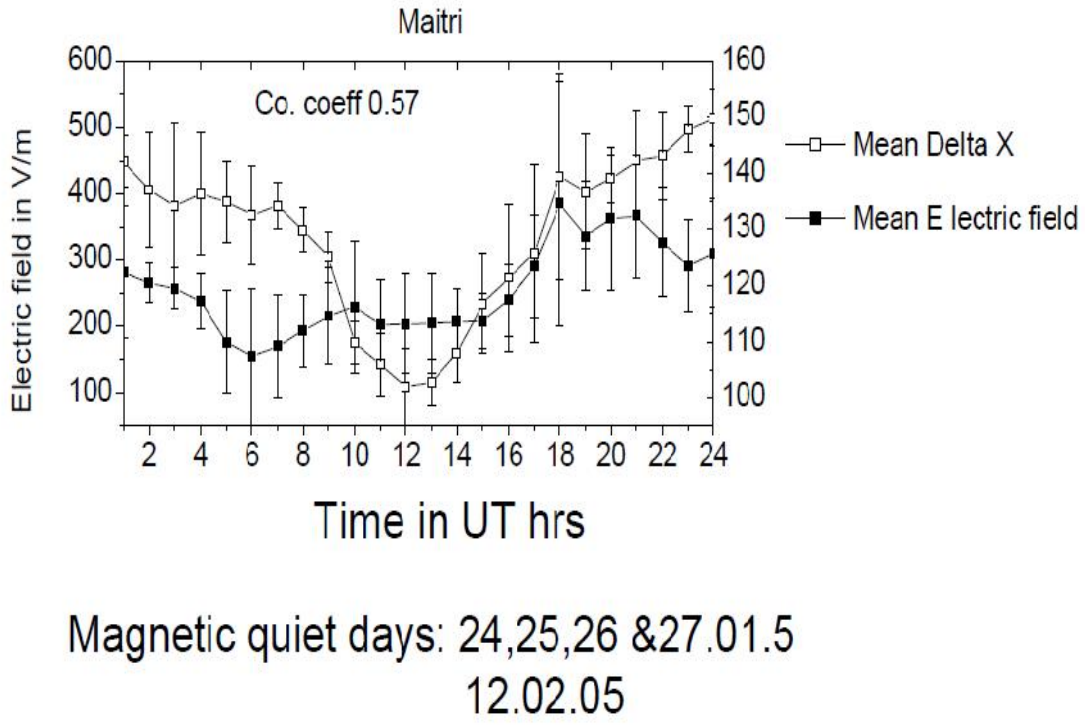

Fig. 6. 10 Diurnal variation o f magnetic field and electric field

With the selected fair-weather days data we have made an attempt to explain the influence of upper atmospheric contribution during geomagnetic disturbed periods. During geomagnetically quiet days the variations of measured atmospheric electrical parameters are similar to the famous fair weather "Carnegie curve". But, during geomagnetically disturbed days the diurnal pattern is different from the Carnegie curve and is modified by the ionospheric / magnetospheric contributions. This is another result for supporting the study of GEC, which is modified by the upper atmospheric contribution during geomagnetic disturbed conditions.

6. 3 Method used for the separation of different atmospheric generators

In this section we are discussing about the separation method used for the separation of different atmospheric generators that operates Global Electric Circuit (GEC). To separate the thunderstorm, ionospheric/magnetospheric contribution we have carried out the principal component analysis (Gnanadesikan 1977) for the electrical parameters. The most widely used multivariate method, is the principal component analysis (PCA), which is a classical statistical method. PCA is a transformation, which transforms a number of (possibly) correlated variables into a (smaller) number of uncorrelated variables called 'principal components' (PCs).

The objectives of this analysis are to reduce the dimensionality of the dataset and to identify new meaningful underlying variables. The basic idea of principal component analysis is to describe the dispersion of an array of n points in p-dimensional space by introducing a new set of orthogonal linear coordinates so that the sample variances of given points with respect to these derived coordinates are in decreasing order of magnitude. The mathematical technique used in PCA is called eigen analysis: we solve for the eigenvalues and eigenvectors of a square symmetric matrix of covariance. The eigenvector associated with the largest eigenvalue has the same direction as the first principal component and contains the most variance in the data. The eigenvector associated with the second largest eigenvalue determines the direction of the second principal component and contains the most variance when the first component is removed from the data. The sum of the eigenvalues equals the trace of the square matrix and the maximum number of eigenvectors equals the number of rows (or columns) of this matrix. A common way to find the principal components of

a dataset is by calculating the eigenvectors of the data correlation matrix. These vectors give the directions in which the data cloud is stretched most. The projections of the data on the eigenvectors are the principal components. The corresponding eigenvalues give an indication of the amount of information represented by the respective principal components. Principal components corresponding to large eigenvalues, represent much information in the dataset and thus tell us much about the relations between the data points. This technique of analysis has been used to study the day-to-day variability of the measured atmospheric electrical parameters in the present investigation.

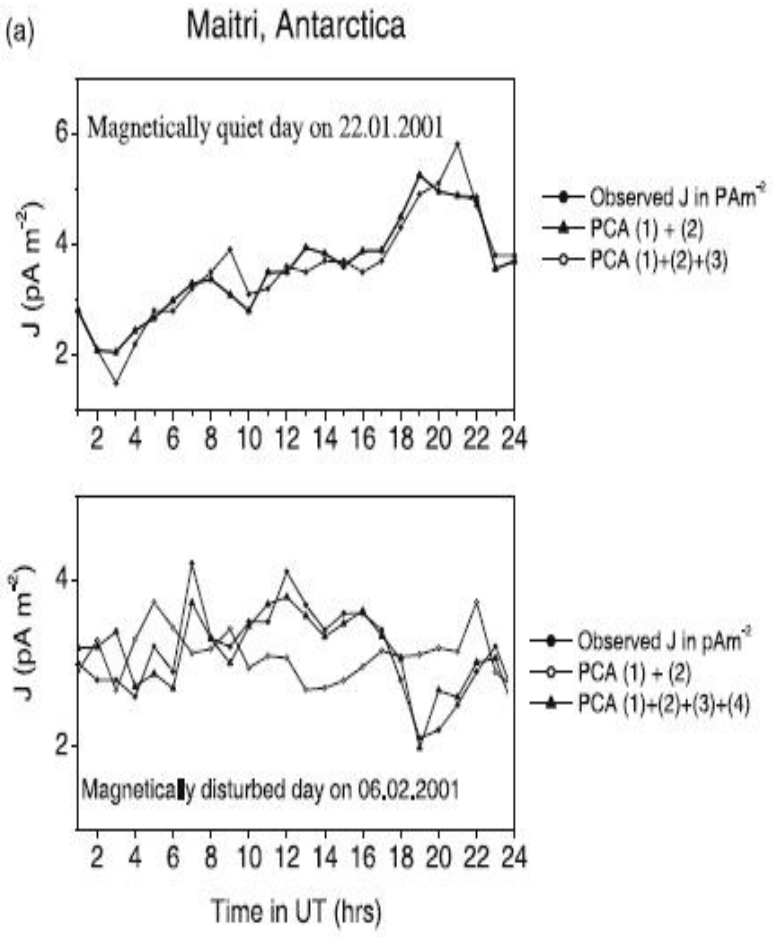

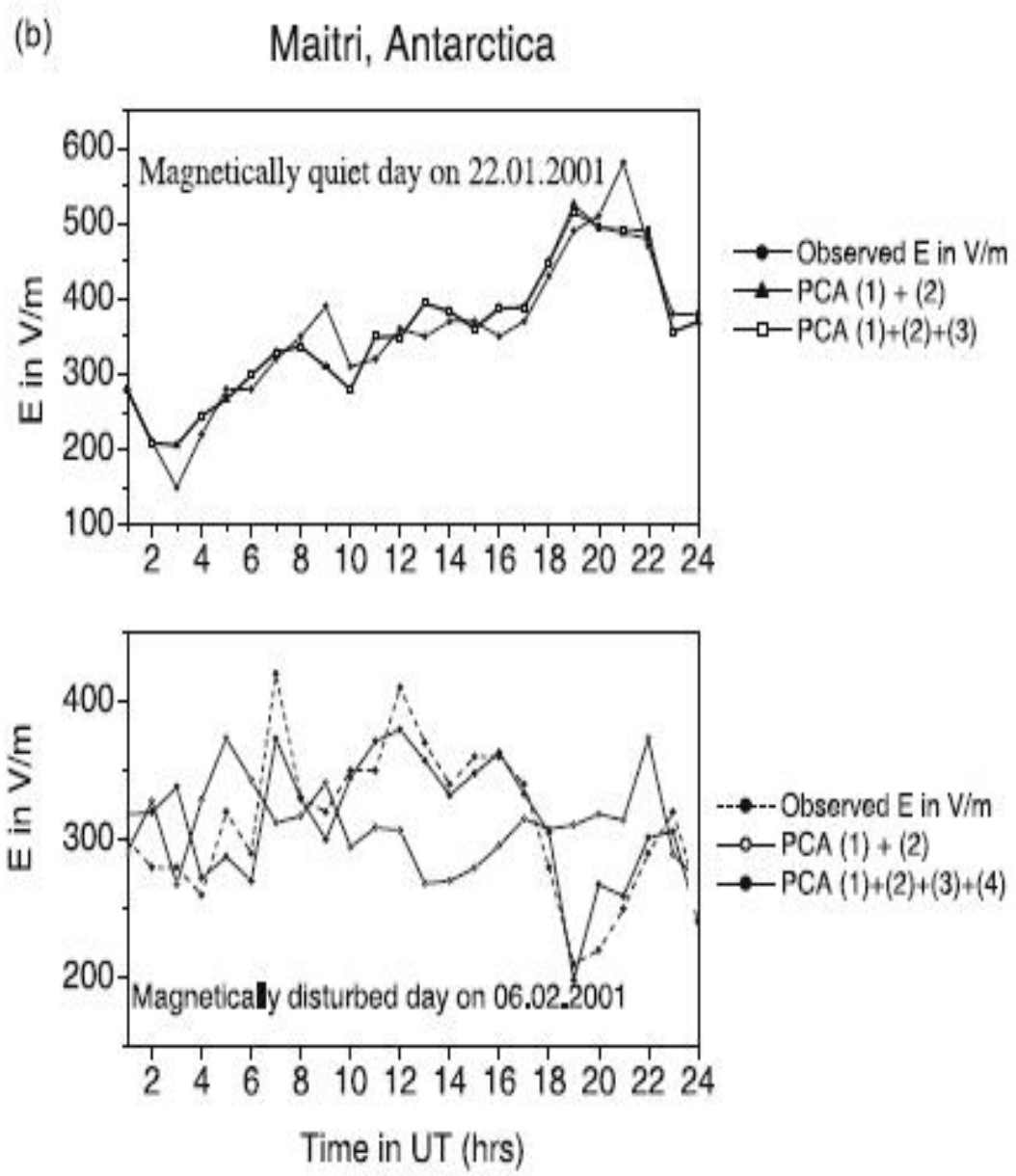

Fig. 6. 11 Diurnal variation of (a) Maxwell current and (b) electric field during magnetic quiet and disturbed days using PCA.

To separate the thunderstorm, ionospheric/magnetospheric contribution we have used the Principal Component Analysis (PCA) for the electric field and Maxwell current density. The first component gives information about the thunderstorm contribution to the global electric circuit. The second and higher components will give us information on the upper atmospheric contribution namely from the ionosphere and the magnetosphere. During magnetic quiet days the first order component (thunderstorm contribution) contributes the maximum. The remaining component's (second and higher) contribution is very less. The measured electrical parameter and the PCA first order component was compared and found identical. Geomagnetically disturbed days were also used for the PCA analysis and the observed diurnal pattern compared with the first order component. We found that there is a deviation from the measured atmospheric electrical parameters. Then we have added the second and third order component with first order, the PCA first order with the second and third order components compared with the observed diurnal curve and we found it is identical. From the PCA it is clearly seen that during magnetically disturbed days the ionospheric/magnetospheric contribution modifies the diurnal pattern of the measured atmospheric electrical parameters, which is shown in figure 6.11(a) and 6. 11(b). Further detailed study will be carried in future.

7. Conclusions and suggestions for future work

7.1 Overview of the studies completed

- Fairweather monthly / long term means of potential gradient, Maxwell current and Air-Earth conduction current density diurnal variations observed at Tirunelveli, a low latitude station in India and Maitri, a high latitude station in Antarctica, proved that the low latitude continental station Tirunelveli is also suitable for the measurement of atmospheric electrical parameters.

- The Passive wire antenna sensor have been designed and put in operation at Tirunelveli and Maitri, Antarctica, proves to be successful in the measurement of atmospheric potential (Electric field), which is first hand and new technique adopted.

- Mean diurnal variation of potential gradient, conduction current density and total air conductivity have been measured and analyzed for the period 1996 to 2005. Atmospheric electrical parameters were found to be largely dependent on routine meteorological parameters.

- Surface atmospheric electrical parameters were found to be sensitive to convective clouds, fog, rain and snow. The variations of electrical parameters will always be in the positive side, and goes to well in negative side at about 3 hours before the onset of a blizzard at the measuring site. Hence at high latitude station Maitri, it may perhaps be used as a tool for forecasting the onset of blizzards.

- Ohm's Law is in good agreement with the measured atmospheric electrical parameters like current density, conductivity and electric field at Maitri during fairweather days.

- Diurnal variability of surface Conduction current, electric field and conductivity measurements on fairweather days were most likely to be dominated by global sources and follow the famous Carnegies curve with a minimum at about 4:00 UT and a maximum at about 19:00 UT.

- Separation of different atmospheric currents carried out during this course of study using the data collected with different instruments like Field mill, Passive antenna, Maxell antenna and long wire antenna at high latitude station Maitri, Antarctica.

- Influence of geomagnetic storms and sub- storms on atmospheric electricity at high latitude auroral station was studied. Different atmospheric electrical generators and their contributions to the atmospheric electrical parameters were identified and separated using mathematical techniques.

7.2 Summary and future work

The Maxwell wire antenna, Gerdian conductivity meter and passive wire antenna instruments have been proven capable of measuring the atmospheric currents, conductivity and potential respectively during this study. The absolute values of potential gradient from both the passive wire antenna, and the commercially-

purchased field mill were reliable under all atmospheric conditions, and showed high level of accuracy, resolution and thermal stability. With the different instruments for measuring different atmospheric electrical parameters, the comparison work carried out and has good correlation. Apart from the above suggested research work, modeling, and the interaction of atmospheric electricity with climate may be undertaken in near future.

A key scientific question to be answered is whether the effect of space charge (both ionic and charged aerosol) can be effectively incorporated in the vertical profile model. The departure from an otherwise fair-weather model would allow modeling of surface atmospheric electrical parameters during disturbed weather, and quantitatively investigate the influence of space charge and turbulent current density on surface potential and conduction current, allowing the observed non-Carnegie diurnal variations to be replicated. A coupled boundary layer-atmospheric electrical model that simulates convectively-driven changes to the aerosol and ionization rate profiles would allow more accurate determination of surface/columnar sources of potential gradient and conduction current variability. By modeling and compensating for these local effects, including space charge, it may be possible to retrieve global signals from polluted sites such as the Tirunelveli on a daily basis during all seasons, not just from fair-weather monthly / long term means as demonstrated by this study.

The sensors must be capable of continuous measurements of all atmospheric electrical parameters during any weather conditions. An instrument capable of continuously measuring the true total conductivity would be useful for the local meteorological studies and their influence on atmospheric electricity. With such

measurements, it would be possible to quantify the Ohmic fulfillment in terms of absolute values, not just significant correlations.

Measurement of atmospheric electrical vertical profiles (not just surface measurements) would be useful for model accuracy assessment and development, including the possibility of directly determining the columnar resistance (and therefore ionospheric potential using measured conduction current). This will be possible if inexpensive balloon-borne atmospheric electrical sensors capable of operating in the conditions except during the ascent (extreme cold, high and low humidity, cloud etc) are developed. Continuous, long term measurements of atmospheric electrical parameters at a low-pollution site would offer a useful comparison with those of the Maitri, and may serve as a reference source for "realtime" variability of the global circuit, without the need to average over several days to be confident of a Carnegie-like diurnal cycle. Using times of JC or PG correlation between two clean-air sites (preferably displaced by many degrees longitude so their local diurnal variations are not in phase) it may be possible to observe sub-diurnal variations of the global circuit. The continuation of atmospheric electrical measurements both at Tirunelveli and Maitri sites will eventually allow investigation of inter-annual and decadal changes to both local and global sources of variability; vital if the effect of climate change on the global electric circuit is to be studied. A key benefit of atmospheric electrical measurements even when they are not giving global-circuit data, is the additional insight provided into cloud and atmospheric physical processes. More investigation into the effect of local meteorological conditions on conduction current, conductivity and potential gradient will enable a more quantitative use of atmospheric electrical measurements for

meteorological research in areas such as now casting, aerosol studies, convective clouds and boundary-layer processes. Measurement of short-period (order of minutes) variability in conduction current due to the passage of convective cloud is now possible using the geometrical method, as the requirement for ~1000s measurement lag using the more traditional "matching circuit" method is not required.

References

Adlerman, E. J. and Williams, E. R., (1996). Seasonal variation of the global electric circuit, Journal of Geophysical Research 101 D23 29679-29688.

Ahrens, C. D. (1991) Meteorology Today. 4th Edition, West Publishing Company, St Paul, 576 pp

Akasofu, S.I., 1981. Prediction of developments of geomagnetic storms using the polar wind-magnetosphere energy coupling function ε. Planet. Space Sci. 29, 1151–1158.

Anderson, R. V., (1969). Universal Diurnal Variations in the Air-Earth Current Density, Journal of Geophysical Research 74(6) 1697-1700.

Anderson, R. V., (1967). Measurement of worldwide diurnal atmospheric electricity variations, Monthly Weather Review 95(12) 899-904.

Anisimov, S. V., E. A. Mareev, A. E. Sorokin, N. M. Shikhova, and E. M. Dmitriev, Electrodynamical properties of the fog. Izv., Atmos. Ocean. Phys., 39(1), 341–347, 2003.

Anisimov, S. V., E. A. Mareev, N. M. Shikhova, A. E. Sorokin, and E. M. Dmitriev, On the electro-dynamical characteristics of the fog, *J.* Atmos. Res., 76, 16–28, 2005.

Aplin, K. L., (2000). PhD Thesis. University of Reading, UK.

Anil Kumar, C.P., Panneerselvam, C., Nair, K.U., Jeeva, K., Selvaraj, C., Gurubaran, S., Rajaram, R., 2006. Influence of azimuthal and vertical components of IMF on atmospheric electrical parameters at Maitri, Antarctica. National Space Science Symposium, p. 65.

Aplin, K. L. and McPheat, R. A., (2005). Absorption of infra-red radiation by atmospheric molecular cluster-ions, Journal of Atmospheric and Solar-Terrestrial Physics 67, 775-783.

Atkins P.W. (1989), Physical Chemistry, 4th edition, Oxford University Press

Anonymous (1915) The home of the blizzard. Symon's Meteorological Magazine, 50, pp. 37-41

Barlow, J. F., (1999). PhD Thesis. University of Reading, UK.

Barnhart, C. L. and Barnhart, R. K. (1984) The World Book Dictionary. Volume 1, A-K, World Book Inc., Chicago, pp. 214

Beccaria, G., (1775). Della elettricite terrestre atmosferica a cielo serno, Turin.

Bozman, E. F. (1970) Everyman's Encyclopaedia. Volume 2, 6th Edition, J. M. Dent and Sons Ltd, London, pp. 282-283

Bostwick, A. E. (1916) Meteorological conditions of a blizzard. Nature, 47, pp. 261

Breton, H. H. (1928) The Great Blizzard of Christmas 1927, Its Causes and Incidents. Hoyten and Cole, Plymouth, pp. 56

Brownlee J.N. (1973), *A* fast mobility spectrometer for atmospheric ions, PhD Thesis, University of Auckland

Bunker, J., (1982). Sailing the Magnetic Fields: Carnegie, a Sea-Going Observatory, Plotted the Forces That Sent Compasses Awry, *S*urveyor 16(4) 28-31.

Bürgesser, R. E., Pereyra, R. G. and Avila, E. E., (2006). Charge separation in updraft of convective regions of thunderstorm, Geophysical Research Letters 33 L03808.

Burke, H. K. and Few, A. A., (1978). Direct Measurements of the Atmospheric Conduction Current, Journal of Geophysical Research 83(C6) 3093-3098.

Burns, G. B., B. A. Tinsley, A. R. Klekociuk, O. A. Troshichev, A. V. Frank-Kamenetsky, M. L. Duldig, E. A. Bering, and J. M. Clem, Antarctic polar plateau vertical electric field variations across heliocentric current sheet crossings, *J.* Atmos. Terr. Phys., (68), 639–654, 2006.

Canton, J., (1753). A Letter to the Right Honorable the Earl of Macclesfield, President of the Royal Society, concerning Some New Electrical Experiments. Philosophical Transactions 48, 780-785.

Chalmers, J.A., (1956). The vertical electrical currents during continuous rain and snow. *J.* Atmos. Terres. Phys., 9, 311-321.

Chalmers, J. A., (1967). Atmospheric Electricity (2nd Edition), Pergamon Press Ltd.

Cobb, W. E., (1967). Evidence of a solar influence on the atmospheric electric elements at Mauna Loa Observatory, Monthly Weather Review 95(12) 905-911.

Considine, D. M. (1976) Van Nostrand's Scientific Encyclopedia. 5th Edition, Van Nostrand Reinhold Company, New York, 2370 pp

Devendra Siingh, Gopalakrishnan, V., Singh, R.P., Kamra, A.K., Shubha Singh, Vimlesh Pant, Singh, R., Singh, A.K., 2007. The atmospheric global electric circuit: An overview. Atmospheric Research 84, 91–100.

Deshpande, C. G. and A. K. Kamra, Diurnal variations of the atmospheric electric field and conductivity at Maitri, Antarctica, *J.* Geophys. Res., 106, 14,207–14,218, 2001.

Despiau, S. and E. Houngninou, Raindrop charge, Precipitation and Maxwell currents under tropical storms and showers, *J.* Geophys. Res., 101, 14,991–14,997, 1996.

Dolezalek, H**.,** The atmospheric electric fog effect, Rev. Geophys., 1, 231– 282, 1963.

Dolezalek, H., (1978). The application of atmospheric electricity concepts and methods to other parts of meteorology, *World* Meteorological Organisation Technical Note 162 130pp.

Dolezalek, H., (1972). Discussion of the Fundamental Problem of Atmospheric Electricity, Pure and Applied Geophysics 100 8-43.

Dungey, J. W., 1961. Interplanetary magnetic field and auroral zones. Phys. Rev. ett., 6, 47-48.

Everett, J. D., (1868). Results of observations of atmospheric electricity at Kew Observatory, and at Kings College, Windsor, Nova Scotia Phil. Trans. Roy. Soc. Lond. A. 158, 347-361.

Fishman, G., Bhat, P.N., Mallozzi, R., Horack, J.M., Koshut, T., Kouveliotou, C., Pendleton, G.N., Meegan, C.A., Wilson, R.B., Paciesas, W.S., Goodman, S.J., Christian, H.J., 1994. Discovery of intense gamma rays flashes of atmospheric origin. Science, 264, 1313-1316.

Fleming, J. A., (1949). Physics of the Earth VIII - Terrestrial Magnetism and Electricity, Dover publications, New York.

Forbes, J.M., 1981. The equatorial electrojet. Rev. Geophys. Space Phys. 19, 469-504.

Funk, C. E. (1956) New Practical Standard Dictionary of the English Language. Volume 1, Funk and Wagnalls Company, New York, 1572 pp

Galeev, A. A., Kuznetsova, M. M. Zelenyi, L. M., 1986. Magnetopause stability threshold for patchy reconnection. Space Sci. Rev., 44, 1.

Gerdien, H., (1905a). Messungen der Dichte des vertikalen elektrische in der freien Atmosphäre bei der Ballonfahrt am 11 V 1905 Nachrichten von der Gesellschaft der Wissenschaften zu Göttingen 1905, 258-270.

Gerdien, H., (1905b). Messungen der Dichte des vertikalen elektrische in der freien Atmosphäre bei der Ballonfahrt am 30 VIII 1905 Nachrichten von der Gesellschaft der Wissenschaften zu Göttingen 1905, 447-458.

Gish, O. H., (1944). Evaluation and interpretation of the columnar resistance of the atmosphere, Terrestrial Magnetism and Atmospheric Electricity 36 159-160.

Gringel, W., Rosen, J. M. and Hofmann, D. J., (1986). The Earth's Electrical Environment, Ch. 12, Studies in Geophysics. National Academy Press, U. S. A.

Gretz, P. W. (1986) The New Encyclopaedia Britannica. Volume 2, 15th Edition, Encyclopaedia Britannica Inc., Chicago, pp. 285

Gnanadesikan R 1977 Methods for statistical data analysis of multivariate observations; John Wiley and Sons, New York.

Gove, P. B. (1961) Webster's Third New International Dictionary of the English Language A-K. G. Bell and Sons Ltd, London, pp. 235

Gonzalez, W. D., Joselyn, J. A., Kamide, Y., Krochl, H. W., Rostoker, G., Tsurutani, T., Vasyliunas, V. M., 1994. What is geomagnetic storm? J. Geophys. Res. 99, 5771.

Hanks, P. (1976) Encyclopedic World Dictionary. The Hamlyn Publishing Group, London, 1856 pp

Harrison, H., (2006a). Atmospheric electric fields at the Kennedy Space Center, 1997-2005: No evidence for effects of global warming or modulation by galactic cosmic rays, Geophysical Research Letters 33 L10814.

Harrison R. G., (1997a) An antenna electrometer system for atmospheric electrical measurements Rev. Sci. Inst. 68(3) 1599-1603.

Harrison R.G. and Aplin K.L. (2000a), Femtoampere current reference stable over atmospheric temperatures, Rev. Sci. Instrum., 71, 8, 3231-3232

Harrison, R. G., (2004b). Long-range correlations in measurements of the global atmospheric electric circuit, *J*ournal of Atmospheric and Solar-Terrestrial Physics 66 1127-1133.

Harrison, R. G., (2004c). The global atmospheric electrical circuit and climate, Surveys in Geophysics 25 441-484.

Harrison, R. G., (2005b). Columnar resistance changes in urban air, *Journal of* Atmospheric and Solar-Terrestrial Physics 67 763-773.

Harrison, R. G. and Bennett, A. J., (2007a). Cosmic ray and air conductivity profiles retrieved from early twentieth century balloon soundings of the lower troposphere Journal of Atmospheric and Solar-Terrestrial Physics 69 515-527.

Harrison, R. G. and Ingram, W. J., (2005). Air-earth current measurements at Kew, London, 1909-1979, Atmospheric Research 76(1-4) 49-64.

Hays, P. B. and Roble, R. G., (1979). A Quasi-Static Model of Global Atmospheric Electricity 1. The Lower Atmosphere, Journal of Geophysical Research 84(A7) 3291-3305.

Hatakeyama H., Kobayashi J., Kitaoka T., Uchikawa K. (1958), A radiosonde instrument for the measurement of atmospheric electricity and its flight results, In: Smith L.G. (ed.), Recent advances in atmospheric electricity, Pergamon Press, Oxford Herman J R and Goldberg R A 1978 Sun, Weather and Climate; Scientific and Technical Information Branch, National Aeronautics and Space Administration, Washington, D.C.

Hess, V. F., (1912). Über Beobachtungen der durchdringenden Strahlung bei sieben Freiballonfahrten Phys.Zeitschr. 13 1084.

Higazi K.A. and Chalmers J.A. (1966), Measurements of atmospheric electrical conductivity near the ground, *J.* Atm. Terr. Phys., 25, 327-330

Hatakeyama H., Kobayashi J., Kitaoka T., Uchikawa K. (1958), A radiosonde instrument for the measurement of atmospheric electricity and its flight results, In: Smith L.G. (ed.), Recent advances in atmospheric electricity, Pergamon Press, Oxford

Hoppel, W., Anderson, R. V. and Willett, J. C., (1986). The Earth's Electrical Environment, Ch. 11, Studies in Geophysics. National Academy Press, U. S. A.

Hudson, I. C. (1979) The Highland blizzard 27 to 29 January 1978. Journal of Meteorology, 4, pp. 37-47

Huschke, R. E. (1959) Glossary of Meteorology. American Meteorological Society, Boston Massachusetts, 638 pp

Iribarne**,** J. V., and H. R. Cho, 1980: Atmospheric Physics. Reidel Publishing, pp 212

Israel, H. 1954, Mitt. dt. Wetterd. No. 7.

Israel, H. (1970), Atmospheric Electricity, Vol. I, Israel Program for Scientific Translations Ltd., The National Science Foundation, Washington, D. C., pp. 317.

Israel H 1973 Atmospheric Electricity; vol. II, Isr. Program for Sci. Transl., Jerusalem.

Israelsson, S., (1978). On the Conception 'Fair Weather Condition' in Atmospheric Electricity, Pure and Applied Geophysics 116 149-158.

Israelsson**,** S. and Tammet, H., (2001). Variation of fair weather atmospheric electricity at Marsta Observatory, Sweden, 1993-1998, Journal of Atmospheric and Solar-Terrestrial Physics 63 1693-1703.

Kamra, A. K., Effect of wind on diurnal and seasonal variations of atmospheric electric field, J. Atmos. Terr. Phys., 31, 1281-1286, 1969.

Kamra, A. K., Measurements of the electrical properties of dust storms J Geophys Res. pp 5856-5869, 1972

Kamra, A. K., Deshpande, C. G. and Gopalakrishnan, V., (1994). Challenge to the assumption of the unitary diurnal variation of the atmospheric electric field based on observations in the Indian Ocean, Bay of Bengal, and Arabian Sea, Journal of Geophysical Research 99(D10) 21043-21050.

Karasnogorskaya , N. A. and D. A. Pokhmelnik, On the origin of Variations in the Electric field of the Earth's Atmosphere, Proceedings in Atmospheric Electricity, 79–84, 1983.

Kan, J.R., Lee, L.C., Akasofu, S.I., 1980. The energy coupling function and the power generated by the solar wind-magnetosphere dynamo. Planet. Space Sci. 28, 823–831.

Kasemir**,** H.W., (1950) Qualitative Uebersicht áber Potential -, Feld -, und Ladungsverhaltnisse bei einer Blitzentlandung in der Gewitterwolke. In Das Gewitter*,* H. Israel, Akad. Verlags. Ges. Geest and Portig K.-G., Leipzig.

Kasemir, H. W., (1951). An apparatus for simultaneous registration of potential gradient and air-earth current (description and first results), Journal of Atmospheric and Terrestrial Physics 2 32-37.

Kasemir, H.W. and L. H. Ruhnke, Antenna problems of measurement of the air-Earth current, in Recent advances in Atmospheric Electricity*,* edited by L. G. Smith, pp. 137–147, Pergamon, New York, 1959.

Kasemir, H. W., (1972). Atmospheric Electric Measurements in the Arctic and Antarctic, Pure and Applied Geophysics 100 70-80.

Klein, E. (1971) A Comprehensive Etymological Dictionary of the English Language. Elsevier Scientific Publishing Company, Amsterdam, pp. 48 and 86

Krumm**,** H., (1962). Der weltzeitliche Tagesgang der Gewitterhäufigkeit, Zeitschrift für Geophysik 28 85-104.

Lazzara, M. A., Wang, P. K. and Stearns, C. R., Observations of Antarctic fog particles. In 7th Conference on Polar Meteorology and Oceanography and Joint Symposium on High-Latitude Climate Variations, Hyannis MA, 12–16 May 2003;

Lester, M., Cowley, S. W. H., 2000. The solar terrestrial interaction and its importance for space-weather. Adv. Space Res. 26, 79-88.

Lee, L. C., Johnson, J. R. Ma, Z. W., 1994. Kinetic Alfven wave as a source of plasma transport at the dayside magnetopause. J. Geopgys. Res., 99, 17405.

Lutz, C.W. 1939, Gerl. Beitr. ys. Geophys. 54, 337.

Markson, R., (2007). The global circuit intensity, *Bulletin* of the American Meteorological Society 88 (2), pp. 223–241.

Märcz, F. and Harrison, R. G., (2005). Further signatures of long-term changes in atmospheric electrical parameters observed in Europe, Annales Geophysicae 23(6) 1987- 1995.

Mareev, E. A. and Anisimov, Global electric circuit as an open dissipative system, Proc. 12th Int. Conf. On atmospheric electricity, Versailles, vol. 2, pp 781–784, 2003.

Markson, R., (1976). Ionospheric Potential Variations Obtained From Aircraft Measurements of Potential Gradient, Journal of Geophysical Research 81(12) 1980-1990.

Matsushita, S., 1967. Solar quiet and lunar daily variation fields. In: Matsushita, S., Campbell, W.H. (Eds), Physics of Geomagnetic Phenomena. Academic Press, New Yark,, pp. 301.

Mauchly, S. J., (1921). Note on the Diurnal Variation of the Atmospheric-Electric Potential Gradient Physic. Rev. 18 p.161, 477.

Mauchly, S. J., (1923). On the Diurnal variation of the potential gradient of atmospheric electricity. Terr. Magn. Atmos. Electr. 28, 61-81.

Mauchly, S. J., (1926). Atmospheric-electric results obtained aboard the Carnegie, 1915- 1921, Carnegie Institute, Washington 175(3) 197-211.

McCracken, K. G., Beer, J. and McDonald, F. B., (2004). Variations in the cosmic radiation, 1890-1986, and the solar and terrestrial implications, Advances in Space Research 34 397-406.

McLeod, W. T. and Hanks, P. (1982) The New Collins Concise Dictionary of the English Language. William Collins Sons and Co. Ltd, Glasgow, 1379 pp

Miura, A., 1987. Simulation of Kelvin-Helmholtz instability at the magnetosphere boundary. J. Geophys. Res., 92, 3195-3206.

Milikh, G., Valdivia, J.A., 1999. Model of gamma rays flashes fractal lightning. Geophys, Res. Lett. 26, 525.

Monkhouse, F. J. (1970) A Dictionary of Geography. 2nd Edition, Edward Arnold, London, 378 pp

Monkhouse F. J. and Small, J. (1978) A Dictionary of the Natural Environment. Edward Arnold (Publishers) Ltd, London, 320 pp

Muir, M. S., The ionosphere as the source of the atmospheric electric sunrise effect, *J.* Atmos. Terr. Phys., 37, 553–559, 1975.

Muir, M. S., The potential gradient sunrise effect in atmospheric electricity, J. Atmos. Terr. Phys, 39, 229–233, 1977.

Nickolaenkoko, A. P., Hayakawa, M. and Sekiguchi, M., (2006). Variations in global thunderstorm activity inferred from the OTD records, Geophysical Research Letters 33 L06823.

Ogawa**,** T., (1985). Fair-Weather Electricity, Journal of Geophysical Research 90(D4) 5951-5960.

Owon, C. J., Cowley, S. W. H., 1991. Heikkila mechanism for impulsive plasma transport through the magnetopause a re-examination. J. Geophys. Res., 96, 5575-5574.

Panneerselvam, C., K. U. Nair, K. Jeeva, C. Selvaraj, S. Gurubaran, and R. Rajaram, A comparative study of atmospheric Maxwell current and electric field from a low latitude station Tirunelveli, Earth Planets Space, 55, 697–703, 2003.

Panneerselvam, C., K. U. Nair, C. Selvaraj, K. Jeeva, C. P. Anil Kumar, and S. Gurubaran, Diurnal variation of atmospheric Maxwell current over the low-latitude continental station, Tirunelveli, India (8.7◦N, 77.8◦E), Earth Planets Space, 59, 429–435, 2007.

Perreault, P., Akasofu, S.I., 1978. A study of geomagnetic storms. Geophys. J. R. Astron. Soc. 4, 547–556.

Petterssen, S., *Introduction to Meteorology*, McGraw-Hill and Kogakusha Co Ltd, Tokyo, 1958, pp 1–313.

Price, C. and D. Rind, A simple lightning parameterization for calculating global lightning Distributions, *J.* Geophys. Res., 97, 1919–1927, 1992.

Raina, B. N., Surface measurements of the components of air-earth current density, Cloud Physics and Atmospheric Electricity Frontiers, Vol. II, 973–988, 2002.

Rajaram G, Dhar A and Kumar S 2001 Response of geomagnetic variations and 30MHz riometer absorption at Indian Antarctic station Maitri, to conditions of ‘Zero’ and ‘high’ solar wind; Adv. Space Rev. 28(11) 1661–1667.

Rastogi, R.G., Patel, V.L., 1975. Effect of interplanetary magnetic field on ionosphere over the magnetic equator. Proc. Indian Acad. Sci. (Earth Planet. Sci.) 82, 121-141.

Reddell, B. D., Benbrook, J. R., Bering, E.A., Cleary, E. N. and Few, A. A., (2004). Seasonal variations of atmospheric electricity measured at Amundsen-Scott South Pole station, Journal of Geophysical Research 109 A09308.

Retalis, D. A., (1991). Study of the Air-earth Electrical Current Density in Athens, Pure and Applied Geophysics 136 217-233.

Richmond, A.D., 1976. Electric field in the ionospheric and plasmaspheric on quiet days. J. Geophys. Res. 81, 1447-1450.

Richmond**,** A.D., 1986. Upper-atmospheric electric field sources. In: Study in Geophysics-The Earth's electrical Environment, National Academy Press, Washington, D.C., 195-205.

Rishbeth**,** H., (2006). F-region links with the lower atmosphere?, Journal of Atmospheric and Solar-Terrestrial Physics 68 469-478.

Rutherford E. (1897), The velocity and rate of recombination of the ions in gases exposed to Rontgen radiation, Phil. Mag., 44, 422-440

Roble, R. G., On solar-terrestrial relationships in atmospheric electricity, *J.* Geophys. Res., 90, 6000–6012, 1985.

Rodger, C. J., 1999. Red sprites, upward lightning and VLF Perturbations. Rev. Geophys. 37, 317-336.

Ruhnke, L. H., Area averaging of atmospheric electric currents, *J.* Geomagn. Geoelectr, 21, 453–462, 1965.

Russell, C. T., Fleishman, M., 2002. Joint control of region-2 field aligned current by the east-west component of the interplanetary electric field and polar cap illumination. J. Atmos. Solar Terr. Phys. 64, 1803-1808.

Sagalyn, R. C. and Faucher, G. A., (1954). Aircraft investigation of the large ion content and conductivity of the atmosphere and their relation to meteorological factors, Journal of Atmospheric and Terrestrial Physics 5 253-272.

Sagalyn, R. C. and Faucher, G. A., (1956). Space and time variations of charged nuclei and electrical conductivity of the atmosphere, Quarterly Journal of the Royal Meteorological Society **82** 428-445.

Sapkota, B. K. and Varshneya, N. C., (1990). On the global atmospheric electrical circuit, Journal of Atmospheric and Terrestrial Physics 52(1) 1-20.

Schindler, K., 1979. On the role of irregularities in plasma energy into the magnetosphere. J. Geophys. Res., 84, 7257-7266.

Schmidt, D. S. and Dent, J. D.: 1994, 'Measurements of The Electric Field Gradient in a Blizzard', Proc. Int. Snow Sci. Workshop, Oct. 30–Nov. 3, 1994, Snowbird, UT, U.S.A., pp. 197–202.

Schonland B.F.J. (1953), Atmospheric electricity, 2nd edition, Methuen, London

Schwarz, C.; Davidson, G.; Seaton, A. and Tebbit, V. (1989) Chambers English Dictionary. W and R Chambers Ltd, Edinburgh and Cambridge University Press, Cambridge, pp. 151

Schwarz, C. (1993) The Chambers Dictionary. Chambers Harrap Publishers Ltd, Edinburgh, pp. 178

Serbu, G. P. and E. M. Trent, A study of the use of atmospheric electric measurements in fog forecasting, Trans. Am. Geophys. UN, 39, 1034, 1958.

Simpson G. C., (1919), British Antarctic Expedition 1910–1913. Thacker, Spink and Co., 326 pp.

Simpson, J. A. and Weiner, E. S. C. (1989) The Oxford English Dictionary. 2nd Edition, Volume 2, Clarendon Press, Oxford, pp. 294 and 662

Sinclair, J. (1992) Collins Cobuild English Language Dictionary. Harper Collins Publishers, London, 1703 pp

Smirnov, V. V., Ionization in the troposphere, Gidrometeoizdat, St Petersbourg, pp. 312, 1992.

Somayajulu, V.V ., Reddy, C.A., Viswanathan, K.S., 1985. Simultaneous electric field changes in the equatorial electrojet in phase with polar caps latitude changes during a magnetic storm. Geophys. Res. Lett. 12**,** 473-475.

Sorokin, A. E., S. V. Anisimov, and E. A., Mareev, Horizontal long-wire antenna as a fog electrical properties analyzer, Proc. of Conference on Fog and Fog Collection. St. John's Canada, pp. 473–476, 2001.

Spiro, R. W., Wolf, R. A. 1984. Electrodynamics of convection in the inner magnetosphere, In Magnetospheric current (ed. Poterma*,* T. A.) (American Geophysics Union, Washington, D.C.) pp 247-259.

Strangeways, R. J., Raeder, J., 2001. On the transition from collision to collisional magnetohydrodynamics. J. Geophys. Res., 106, 1955-1960.

Swann W.F.G. (1914), The theory of electrical dispersion into the free atmosphere, with a discussion of the theory of the Gerdien conductivity apparatus, and of the theory of the collection of radioactive deposit by a charged conductor, J. Terr. Mag. Atmos. Elect., 19, 81-92

Takagi, M. and Masahiro, K., (1972). Global Variation in the Atmospheric Electric Field, Pure and Applied Geophysics 100 44-53.

Takeda, M., Maeda, H., 1980. Three dimensional structure of ionospheric currents-1. Currents caused by diurnal tidal winds. J. Geophys. Res. 85, 6895-6899.

Tammet, H., Israelsson, S., Knudsen, E. and Tuomi, T. J., (1996). Effective area of a horizontal long-wire antenna collecting the atmospheric vertical current, Journal of Geophysical Research 101 29671-29677.

Thompson, S. P., (1910). The Life of William Tomson, Vol. I, MacMillan.

Thomson, J. J., (1924). Recombination of gaseous ions, the chemical combination of gases and monomolecular reactions Phil. Mag. 47, 337-378.

Thompson**,** W., (1859). On the Necessity for incessant Recording, and for Simultaneous Observations in different Localities, to investigate Atmospheric Electricity, *2*9th Meeting, British Association for the Advancement of Science (Aberdeen).

Thomson, W., (1872). Reprint of papers on Electrostatics and Magnetism (Section XVI, Atmospheric Electricity). Macmillan, London.

Tinsley, B. A. and R. A. Heelis (1993), Correlations of atmospheric dynamics with solar activity. Evidence for a connection via the solar wind, atmospheric electricity and cloud microphysics, J. Geophys. Res. 98, 10375–10384.

Tinsley, B.A., 1996. Correlations of atmospheric dynamics with solar wind induced changes of air– earth current density into cloud tops. J. Geophys. Res. 101, 29,701–29,714.

Tinsley, B. A. and Zhou, L. (2006). Initial results of a global circuit model with variable stratospheric and tropospheric aerosols, Journal of Geophysical Research 3 D16205.

Torreson O.W. (1949), Instruments used in observations of atmospheric electricity, In: Fleming J.A. (ed.), Terrestrial Magnetism and Electricity, 2nd edition, Dover, New York

Tsurutani, B.T., and Gonzalez, W.D., 1995. The efficiency of 'viscous interaction' between the solar wind and magnetosphere during intense northward IMF event. Geophys. Res. Lett. 22, 663-666.

Tufty, B. (1987) 1001 Questions Answered about Hurricanes, Tornadoes and other Natural Air Disasters. Dover Publications Inc., New York, 381 pp

Uchikawa, K., (1972). On the Seasonal Variations of the Atmospheric Electric Elements, Pure and Applied Geophysics 100 54-59.

Venkiteshwaran S.P. (1958), Measurement of the electrical potential gradient and conductivity by radiosonde at Poona, India, In: Smith L.G. (ed.), Recent advances in atmospheric electricity, Pergamon Press, Oxford

Volland, H., 1987. Electromagnetic coupling between lower and upper atmosphere. Physica Scripta T18, 289-297.

Watson, W. M., (1746). Observations upon So Much of Monsieur Le Monnier the Younger's Memoir, Lately Presented to the Royal Society, as Relates to the Communicating the Electric Virtue to Non-Electrics, Philosophical Transactions (1683- 1775) 44 388-395.

Wåhlin L. (1986), Atmospheric electrostatics, Research Studies Press, Letchworth

Wahlin, L. and Kasemir, H. (1985) Electrochemical charging in the atmosphere measured by a Gerdien cylinder. Journal of Electrostatics 379–386.

Weiss, L. A., Reiff, P. H., Mosses, J. J., Moore, B. D., 1992, Eur. Space Agency Spec. Publ., ESA-SP 335, 309.

Wormell, T.W., Vertical electric currents below thunderstorms and showers, Proceedings of the Royal Society *A* 127 (1930), pp. 567–590.

Whipple, F. J. W., (1929). On the association of the diurnal variation of electric potential gradient in fine weather with the distribution of thunderstorms over the globe, Quarterly Journal of the Royal Meteorological Society 55(229) 1-17.

Whipple, F.J.W. 1932, Terr. Magn. Atmos. Elect. 37, 355.

Whittow, J. B. (1984) The Penguin Dictionary of Physical Geography. Penguin Books Ltd, London, 591 pp

Williams, E. R., (1992). The Schumann Resonance: A Global Tropical Thermometer, Science 256 1184-1187.

Williams, E. R. and Sátori, G., (2004). Lightning, thermodynamic and hydrological comparison of the two tropical continental chimneys, Journal of Atmsopheric and Solar- Terrestrial Physics 66 1213-1231.

Wilson, C. T. R., (1906). On the Measurement of the Earth-Air Current and on the Origin of Atmospheric Electricity, Cambridge Proc. Phil. Soc. 13(6) 363-382.

Wilson, C.T.R., (1916). On some determinations of the sign and magnitude of electric discharges in lightning flashes. Proc. Roy. Soc. Lond*., A, 92,* 555-574.

Wilson C. T. R., (1925). The electric field of the thundercloud and some of its effects; Proc. Phys. Soc. London, Sect. A 111 32D.

Wilson, C.T.R., (1929). Some thundercloud problems, J. Franklin Inst., *208,* 1-12.

Wilson C. T. R., (1960). Reminiscences of my early years. Notes and Recollections of the Royal Society of London 14(2), 163-173 .